
Doctoral Dissertations


Student Theses and Dissertations

Fall 2019

Mass spectrometry analysis of contaminants of emerging concern: Nanoparticles, algal toxins, and cyanotoxins in natural waters and their potential health impacts

Ariel R. Donovan

Follow this and additional works at: https://scholarsmine.mst.edu/doctoral_dissertations

 Part of the [Chemistry Commons](#), [Environmental Sciences Commons](#), and the [Nanoscience and Nanotechnology Commons](#)

Department: Chemistry

Recommended Citation

Donovan, Ariel R., "Mass spectrometry analysis of contaminants of emerging concern: Nanoparticles, algal toxins, and cyanotoxins in natural waters and their potential health impacts" (2019). *Doctoral Dissertations*. 3034.

https://scholarsmine.mst.edu/doctoral_dissertations/3034

This thesis is brought to you by Scholars' Mine, a service of the Missouri S&T Library and Learning Resources. This work is protected by U. S. Copyright Law. Unauthorized use including reproduction for redistribution requires the permission of the copyright holder. For more information, please contact scholarsmine@mst.edu.

MASS SPECTROMETRY ANALYSIS OF CONTAMINANTS OF EMERGING
CONCERN: NANOPARTICLES, ALGAL TOXINS, AND CYANOTOXINS IN
NATURAL WATERS AND THEIR POTENTIAL HEALTH IMPACTS

by

ARIEL RENEE DONOVAN

A DISSERTATION

Presented to the Faculty of the Graduate School of the
MISSOURI UNIVERSITY OF SCIENCE AND TECHNOLOGY

In Partial Fulfillment of the Requirements for the Degree

DOCTOR OF PHILOSOPHY

in

CHEMISTRY

2019

Approved by:

Honglan Shi, Advisor
Keith Loftin, Co-Advisor
Nuran Ercal
Xinhua Liang
Paul Nam

© 2019

Ariel Renee Donovan

All Rights Reserved

PUBLICATION DISSERTATION OPTION

This dissertation includes two peer-reviewed articles that have been published elsewhere and one manuscript that has been submitted for publication, formatted in the style used by the Missouri University of Science and Technology, in addition to an original introduction and conclusion.

Paper I: Pages 16-41 have been published by *Analytical and Bioanalytical Chemistry* 408(19), 5137-5145 (2016).

Paper II: Pages 42-73 have been published by *Chemosphere* 195, 531-541 (2018).

Paper III: Pages 74-107 are intended for submission to *Harmful Algae*.

ABSTRACT

The analysis of contaminants of emerging concern is critical to protecting environmental health. In the presented dissertation, two groups of contaminants of emerging concern were assessed using mass spectrometry methods: nanoparticles and algal and cyanotoxins.

Analysis of metal oxide nanoparticles in environmental matrices has been a challenging issue, as most traditional methods require complicated sample preparation methods or that can alter or destroy the nanoparticles in the system. Single particle inductively coupled plasma mass spectrometry (SP-ICP-MS) methods were used to detect metal oxide nanoparticles in surface waters and their removal through drinking water treatment simulations while retaining all information regarding primary particles. Methods were developed to monitor titanium dioxide, cerium dioxide, zinc oxide, citrate-coated silver, and citrated-coated gold nanoparticles directly in surface water and water treated by multiple drinking water treatment methods. Results from these studies indicate that removal depends on the starting water quality, the surface of the nanoparticles, and the type of treatment employed.

Cyanotoxins, produced by freshwater cyanobacteria, are a group of contaminants of emerging concern at the freshwater-marine water continuum. Cyanotoxins and several marine algal toxins were analyzed by a direct injection liquid chromatography tandem mass spectrometry (LC/MS/MS) in estuary samples from the contiguous United States. Anatoxin-a, cylindrospermopsin, domoic acid, and microcystins were detected in U.S. estuaries, indicating that cyanotoxins are transported to or produced in estuary systems.

ACKNOWLEDGMENTS

I owe a sincere thanks to the people who supported me to this point in my career. Firstly, I would like to thank my advisor, Dr. Honglan Shi, for affording me countless opportunities to grow, develop my abilities as a scientist, and to forge my own path to this point. Thanks to my co-advisor at the United States Geological Survey, Dr. Keith Loftin, for providing opportunities to grow as a chemist and researcher. These individuals inspired a love of research, public service, and curiosity to continue digging deeper. Thanks to my committee members, Dr. Nuran Ercal, Dr. Xinhua Liang, and Dr. Paul Nam for their comments and advice on this body of work. Thanks to Dr. Shi's research team for their crucial help performing drinking water treatment simulations, and my co-workers at the USGS. I would also like to thank the support staff in the Chemistry Department at Missouri S&T for their unending help and answers to questions.

Finally, thanks to my family and friends who have supported my efforts throughout this process. To my parents, who encouraged me to bring my best to everything I do and to strive for excellence. Lastly, thanks to my fiancé, Robert Gattenby, for twelve years of love and support.

TABLE OF CONTENTS

	Page
PUBLICATION DISSERTATION OPTION	iii
ABSTRACT.....	iv
ACKNOWLEDGMENTS	v
LIST OF ILLUSTRATIONS.....	xii
LIST OF TABLES.....	xiv
 SECTION	
1. INTRODUCTION.....	1
1.1. CONTAMINANTS OF EMERGING CONCERN AND DETECTION METHODS.....	1
1.2. NANOPARTICLES: AN EMERGING SURFACE WATER CONTAMINANT	3
1.2.1. Toxicity of Nanoparticles.....	3
1.2.2. Nanoparticle Detection Methods.....	5
1.2.3. Nanoparticles in Surface Water and Treated Drinking Water.	7
1.3. CYANOTOXINS: EMERGING COASTAL WATER CONTAMINANTS.....	8
1.3.1. Cyanotoxin Detection in High Salinity Waters.....	9
1.3.2. Microcystins.....	10
1.3.3. Nodularins.....	11
1.3.4. Anatoxins.....	11
1.3.5. Cylindrospermopsins.....	12

1.3.6. Known Marine Algal Toxins.....	12
1.3.6.1. Domoic acid.....	13
1.3.6.2. Okadaic acid, dinophysistoxins, and pectenotoxins.	13
1.3.6.3. Pectenotoxins.....	14
1.3.6.4. Gymnodimine and spirolides.....	14
1.3.7. Occurrence of Algal Toxins and Cyanotoxins in Coastal Waters.....	15

PAPER

I. DETECTION OF ZINC OXIDE AND CERIUM DIOXIDE NANOPARTICLES DURING DRINKING WATER TREATMENT BY RAPID SINGLE PARTICLE ICP-MS METHODS.....	16
ABSTRACT.....	17
1. INTRODUCTION.....	18
2. MATERIALS AND METHODS.....	21
2.1. MATERIALS AND INSTRUMENTATION.....	21
2.2. SINGLE PARTICLE ICP-MS METHODS.....	22
2.3. WATER SAMPLE COLLECTION AND WATER QUALITY PARAMETER MEASUREMENT.....	23
2.4. DRINKING WTAER TREATMENT SIMULATIONS.....	24
3. RESULTS AND DISCUSSION.....	25
3.1. NANOPARTICLE CHARACTERIZATION.....	25
3.2. SP-ICP-MS METHOD PERFORMANCE.....	26
3.3. FATE OF ZnO AND CeO ₂ NPs DURING SIMULATED DRINKING WATER TREATMENTS.....	28
3.3.1. Fate of Zn-Containing NP without ZnO NP Addition.....	30

3.3.2. Fate of ZnO NPs with ZnO NP Addition.....	31
3.3.3. Fate of Ce-Containing NP without NP Addition.....	33
3.3.4. Fate of CeO ₂ NP with CeO ₂ NP Addition.....	33
3.4. ZnO AND CeO ₂ NP OCCURRENCE IN WATER FROM THREE DRINKING WATER TREATMENT FACILITIES.....	35
ACKNOWLEDGEMENTS.....	37
CONFLICT OF INTEREST.....	38
REFERENCES.....	38
II. FATE OF NANOPARTICLES DURING ALUM AND FERRIC COAGULATION MONITORED USING SINGLE PARTICLE ICP-MS.....	42
ABSTRACT.....	43
1. INTRODUCTION.....	44
2. MATERIALS AND METHODS.....	47
2.1. MATERIALS.....	47
2.2. NATURAL WATERS.....	47
2.3. INSTRUMENTATION.....	48
2.4. SP-ICP-MS ANALYSIS.....	49
2.5. JAR TEST PROCEDURE.....	50
3. RESULTS AND DISCUSSION.....	51
3.1. SP-ICP-MS ANALYSIS.....	51
3.2. NANOPARTICLE CHARACTERIZATION.....	52
3.3. NANOPARTICLE FATE AND REMOVAL BY CHARGE NEUTRALIZATION (ZONE 2) COAGULATION.....	54

3.4. NANOPARTICLE FATE AND REMOVAL BY SWEEP FLOC (ZONE 4) COAGULATION.....	60
4. CONCLUSIONS	66
SUPPLEMENTARY INFORMATION.....	67
CONFLICT OF INTEREST	67
ACKNOWLEDGEMENTS	68
REFERENCES.....	68
III. CYANOTOXIN OCCURRENCE, RELATION WITH SALINITY, AND POTENTIAL RECREATIONAL HEALTH RISKS IN U.S. ESTUARIES IN THE 2015 EPA NATIONAL COASTAL ASSESSMENT	74
ABSTRACT	74
1. INTRODUCTION.....	76
2. METHODS AND MATERIALS	80
2.1. STUDY DESIGN	80
2.2. SAMPLE COLLECTION AND PRESERVATION AND IN-SITU SALINITY MEASUREMENT	80
2.3. SAMPLE PROCESSING FOR ALGAL TOXIN AND CYANOTOXIN ANLAYSIS BY LC/MS/MS.....	81
2.4. LIQUID CHROMATOGRAPHY TANDEM MASS SPECTROMETRY (LC/MS/MS) ANALYSIS FOR ALGAL TOXINS AND CYANOTOXINS .	82
2.5. DETECTION OF MICROCYSTINS BY ENZYME-LINKED IMMUNOSORBENT ASSAY (ELISA)	83
2.6. DETERMINATION OF CHLOROPHYLL.....	84
2.7. DATA ANALYSIS.....	84
3. RESULTS.....	85
3.1. CLIMATE AND SALINITY.....	85

3.2. OCCURRENCE OF ALGAL TOXINS AND CYANOTOXINS IN U.S. ESTUARIES AND COASTAL WATERS BY LIQUID CHROMATOGRAPHY TANDEM MASS SPECTROMETRY (LC/MS/MS)	86
3.3. CHLOROPHYLL IN U.S. ESTUARIES AND COASTAL WATERS.....	87
3.4. ALGAL TOXINS AND CYANOTOXINS OCCURRENCE IN THE CONTEXT OF MEASURED SALINITY	91
3.5. RECREATIONAL RISK ASSESSMENT FOR MICROCYSTIN EXPOSURE IN U.S. ESTUARIES AND COASTAL WATERS BASED ON WORLD HEALTH ORGANIZATION AND U.S. ENVIRONMENTAL PROTECTION AGENCY FRESHWATER GUIDELINES	91
4. DISCUSSION	95
4.1. DOMOIC ACID WAS DETECTED IN MANY COASTAL CONTIGUOUS U.S. ESTUARY SYSTEMS TESTED	95
4.2. MULTIPLE CLASSES OF CYANOTOXINS OCCURRED IN U.S. ESTUARIES AND COASTAL SYSTEMS	96
4.3. SALINITY AND TOXINS.....	97
4.4. UNKNOWN IMPACTS OF MULTIPLE TOXIN CLASSES PRESENT IN ESTUARIES AND COASTAL WATER SYSTEMS	97
SUPPORTING INFORMATION	98
ACKNOWLEDGEMENTS	98
REFERENCES	99
SECTION	
2. CONCLUSIONS	108
2.1. SINGLE PARTICLE ICP-MS DETECTION OF NANOPARTICLES IN SURFACE AND TREATED WATER.....	108
2.2. CYANOTOXINS IN ESTUARINE ENVIRONMENTS BY LC/MS/MS	108

APPENDIX.....110

BIBLIOGRAPHY.....114

VITA.....125

LIST OF ILLUSTRATIONS

	Page
PAPER I	
Figure 1. SP-ICP-MS and SEM characterizations of NPs.....	26
Figure 2. Change in size distribution histograms after sequential simulated drinking water treatments in Missouri River water for a) ZnO without NP addition (n=2), b) ZnO with 80-200 nm ZnO addition (7 µg/L mass concentration) (n=2), c) CeO ₂ without NP addition (n=2), and d) CeO ₂ with 30-50 nm CeO ₂ addition (4 µg/L mass concentration) (n=2).....	32
PAPER II	
Figure 1. Size distribution histograms for all studied NPs after Zone 2 (charge neutralization) treatment in river water.	57
Figure 2. a) Ag NP, Au NP, and turbidity removal and b) TiO ₂ , CeO ₂ , ZnO NP and turbidity removal after various Zone 2 coagulation and polymer treatments in river water.	58
Figure 3. Dissolved Ti and Zn removal during Zone 2 coagulation experiments in river water.....	59
Figure 4. Size distribution histograms for all studied NPs after Zone 4 (sweep floc) treatment in river water.	61
Figure 5. Size distribution histograms for all studied NPs after Zone 4 (sweep floc) treatment in lake water.	62
Figure 6. a) Ag NP, Au NP, and turbidity removal and c) TiO ₂ , CeO ₂ , ZnO NP and turbidity removal after various Zone 4 coagulation and polymer treatments in river water; b) Ag NP, Au NP, and turbidity removal and d) TiO ₂ , CeO ₂ , ZnO NP and turbidity removal after various Zone 4 coagulation treatments in river water.	64
Figure 7. Dissolved Ti and Zn removal during Zone 4 coagulation experiments in a) river water and b) lake water.....	66

PAPER III

Figure 1. Salinity tolerance range of several potential toxin producing cyanobacteria genera where n is the number of instances reported salinity tolerance data. ...	77
Figure 2. Anatoxin-a occurrence in U.S. estuarine and coastal samples by LC/MS/MS.	88
Figure 3. Cylindrospermopsin occurrence in U.S. estuarine and coastal samples by LC/MS/MS.	88
Figure 4. Total microcystin occurrence in U.S. estuarine and coastal samples by LC/MS/MS.	89
Figure 5. Microcystins occurrence in U.S. estuarine and coastal samples by ELISA.	89
Figure 6. Domoic acid occurrence in U.S. estuarine and coastal samples by LC/MS/MS.	90
Figure 7. Chlorophyll occurrence in U.S. estuarine and coastal samples.	90
Figure 8. Comparison of a) anatoxin-a (ANAA) and cylindrospermopsin (CYLS), b) domoic acid (DMAC), c) microcystins by LC/MS/MS and ELISA, and d) chlorophyll to measured salinity.	92
Figure 9. Comparison of microcystins measured by ELISA and chlorophyll with WHO relative health risk thresholds noted.	93
Figure 10. Comparison of microcystins measured by LC/MS/MS and chlorophyll with WHO relative health risk thresholds noted.	94

LIST OF TABLES

	Page
 PAPER I	
Table 1. SP-ICP-MS instrument and method parameters for ZnO and CeO ₂ NP and dissolved element analysis.....	27
Table 2. Change in pH, DOC, and turbidity after each treatment step during the simulated drinking water treatment process (value±standard deviation, n=6)..	29
Table 3. General water quality parameters for Facilities 1-3.....	36
Table 4. Zn- and Ce-containing NP occurrence and dissolved Ce and Zn through drinking water treatments at three drinking water treatment facilities.	37
 PAPER II	
Table 1. SP-ICP-MS size distribution histograms, TEM images, ZPC (point of zero charge), and SP-ICP-MS statistical variation for the five selected NPs.....	53
 PAPER III	
Table 1. Percentage of samples by ELISA, LC/MS/MS, and chlorophyll that fall into WHO recreational health threshold categories for potential microcystin exposure.	93

1. INTRODUCTION

1.1. CONTAMINANTS OF EMERGING CONCERN AND DETECTION METHODS

Environmental contaminants can arise from many sources, be inorganic or organic compounds, and can impact human and ecological health (environmental health). Given the staggering numbers of chemicals produced anthropogenically and naturally, the challenge of prioritizing research and determining toxic effects of these chemicals is enormous.¹ Generally, these compounds are identified as the result of some observed toxic effect in humans and animals, as a result of environmental impacts over the long-term, or are identified and prioritized based on exposure potential.^{1,2} Analytical challenges associated with the detection of contaminants of emerging concern include contaminant identification, sample preparation, compound identification, and quantitation. In this body of work two contaminant types of emerging concern, metal-based nanoparticles and cyanotoxins, are examined in the context of detection methodology, environmental occurrence, and potential for human and environmental health risks.

Engineered nanoparticles (ENPs) are an example of emerging contaminants that have received significant attention in recent years due to numerous applications in personal care products, sunscreen, and medicine among many others.³ ENPs can enter the environment through a variety of applications ranging from personal care products to medicines, with the potential for human dermal, oral, and inhalation exposure.⁴ There are significant challenges associated with determining human and environmental health risks of these materials due to their size and nature: nanoparticles are too small for most

filtration methods, can sorb to organic materials in environmental systems, stability, dissolution, and the presence of background nanoparticles make detection challenging.⁵ Mass spectrometry methods have recently been employed to determine ENPs in natural and treated waters, food, and plants and is a promising technique for future investigations into toxicity and occurrence.⁶⁻¹²

Cyanotoxins are an emerging topic in human and environmental health due to their implications in human and animal illnesses worldwide.^{13,14} Only a handful of cyanotoxins are monitored (a few microcystin congeners and cylindrospermopsin), but there are many more that have yet to be identified. In the case of microcystins, there are over 250 known congeners.¹⁵ Cyanotoxins are an emerging contaminant in marine water systems, where they have not historically been monitored as a result of their primary occurrence in freshwater systems; however, recent events indicating cyanotoxin exposure of marine wildlife indicates the need for cyanotoxin monitoring in marine environments.^{16,17} Detection is complicated due to a lack of reference materials for many of the known cyanotoxins, and the understanding that there are many more cyanotoxins that have yet to be identified. Enzyme-linked immunosorbent assay (ELISA) methods are a common screening tool for major toxin classes. These methods are rapid and can be performed with minimal expertise, but interpretation is complicated when multiple congeners are detected and have varying toxicity.^{15,18} Mass spectrometry methods are often employed in research efforts to accurately quantitate specific cyanotoxin compounds, but require reference materials that may not be available for accurate quantitation.¹⁹

1.2. NANOPARTICLES: AN EMERGING SURFACE WATER CONTAMINANT

Inorganic nanoparticles have increased in global production over the last decade due to unique physiochemical properties, and production is projected to increase in the next decade.²⁰ Nanoparticles are materials with at least one dimension smaller than 100 nm, and can be made of organic and inorganic components.²¹ Nanoparticles have been used for a multitude of applications, ranging from paints and coatings, electronics, personal care products, sunscreen, food additives, antimicrobial uses, and drug delivery.^{22–25} The most commonly used metallic nanoparticles include titanium dioxide (TiO₂), zinc oxide (ZnO), cerium dioxide (CeO₂), silver (Ag), and gold (Au). While nanoparticles have long been used in photocatalysis, particularly TiO₂, more recent applications have significantly increased production of nanosized materials worldwide.²⁰ As nanomaterials are used in consumer products, they will inevitably be released into the environment, where their human and environmental health impacts are not yet well understood.

1.2.1. Toxicity of Nanoparticles. The toxicity of ENPs depends on the type of material the particle is made from, size of the ENPs, the solubility of the ENPs, and the presence of other toxins. An exhaustive review of literature regarding the toxicity of titanium dioxide nanoparticles in humans and mammals was conducted by Fabian et al. 2019.²⁶ The major findings of this review indicated that regularly consumed titanium dioxide nanoparticles can impact the brain, heart, internal organs, and intestinal mucosa as well as increase the risk of disease development. An additional consideration for titanium dioxide nanoparticles is the toxicity difference between crystal structures: anatase, rutile, and brookite. There is some evidence that anatase may induce more toxic

response to human peripheral blood monocytes compared to rutile titanium dioxide nanoparticles, but more work needs to be done to fully understand the variability.²⁶

Zinc oxide ENPs have been used in sunscreens due to their UV absorption properties and food packing due to antimicrobial properties.²⁷ Thus the main routes of human exposure to these ENPs is dermal and oral ingestion. In vitro studies of zinc oxide ENP exposure on human cell types primarily indicate that toxic effects are the result of dissolution outside of cells.²⁸ Others suggest that toxic effects on human cancer cells are the result of the production of reactive oxygen species by zinc oxide ENPs.²⁹⁻³¹

Cerium dioxide ENPs are used in a wide variety of applications, including catalysis, oxygen sensing, solar cells, polishing, and are used as diesel fuel additives. These ENPs have been reported to be toxic to human monocytes at low doses (0.5 – 10 $\mu\text{g/L}$).³² Similar concentrations have been reported to be toxic to human lung cancer cells.^{33,34} In rats, acute toxicity was observed after inhalation of cerium dioxide ENPs, resulting in cytotoxicity.³⁵

Silver ENPs are often used as an antimicrobial agent in clothing and colloidal silver is produced and used as a medicinal cure-all by a small portion of the population. Animal exposure to nanoparticle silver has been reported to cause weight loss, hypoactivity, changes brain chemistry, enlarged hearts, and death.³⁶ Nanoparticle silver caused apoptosis in several human cell lines while ionic silver resulted in cell necrosis.³⁷ This result may be used in future studies to assist in cell effect determinations when testing silver nanoparticles. Gold ENPs have been found to be useful in biomedical applications such as drug delivery. The toxicity of gold ENPs is unclear, as there are

many conflicting reports, but it has been suggested that the uptake and toxicity of these ENPs can be controlled through the use of ligands on the surface.^{38,39}

Dermal absorption is of interest as nanoparticles are often used in personal care products and sunscreens which are directly applied to skin, primarily titanium dioxide and zinc oxide. Titanium dioxide ENPs have been shown to penetrate dermal layers in some cases, and no penetration was observed in others.⁴⁰ There are also conflicting reports on the impacts of zinc oxide ENPs on skin.⁴⁰⁻⁴² Few reports exist on dermal exposure for gold and silver ENPs. Gold ENPs have been observed to have a size dependent permeation of skin layers,⁴⁰ and when they have entered cells, non-toxic results were observed.⁴³ Dermal exposure to silver ENPs is primarily through the use of antimicrobial clothing. Studies have shown that the silver ENPs in these materials can dissolve into sweat and saliva, but depended on how the materials were processed.⁴⁴ Other studies report minimal adverse effects of silver ENPs in dermal toxicity testing.⁴⁵

1.2.2. Nanoparticle Detection Methods. The detection of metal based ENPs in environmental matrices is complex due to matrix interferences, sample preparation requirements, and the presence of dissolved metals in the samples.⁵ Identification of ENPs is further complicated by the presence of naturally occurring metal-oxide nanoparticles. When considering nanomaterials, there are multiple parameters that are important: diameter, hydrodynamic diameter, specific surface area, mass, surface charge, shape, aggregation, and composition. There is not one single technique that can provide information regarding all parameters, rather, multiple techniques that provide information regarding one or more parameters. Traditional methods to analyze ENPs including imaging, field flow fractionation (FFF) methods, zeta-potential measurements, and

inductively coupled plasma mass spectrometry (ICP-MS) on acid digested materials.⁵ Many of these techniques require sample preparation for natural water samples, such as evaporation, ultrafiltration, and digestion with acid, to analyze samples for one or more parameter using the techniques previously mentioned. Imaging techniques including transmission electron microscopy (TEM) and scanning electron microscopy (SEM) provide information on particle size, shape, and when coupled to X-ray fluorescence (XRF) can provide elemental compositions of the surface of ENPs. Methods such as FFF separate particles based on hydrodynamic diameter by applying a perpendicular flow across a membrane that the particles cannot pass.⁴⁶ However, there are disadvantages to this method in that run times are long, usually an hour or more, and complicated sample preparation is required.⁴⁷

Single particle inductively coupled plasma mass spectrometry (SP-ICP-MS) is an emerging technique for the analysis of ENPs, particularly in environmental samples. Using this method, water samples can be directly injected into an ICP-MS and dissolved element fraction and particulate fractions can be simultaneously detected as well as particle concentration, agglomeration state, size, size distribution, and composition. Other matrices, such as biological material, sunscreen, and plants require some sample preparation before analysis. ICP-MS systems are modified to have a low sample flow rate and short dwell time. Under these conditions, an ENP from a sample will enter the plasma torch, is ionized into a packet of ions, and is transported through the quadrupole to the detector. This number of ions is directly related to the size of the ENP, and can be used to back-calculate the particle size based on a known particle shape, in most cases assumed to be spherical.⁴⁸ It is critical that only one particle reaches the detector at a time

to accurately determine particle size and frequency, which is used to determine particle concentration.^{11,49,50} The dissolved portion of an element appears as a constant background signal, while particles appear as sharp peaks in the spectrum.⁵¹ There are a few key assumptions that are made when performing this type of analysis: regular and known particle shape, density, and composition, all particles are completely ionized in the plasma torch, and that agglomerations are not altered during sample introduction. This technique has proven to be useful when characterizing ENPs in a variety of matrices including surface waters and during drinking water treatments^{11,52-54}, in wastewater effluent^{55,56}, soils⁸, chicken meat^{57,58}, other biological matrices⁵⁹, sunscreen⁶⁰, and plants^{61,62}.

1.2.3. Nanoparticles in Surface Water and Treated Drinking Water. The analysis of ENPs in surface waters and their fate through drinking water treatment processes has been of interest to researchers due to the unknown health effects they may have on humans. Several studies have been conducted regarding the fate of metal ENPs through drinking water treatment procedures. Alum, a popular coagulant, has been used to remove titanium dioxide, zinc oxide, iron(III) oxide, nickel oxide, and silica ENPs in tap water and nanopure water, with 20-60% removal.⁶³ Alum coagulation was shown to remove up to 99% of zinc oxide ENPs, 8% of titanium dioxide ENPs, and 20% of silver ENPs.⁶⁴ Polyferric sulfate, ferric chloride, polyaluminum chloride, and alum coagulation methods were shown to remove titanium dioxide ENPs from water, with iron-based coagulants resulting in the highest removal efficiency.⁶⁵ Optimized conditions for removal by polyferric sulfate and ferric chloride coagulants resulted in up to 90% removal of titanium dioxide ENPs in a follow-up report.⁶⁶ However, each of these studies

relied on methods that destroyed the ENPs to analyze removal. SP-ICP-MS methods were employed in one study to determine the behavior of silver, gold, and titanium dioxide ENPs throughout a simulated drinking water treatment process including lime softening, alum coagulation, filtration, and disinfection by free chlorine.⁵² The ENPs in this study were primarily removed during the lime softening treatment ($97 \pm 3\%$). Further study to include other types of ENPs and drinking water treatment processes are imperative to understand potential risk assessments for ENPs in the drinking water supply.

1.3. CYANOTOXINS: EMERGING COASTAL WATER CONTAMINANTS

There is a perceived global increase in the occurrence of cyanobacteria and associated toxins, known as cyanotoxins, globally. Cyanobacteria are generally categorized as freshwater harmful algal blooms resulting in anoxic conditions, taste and odor problems, and in some cases the release of cyanotoxins^{67,68}; however, the presence of cyanobacteria and cyanotoxins are becoming of more concern in coastal and estuarine environments as monitoring efforts increase.^{16,17,69,70} Factors that can transport cyanobacteria and cyanotoxins from freshwater to coastal and estuarine environments include weather events (rain, drought, snow melts), tides, and anthropogenic water discharge.¹⁶ As such, cyanotoxins are considered a contaminant of emerging concern in coastal areas that may be susceptible to their occurrence. There are several major groups of cyanotoxins including microcystins, nodularins, anatoxins, cylindrospermopsins, and saxitoxins.¹⁸ Detection of cyanotoxins in coastal and estuarine environments is

complicated due to salinity in water samples, which may dictate extensive sample preparation before analysis.

1.3.1. Cyanotoxin Detection in High Salinity Waters. Enzyme-linked immunosorbent assays (ELISAs) are a rapid screening technique that use antibodies designed for a specific toxin or class of toxins (i.e. microcystins) to target and detect the compounds in samples.⁷¹ For freshwater samples, little-to-no sample preparation is required. However, when samples have salts present (in the case of estuary samples), sample preparation is required to minimize interferences associated with binding during the assay (such as salt removal) or the use of ELISA kits designed to tolerate saline samples. While ELISA remains a rapid screening tool for toxins, the cross-reactivity of these kits can in some cases overestimate the toxicity when less toxic congeners are bound.¹⁵ Furthermore, cross-reactive kits lack specificity required to detect toxins on a compound-by-compound basis. Capillary electrophoresis (CE) has been applied to separate cyanotoxins, however microcystins congeners have not been successfully resolved from each other, and sensitivity is inadequate without sample preconcentration.⁷²⁻⁷⁴ CE methods have not currently been applied to high salinity samples. Thus, liquid chromatography - mass spectrometry (LC-MS) is the most ubiquitous technique to monitor cyanotoxins in environmental samples with the specificity and sensitivity required for environmental applications. When considering the analysis of high salinity samples using LC-MS, passing samples with high salt content to the MS source can cause several major issues: ion suppression, physical build-up in the source assembly, and sodium adduct formation. However, steps can be taken to mitigate these effects including starting the mobile phase gradient at 100% aqueous phase to form

a salt head that will elute first, and by diverting the first few minutes of the injection to waste, bypassing the potential build-up on the source assembly. This dictates that compounds of interest must elute after the diver time. Sodium adduct formation can be minimized through the use of mobile phase additives such as ammonium formate.⁷⁵

1.3.2. Microcystins. Microcystins are a group of hepatotoxic cyclic heptapeptides first identified in the early 1980s.¹⁸ Most compounds in this class have a common ADDA group (4E,6E-3-amino-9-methoxy-2,6,8-trimethyl-10-phenyldeca-4,6-dienoic acid) attached to a ring of seven amino acids.⁷⁶ There are over 250 reported congeners of microcystins¹⁵ and have been isolated from freshwater cyanobacteria genera including *Anabaena*, *Microcystis*, *Oscillatoria*, *Planktothrix*, *Synechococcus*, and *Synechocystis*.^{15,67} The marine cyanobacteria *Trichodesmium* has been shown to produce microcystins and saxitoxin in coastal environments.⁷⁷ Toxicity of these compounds has been shown to be congener dependent, and dominant forms vary based on unknown factors.^{18,67,68,78} Microcystins and microcystin-producing cyanobacteria have been detected in freshwater globally.⁷⁹ The World Health Organization (WHO) and U.S. Environmental Protection Agency (EPA) have issued guidelines for assessing potential recreational exposure to microcystins. The WHO guidelines use three metrics to determine potential risk assessment: microcystins concentration, chlorophyll-a concentration, and cyanobacteria abundance.¹⁸ The EPA threshold is 8 µg/L for microcystins.⁸⁰ Interest in microcystins at the land-sea interface has increased in recent years, and were the causative agent in the deaths of 21 southern sea otters in California.^{16,69,81} *Microcystis aeruginosa*, one of the most well-studied microcystin producing cyanobacteria species studied, has been found in coastal California creeks and

lagoons with relatively high salinity (23 parts per thousand, PPT). Microcystin accumulation in shellfish has been reported, and it is possible that some species may be vectors for human exposure to microcystins.⁸²⁻⁸⁵

1.3.3. Nodularins. Nodularins, like microcystins, are cyclic peptides. They have an ADDA group attached to a ring of five amino acids, and there are 12 known congeners.^{86,87} Nodularins have been reportedly produced by cyanobacteria genera *Nodularia*, *Nostoc*, and *Inigainema*.^{15,88} Nodularin-R is the most commonly detected congener⁶⁷, and is hepatotoxic in humans and other mammals.⁸⁹ There has been one reported case of nodularin causing illness in humans and several reported cases of animal illness.¹⁴ *Nodularia*, the most predominant producer of nodularins, forms blooms in brackish water, resulting in significant concern for the land-sea interface.⁹⁰ Recently, nodularins were detected in coastal California waters.¹⁶ Nodularin uptake into blue mussels has been investigated, resulting in low levels of accumulation in the mussels.⁹¹

1.3.4. Anatoxins. Anatoxins are a class of freshwater toxins produced by various filamentous cyanobacteria genera including *Anabaena*, *Aphanizomenon*, *Cuspidothrix* sp. *Cylindrospermopsis*, *Dolichospermum*, *Microcoleus*, *Oscillatoria*, *Phormidium*, *Pseudoanabaena*, *Raphidiopsis*, and *Tychomena*.^{67,92-94} Anatoxin-a, anatoxin-a(s), and homoanatoxin-a are included in the group, with at least four other analogues known.⁹⁵ Anatoxins are nicotinic acetylcholine receptor agonists, a fatal dose of which can kill within 2-30 minutes.^{18,94} There have been five reported incidents of human exposure to anatoxin-a via recreational use of freshwater, of which four cases were associated with other toxins.¹⁴ Anatoxins have been reported in freshwaters across Europe and North America^{18,67} and have been detected in brackish water and coastal creeks and

lagoons.^{16,17,96} There is currently no information regarding the uptake of anatoxins by shellfish.

1.3.5. Cylindrospermopsins. The most famous case of cylindrospermopsin intoxication is the Palm Island mystery disease in 1979. During this event, over 100 people were hospitalized in Australia, later cylindrospermopsin was implicated.^{89,97} Five analogues of cylindrospermopsin are known¹⁵ and have reportedly been produced by multiple freshwater cyanobacteria genera including *Anabaena*, *Aphanizomenon*, *Chrysochloris*, *Cylindrospermopsis*, *Lyngbya*, *Raphidiopsis*, and *Umezakia*.^{15,67,89} The toxic effects of cylindrospermopsins have been reported to be cytotoxic, dermatotoxic, genotoxic, hepatotoxic, and they are possibly carcinogenic.⁹⁸ Cylindrospermopsins have been detected worldwide and across the United States.^{67,99} Recently, they have been reported in coastal creeks and lagoons in California.^{16,17} Few studies have been conducted regarding the uptake of cylindrospermopsin in shellfish. However, there is some evidence that mussels can accumulate cylindrospermopsin, and that monitoring should be increased.^{85,100}

1.3.6. Known Marine Algal Toxins. Cyanobacteria and cyanotoxins are of emerging concern in estuarine and coastal water systems due to recent toxic events⁸¹, but water at the marine-freshwater continuum may also have of marine algal toxins produced by dinoflagellates and diatoms including domoic acid, okadaic acids (okadaic acid, dinophysitoxins), pectenotoxins, and gymnodimine and spirolides.¹⁰¹ These are typically grouped by common symptoms, which generally occur after oral consumption of contaminated fish or shellfish. Contrary to the case of cyanotoxins, marine algal toxins are primary monitored in fish and shellfish rather than in water bodies.¹⁰²

1.3.6.1. Domoic acid. Domoic acid is the causative agent in amnesic shellfish poisoning (ASP) produced by a *Pseudo-nitzschia* species.^{103,104} Toxicogenic varieties of *Pseudo-nitzschia* have been detected in coastal waters worldwide, with significant impacts on the United States west coast.¹⁰⁵ The primary exposure route for domoic acid is consumption of fish and shellfish products that have accumulated the toxin. Domoic acid was first identified after an outbreak of illnesses related to consumption of domoic acid contaminated mussels harvested from Prince Edward Island, Canada. Over 143 people fell ill after eating the mussels and 3 people died.¹⁰⁶ Symptoms associated with domoic acid consumption include vomiting, abdominal cramps, diarrhea, headache, loss of short-term memory, seizures, and in severe cases death.¹⁰⁷ Domoic acid is regulated by the FDA to 20 mg/g in shellfish meat tissue and 30 mg/g in the viscera of Dungeness crab (which may be important for human health depending on the cooking method) to prevent amnesic shellfish poisoning in humans.¹⁰² However, the long-term effects of low-level consumption are still under investigation. Recently, chronic low-level oral consumption of domoic acid has been shown to cause cognitive deficits in mice¹⁰⁸ and changes to brain physiology and chemistry in nonhuman primates.¹⁰⁹ Since the implementation of shellfish regulations, human intoxication events have not been reported.¹⁰⁴ However, wildlife are regularly impacted, notably sea lions in California with acute and chronic symptoms.^{105,110}

1.3.6.2. Okadaic acid, dinophysistoxins, and pectenotoxins. Okadaic acid was first identified in Japan after a series of food poisoning events associated with mussel and scallop consumption, resulting in gastrointestinal issues.¹¹¹ This class of toxin is identified as diarrhetic shellfish poisoning (DSP) toxins due to the symptoms associated

with consumption. Since this initial incident there have been multiple variants identified including dinophysistoxins. Okadaic acids and dinophysistoxins are produced by marine dinoflagellates, including *Dinophysis* and *Prorocentrum* genera.^{112,113} The first United States shellfish harvest closure due to okadaic acid was detected in oysters from the Gulf of Mexico coastline in Texas, resulting in the deaths of over 100 bottlenose dolphins.^{114,115} Concentrations of okadaic acid in the oysters exceeded the USFDA action level of 0.16 mg/g total okadaic acid equivalents including okadaic acid, dinophysistoxins, and their acyl-esters.¹⁰² Okadaic acid has since been detected in Florida and Washington.^{116,117}

1.3.6.3. Pectenotoxins. Pectenotoxins are a group of cyclic polyethers with symptoms similar to okadaic acid and other DSP toxins.¹¹⁸ They were first discovered in shellfish during an outbreak of illness along side okadaic acid and dinophysistoxins.^{111,119} Pectenotoxins are categorized as DSP toxins due to symptoms exhibited after exposure. There are currently no regulations for pectenotoxins in the United States.

1.3.6.4. Gymnodimine and spirolides. Gymnodimine and spirolides are cyclic imines identified to be produced by *Alexandrium* and *Karenia* genera of marine dinoflagellates.^{118,120,121} Symptoms associated with intraperitoneal injection of gymnodimine in mice included nervous systems effects and respiratory distress, and death.¹²² Similar effects have been observed when mice were dosed with 13-desmethyl spirolide c, reacting very quickly.¹²⁰ Other reports confirm gymnodimine toxicity when administered by intraperitoneal injection, but suggest low toxicity when administered orally.¹²³ There have been no reported cases of human intoxication due to gymnodimine

and spirolides. However, there is evidence of gymnodimine accumulation in shellfish and clams^{124,125} and spirolides in shellfish and crabs.¹²⁶⁻¹²⁸

1.3.7. Occurrence of Algal Toxins and Cyanotoxins in Coastal Waters. As the knowledge of cyanotoxins at the land-sea interface expands, the complexity of toxin monitoring and health risk assessment increases. Synergistic effects between cyanotoxins and marine algal toxins are understudied, and the impacts of toxin mixtures on human and animal health are not understood. The first step toward understanding the co-occurrence of cyanotoxins and algal toxins in estuary and coastal environments is to conduct screening studies for algal toxins and cyanotoxins, toxicity studies with multiple toxins present, and to better understand the accumulation of cyanotoxins in common vectors.

PAPER**I. DETECTION OF ZINC OXIDE AND CERIUM DIOXIDE NANOPARTICLES
DURING DRINKING WATER TREATMENT BY RAPID SINGLE
PARTICLE ICP-MS METHODS**

Ariel R. Donovan^{1,2}, Craig D. Adams^{2,3}, Yinfa Ma^{1,2}, Chady Stephan⁴, Todd Eichholz⁵,
Honglan Shi^{1,2*}

¹Department of Chemistry and Environmental Research Center, Missouri University of Science and Technology, Rolla, Missouri, 65409, United States

²Center for Single Nanoparticle, Single Cell, and Single Molecule Monitoring (CS³M), Rolla, Missouri, 65409, United States

³Department of Civil and Environmental Engineering, Utah State University, Logan, Utah, 84321, United States

⁴PerkinElmer, Inc., 501 Rowntree Dairy Rd, Woodbridge, On, Canada, L4L 8H1

⁵Missouri Department of Natural Resources, Jefferson City, MO 65102, United States

*Corresponding Author

Address: Department of Chemistry

Missouri University of Science and Technology

400 West 11th Street

Rolla, MO 65409

Phone: 573-341-4433; Fax: 573-341-6033

E-mail: honglan@mst.edu

ABSTRACT

Nanoparticles (NPs) entering water systems are an emerging concern as NPs are more frequently manufactured and used. Single particle ICP-MS (SP-ICP-MS) methods were validated to detect Zn- and Ce-containing NPs in surface and drinking water using a short dwell time of 0.1 ms or lower ensuring precision in single particle detection while eliminating the need for sample preparation. Using this technique, information regarding NP size, size distribution, particle concentration, and dissolved ion concentrations were obtained simultaneously. The fates of Zn- and Ce-NPs, including those found in river water and added engineered NPs, were evaluated by simulating a typical drinking water treatment process. Lime softening, alum coagulation, powdered activated carbon sorption, and disinfection by free chlorine were simulated sequentially using river water. Lime softening removed 38-53% of Zn-containing and ZnO NPs and >99% of Ce-containing and CeO₂ NPs. Zn-containing and ZnO NP removal increased to 61-74% and 77-79% after alum coagulation and disinfection, respectively. Source and drinking water samples were collected from three large drinking water treatment facilities and analyzed for Zn- and Ce-containing NPs. Each facility had these types of NPs present. In all cases, particle concentrations were reduced by a minimum of 60% and most were reduced by >95% from source water to finished drinking water. This study concludes that uncoated ZnO and CeO₂ NPs may be effectively removed by conventional drinking water treatments including lime softening and alum coagulation.

KEY WORDS

Single particle ICP-MS, ZnO and CeO₂ nanoparticles, nanoparticle occurrence and removal, nanoparticle characterization, drinking water treatment

1. INTRODUCTION

As nanoparticles (NPs) are increasingly incorporated into commercial products, the risk of environmental exposure increases [1]. Zinc oxide (ZnO) and cerium dioxide (CeO₂) are among the most commonly used NPs with applications in personal care products, paints, and catalysts which will lead to their release via wastewater or runoff into natural water bodies. Studies have suggested that ZnO NPs have a relatively high acute toxicity and result in oxidative stress and oxidative damage [2,3]. Uptake of CeO₂ NPs has been demonstrated by human intestinal epithelial cells [4] by diverse biological systems, and to be toxic to these different systems [5] including human peripheral blood monocytes and human lung cancer cells [4-6]. CeO₂ NPs have been shown in an *in vivo* study to induce oxidative stress in *Caenorhabditis elegans* at environmentally relevant concentrations [7]. Another study, however, suggested that ZnO induced toxicity in mammalian cells while CeO₂ suppressed reactive oxygen species (ROS) production and even protected the cell [8]. Given the uncertainty of human and environmental toxicity of ZnO and CeO₂ NPs, it is imperative to analyze their fate and transport through water treatment processes. Work has been done to evaluate the fates of ZnO and CeO₂ NPs during wastewater treatment, reporting up to 8% of Zn in influent wastewater leaving in the effluent [9,10] and 6% of the initial CeO₂ NPs leaving in the effluent [11,12]. There

are many interactions that dictate the behavior of NPs during wastewater treatment including sorption onto debris and particles, dissolution, settling, and interactions with microorganisms [13]. Among the most important considerations for NP stability in aqueous media are aggregation and dissolution.

Major factors affecting NP aggregation and dissolution in aqueous solution include ionic strength, pH, and organic matter in the system. Low ionic strength and high organic matter content are associated with increased NP stability in water [14,15]. Natural organic matter (NOM) plays a major role in NP stability. It has been shown that NOM can both prevent the dissolution of ZnO NPs in aquatic matrices as well as prevent aggregation [16] and has been demonstrated to keep up to 88% initially added CeO₂ NPs in suspension after 12 days of settling [17]. With typical fresh water NOM concentrations between 0.1-20 mg/L, it is likely that NPs released into water systems will not aggregate or dissolved significantly, indicating that humans, mammals, and aquatic life may be exposed to these NPs [18]. Furthermore, if the exposed water system is used as source water for drinking water treatment it will be a direct route for human consumption of NPs if they are not removed during drinking water treatment processes.

While several studies have been conducted evaluating the fate of NPs during drinking water treatment, there exists a significant research gap regarding specific processes and NP types. CeO₂ and ZnO NP removal by filtration processes alone (sand filtration, microfiltration, and/or ultrafiltration) have been studied by several research groups [19-22]. The results of these studies indicated that typical filtration processes efficiently remove uncoated (non-surface functionalized) NPs. Alum coagulation has been shown to result in between 40-99% removal of ZnO under typical conditions, with

the highest removal observed using sweep floc dosages in buffered nanopure water [22,23]. No published papers have been found on CeO₂ NPs removal during coagulative drinking water treatments, while ZnO NP removal has been evaluated in two studies. In both of these studies, the NP detection methods have only been indirect. Specifically, NP content in effluent water was detected by acid digestion followed by inductively coupled plasma- mass spectrometry (ICP-MS) or graphite furnace atomic absorption (GFAA) resulting in loss of information regarding NP size and aggregation state after treatment. On the other hand, single particle ICP-MS (SP-ICP-MS) has more recently proven to be an emerging and reliable technique for monitoring NPs in aquatic matrices [24-26] including applications to monitor removal of Ag, Au, and TiO₂ NPs during typical drinking water treatments [27]. The key advantages of SP-ICP-MS include high sensitivity for environmentally relevant concentrations and simultaneous data acquisition regarding NP size, size distribution, and dissolved element concentration. SP-ICP-MS coupled with an ion exchange resin (IEC) has been used to monitor ZnO NPs in water using a dwell time of 0.5 ms [28]. Using the IEC improved NP signals by removing high background levels of Zn, which was demonstrated in previous work [29]. However, reducing the analysis dwell time has also been shown to improve the resolution between NP signals and dissolved background [30].

In this study, the fates of ZnO and CeO₂ NPs during conventional drinking water treatments were evaluated. SP-ICP-MS methods were developed using short dwell times of 0.1 ms to monitor the NPs throughout drinking water treatment process to provide increased resolution between the dissolved background and NP signals without the use of ion exchange resins or columns for potentially high dissolved background element. NP

removal was evaluated after lime softening, alum coagulation with simultaneous powdered activated carbon (PAC) sorption, and disinfection by free chlorine. Filtration was not simulated because it has been studied in detail and published for the selected NPs [19,22]. Water samples were collected from three drinking water treatment facilities (DWTfS) and monitored for Zn- and Ce- containing NPs using the developed SP-ICP-MS methods. The removal efficiencies were compared to the simulation results to evaluate the efficacy of the treatments on bench and full scales.

2. MATERIALS AND METHODS

2.1. MATERIALS AND INSTRUMENTATION

CeO₂ NPs (30-50 nm diameter, 40 wt% CeO₂ dispersed in water, Stock # US7120) and ZnO NPs (80-200 nm diameter, nanopowder, Stock # US3555) were purchased from US Research Nanomaterials, Inc. (Houston, TX). These nanoparticles were selected for this study because the size distributions were all or partially in the nanoscale range (≤ 100 nm) and they were larger than the particle size detection limits of the SP-ICP-MS. A dilute CeO₂ solution was prepared by diluting the stock solution 1000 times into ultra-pure water. A dilute stock solution of ZnO NPs was prepared by dispersing a known amount of nanopowder in ultra-pure water. Particle concentrations were calculated using the density, mass, and particle size range of NPs suspended and the volume of ultra-pure water used. The working particle concentrations were determined by averaging calculated particle concentrations for several sizes over the manufacturer size range. Size calibration standard Au NPs (citrate-capped, 50, 80, and 100 nm diameter)

suspended in 2 mM sodium citrate were obtained from nanoComposix, Inc. (San Diego, CA). All purchased NPs were characterized by both scanning electron microscopy (SEM) and SP-ICP-MS. An S-4700 model field emission scanning electron microscope (FESEM) with energy-dispersive X-ray spectroscopy (EDS) capability (Hitachi, Tokyo, Japan) was used to image and confirm elemental composition of NPs. The NPs purchased were original materials without surface modification.

Dissolved Ce and Zn standards (PerkinElmer, Waltham, MA) were used for dissolved element calibrations. Sodium hydroxide (caustic), aluminum sulfate ($\text{Al}_2(\text{SO}_4)_3 \cdot 14.3\text{H}_2\text{O}$), and trace metal grade nitric acid, were purchased from Thermo Fisher Scientific Inc. (Pittsburgh, PA). Hydrodarco B (HDB) powdered activated carbon (PAC) was product of Cabot (Marshall, TX). Sodium hypochlorite solutions and trace metal grade sulfuric acid were purchased from Sigma-Aldrich (St. Louis, MO). A Simplicity185 water purification system from Millipore was used to generate ultra-pure water. Dissolved organic carbon (DOC) was monitored with a TOC-L analyzer with ASI-L liquid autosampler from Shimadzu Scientific Instruments (Columbia, MD) and turbidity was tested using a TB200 Portable Turbidimeter (Orbeco-Hellige, Sarasota, FL). The pH of the water samples was monitored at each step of the simulation treatment.

2.2. SINGLE PARTICLE ICP-MS METHODS

A PerkinElmer (Shelton, CT) NexION 300D/350 ICP-MS equipped with Syngistix Nano Application module operating in single particle mode was used. The instrument parameters were optimized for detection of ZnO and CeO₂ NPs as well as their corresponding ions. The system was equipped with a concentric nebulizer, cyclonic

spray chamber, and platinum sampler and skimmer cones. The RF power was set to 1600 W to ensure complete atomization of NPs. Parameters optimized daily included sample flow rate (between 0.26-0.29 mL/min) and the transport efficiency (between 7.5-8.5%). Masses of ^{140}Ce and ^{67}Zn were monitored with a dwell time of 100 μs over a 100 s sampling time. ^{67}Zn was monitored to avoid $^{50}\text{Ti}^{16}\text{O}$ interferences that occur with the higher abundance ^{66}Zn isotope. Water collected from the Missouri River used in this and our previous study have had high Ti concentrations, rendering the isotope selection necessary [27]. The instrument was calibrated with a filtered matrix blank and three dissolved Ce and Zn matrix spikes (0-20 $\mu\text{g/L}$ spikes). In most cases Ce and Zn were present in the matrix; therefore, a blank subtraction was used. This calibration was used for both dissolved ions and NP sizing.

2.3. WATER SAMPLE COLLECTION AND WATER QUALITY PARAMETER MEASUREMENT

Three DWTFs (referred to as Facilities 1, 2, and 3) were selected for this study. Facility 1 using a blend of ground water and Missouri River water as source water and the other two DWTFs use Missouri River water as source water. The water samples were collected in duplicate from each facility. Each DWTF employed lime softening, ferric coagulation, PAC sorption and chlorine/chloramine disinfection treatments. Detailed treatment information can be found in the Supplementary material of our recent publication [27]. Samples were collected in pre-cleaned 125 mL polypropylene bottles without additives or filtration, and immediately brought back to our laboratory for SP-ICP-MS analysis within eight hours to minimize NP transformations after collection. The other key water quality parameters were also measured for the water samples by using the

same methods as those in our recent publication [27]. Missouri River water was collected during the cold season for the simulated treatments. The collected water was allowed to settle for at least 24 hours before use to remove any non-colloidal materials.

2.4. DRINKING WATER TREATMENT SIMULATIONS

A six-gang stirrer system (Phipps & Bird, Richmond, VA) was used to simulate several major drinking water treatment steps in sequence. Lime softening, alum coagulation with PAC sorption, and disinfection were simulated with and without added CeO₂ and ZnO in Missouri River water using six gang stirrers. The river water was analyzed for Ce- and Zn-containing NPs, dissolved ions, DOC, turbidity and pH before use in jar tests and after each treatment step during the simulation. NPs (30-50 nm CeO₂ and 80-200 nm ZnO) were added to 2-L of Missouri River water at 1×10^6 particles/mL (mass concentrations of ~ 7 $\mu\text{g/L}$ ZnO and ~ 4 $\mu\text{g/L}$ CeO₂) and dispersed by stirring at 100 rpm for 1 min. Lime was dosed with 260 mg/L as Ca(OH)₂ to reach pH 11 before rapid mixing (300 rpm for 30 s), flocculation (10 min each at 58, 42, and 28 rpm), and sedimentation (0 rpm for 180 min). The clear supernatant was decanted into a clean 2-L square beaker, leaving only solids behind. Alum coagulation (60 mg/L as Al₂(SO₄)₃·14.3H₂O, Zone 4 coagulation at pH 7-8) with simultaneous PAC sorption by HDB (20 mg/L) was simulated on the softened water using the same stirring parameters as softening. After alum addition, the pH was quickly adjusted to pH 8 using trace metal grade sulfuric acid during flocculation. After settling, 1-L of the clear supernatant was transferred to a clean 2-L square beaker for disinfection. Sodium hypochlorite solution was added to obtain a residual concentration of 2 to 4 mg/L as Cl₂ (stirred at 28 rpm for

60 min). The water samples were taken before and after each treatment step, and were analyzed by SP-ICP-MS immediately after the simulation treatments were completed.

3. RESULTS AND DISCUSSION

3.1. NANOPARTICLE CHARACTERIZATION

ZnO and CeO₂ NPs used for the drinking water treatment simulations were characterized by SP-ICP-MS and SEM imaging before use. Representative SP-ICP-MS size distribution histograms and SEM images can be seen in Figure 1. In each case, the NPs were suspended in ultra-pure water and sonicated to reduce aggregation before analysis for SP-ICP-MS characterization. ZnO NPs were diluted to 70 µg/L total mass concentration and the CeO₂ NPs were diluted to 40 µg/L total mass concentration. The ZnO NPs used (80-200 nm diameter specification by the manufacturer) had irregular shapes and sizes (Figure 1b), contributing to the wide size distribution histogram obtained by SP-ICP-MS (Figure 1a). The detected particle concentration for the ZnO NPs was 2.16×10^4 particles/mL and a detected dissolved concentration of 16.4 µg/L. The CeO₂ NPs used (30-50 nm diameter specification by the manufacturer) are more regularly shaped and relatively spherical (Figure 1d) which is also reflected in the SP-ICP-MS size distribution histogram (Figure 1c), though more large sizes were observed due to aggregation. The detected particle concentration for the CeO₂ NPs was 4.83×10^4 particles/mL and the detected dissolved concentration was below the method detection limit.

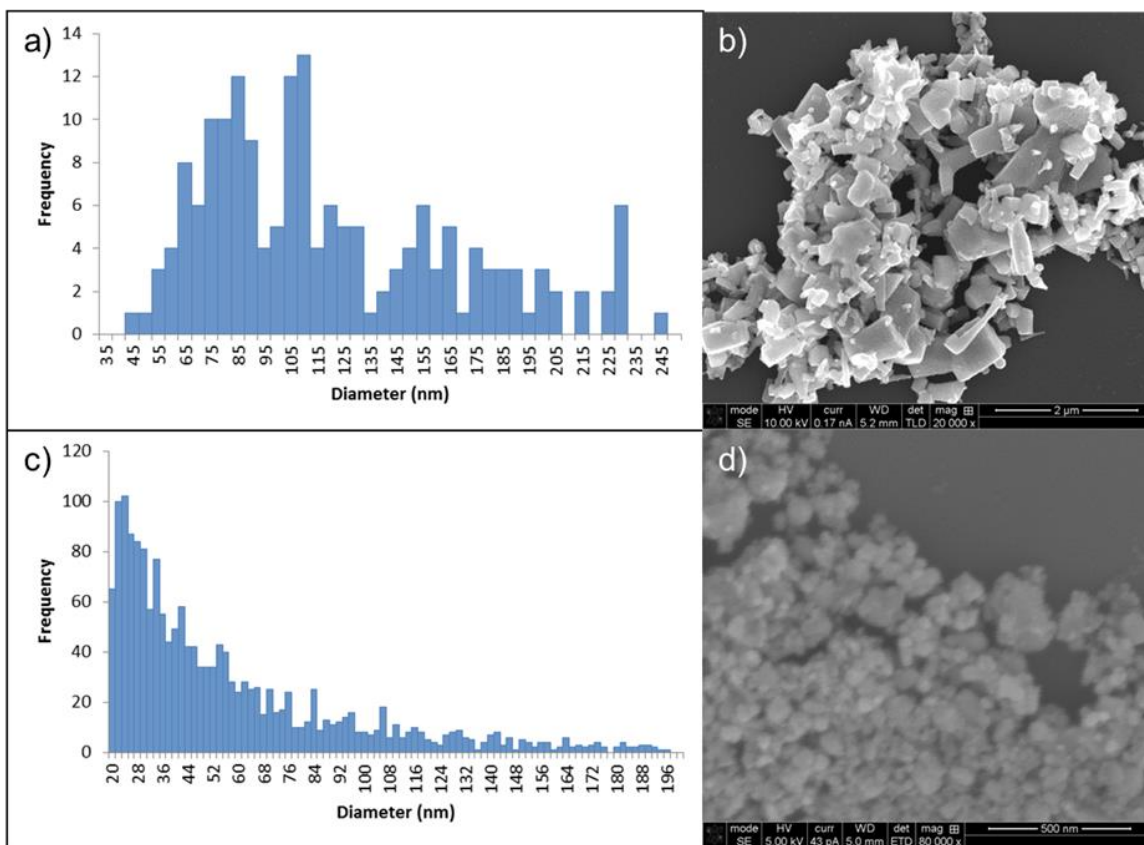


Figure 1. SP-ICP-MS and SEM characterizations of NPs. a) SP-ICP-MS size distribution histogram of ZnO with 70 $\mu\text{g/L}$ total mass concentration (56 $\mu\text{g/L}$ Zn), b) SEM image of ZnO NP, c) SP-ICP-MS size distribution histogram of CeO₂ with 40 $\mu\text{g/L}$ total mass concentration (33 $\mu\text{g/L}$ Ce), d) SEM image of CeO₂ NP.

3.2. SP-ICP-MS METHOD PERFORMANCE

Methods for ZnO and CeO₂ were developed and validated for simultaneous analysis of dissolved ion and NPs by SP-ICP-MS. The instrument was calibrated using 0.45 μm nylon-membrane-filtered matrix water over 0 to 20 $\mu\text{g/L}$ dissolved Zn and Ce using a blank subtraction when the ions were present in the matrix water. Transport efficiency, density, mass fraction, ionization efficiency, and other parameters can be seen in Table 1. The dissolved calibration curve was used to convert NP signals to diameter

based on the mass fraction and density of the material using calculations described elsewhere [24,31].

Table 1. SP-ICP-MS instrument and method parameters for ZnO and CeO₂ NP and dissolved element analysis.

Instrument Parameter	Operation Setting	
Nebulizer	Meinhard	
Spray Chamber	Cyclonic	
Sampler Cone	Platinum	
Skimmer Cone	Platinum	
RF Power (W)	1600	
Nebulizer Gas Flow (L/min)*	1.02-1.06	
Auxiliary Gas Flow (L/min)	1.2	
Plasma Gas Flow (L/min)	18	
Sample Flow Rate (mL/min)*	0.26-0.29	
RPq	0.5	
Dwell Time (ms)	0.1	
Sample Time (s)	100	
Transport Efficiency (%)*	7.5-8.5	
Method Parameters	Zn	Ce
Isotope (amu)	67	140
Density (g/cm ³)	5.61	7.13
Mass Fraction (%)	80.31	81.41
Ionization Efficiency (%)	100	100

*Parameter optimized daily.

The NP detection limits (DLs) were determined to be five times the standard deviation above the background intensity in ultrapure water when analyzed against the dissolved calibration curve in the matrix [32]. This was calculated to be 35 to 40 nm for ZnO and 18 to 20 nm for CeO₂, depending on daily instrument optimization. The ZnO DL is similar to previously reported values, but the CeO₂ DL is ~10 nm higher than previously reported values, most likely due to differences in instrument optimization and

matrix effects when calibrating in the sample matrix [32]. DLs of dissolved ion were determined to be 0.20 and 0.10 $\mu\text{g/L}$ for Zn and Ce, respectively. These detection limits were determined in ultra-pure water and validated in calibrations in the sample matrix. Dissolved DLs were higher than traditional ICP-MS due to the short dwell times used.

3.3. FATE OF ZnO AND CeO₂ NPs DURING SIMULATED DRINKING WATER TREATMENTS

Three typical drinking water treatment steps (lime softening, alum coagulation with PAC sorption, and disinfection by free chlorine) were simulated sequentially to determine the fate of ZnO and CeO₂ NPs. DOC, pH, turbidity, and NP concentration and size distribution were characterized at each treatment step to ensure the treatments were effective and to monitor NP status. The changes in pH, DOC, and turbidity after each treatment step are summarized in Table 2.

The river water used had initial DOC, pH, and turbidity of $2.38 \text{ mg/L} \pm 0.25$, 8.31 ± 0.02 , and $4.04 \text{ NTU} \pm 0.29$, respectively, after aliquoted into six samples at room temperature ($n=6$, relative standard deviation (RSD)). DOC and turbidity were on the low range for river water because they were collected during the cold season when turbidity and organic content are low. After lime softening, the pH increased to 11.35 ± 0.04 (RSD) and DOC and turbidity decreased to 16% and 61% of the original value, respectively. After alum and PAC treatment, the pH decreased to 8.23 ± 0.08 (RSD), and DOC and turbidity decreased to 51% and 93% of the original value, respectively. The pH was 8.21 ± 0.09 (RSD) after sodium hypochlorite disinfection, with no significant change from the pH before disinfection (8.23 ± 0.08 (RSD)). DOC and turbidity were unchanged after disinfection.

Table 2. Change in pH, DOC, and turbidity after each treatment step during the simulated drinking water treatment process (value±standard deviation, n=6).

Water Parameter	Missouri River Water	After NP Spike	After Lime Softening	After Alum + PAC	After Disinfection
pH	8.31±0.02	8.24±0.10	11.35±0.04	8.23±0.08	8.21±0.09
DOC (mg/L)	2.38±0.13	2.41±0.16	1.99±0.25	1.17±0.09	1.21±0.10
Turbidity (NTU)	4.04±0.29	4.12±0.33	1.59±0.34	0.29±0.21	0.16±0.06

At the pH of each step (pH between 8-12), it has been reported that dissolved Zn^{2+} and Ce^{3+} exist as ionic oxides, indicating that dissolved constituents would not result in NP signals during analysis as the pH increased [33]. If, however, these dissolved constituents would form colloidal hydroxides at high pH, the resulting colloidal materials would be formed during drinking water treatment that would be effected by the treatment process.

3.3.1. Fate of Zn-Containing NP without ZnO NP Addition. Zn-containing NPs were present in the river water initially. The real form of the Zn-containing NPs could not be determined by SP-ICP-MS. It was assumed that the NPs were present as ZnO NPs, and measured size was calculated by ZnO NPs. The most frequent ZnO NP sizes were centered on 75 nm with a wide particle size distribution arranged from DL to several hundred nanometers, as shown in Figure 2a. Dissolved Zn (or ZnO NP at size smaller than the particle sized detection limit) was also found in the river water at a concentration 1.11 $\mu\text{g/L}$. It has been demonstrated that ZnO NPs are toxic [2, 3]. If the real forms of the Zn-containing NPs are present as ZnO NPs, the health risk deserved to be evaluated if it not removed during water treatment process Therefore, their fate and removal were evaluated by simulated drinking water treatment first without the addition of the ZnO NPs Control tests were performed in parallel with the treatment tests by adding NPs but not adding treatment materials. The size distribution and concentration of the spiked ZnO NPs in the control samples did not change in the time period of the simulated treatment and until analysis. This indicated that the ZnO NPs in the selected surface water were stable during 12 hours for experiment, presumably stabilized by the water matrix. When the river water was treated by excess lime softening to pH 11, the

Zn-containing NPs exhibited a shift in size distribution to the most frequent size of 35 nm as ZnO and the particle concentration (particles/mL) was reduced by 38% (Figure 2a “After Lime Softening”). This indicated that the ZnO NPs may have been partially dissolved during the treatment, that the larger NPs were removed but smaller ZnO NPs were remained in suspension after softening, or that the formerly soluble zinc in solution transformed into insoluble colloids as the pH increased. After lime softening, the dissolved Zn concentration was reduced from $1.11 \mu\text{g/L} \pm 0.08$ (n=6, RSD) to $0.43 \mu\text{g/L} \pm 0.08$ (n=3, RSD), so dissolution or aggregation could not be confirmed by dissolved concentration and NP results. Alum coagulation with PAC sorption was performed on the softened water and resulted in a particle concentration decrease of 74% relative to the original concentration while maintaining a similar size distribution, indicating that the NPs were not physically changed during this step of treatment but were removed during this step of treatment. The dissolved Zn content was also not significantly changed during this treatment step ($0.48 \mu\text{g/L} \pm 0.02$, n=3, RSD). Minimal dissolution of ZnO was observed after disinfection by free chlorine as evidenced by the further reduction in frequency in the size distribution histogram and particle concentration reduction to 77% of the original concentration in the water (Figure 2a “After Disinfection”) and the dissolved Zn concentration ($0.52 \mu\text{g/L} \pm 0.08$, n=3, RSD). Overall, disinfection had little effect on the Zn-containing NP distribution and dissolved Zn content.

3.3.2. Fate of ZnO NPs with ZnO NP Addition. To evaluate the removal of engineered ZnO NPs during drinking water treatments, 80 to 200 nm diameter ZnO NPs were added to the river water and subjected to the same treatments previously mentioned. The change in size distribution histograms for the ZnO NPs can be seen in Figure 2b.

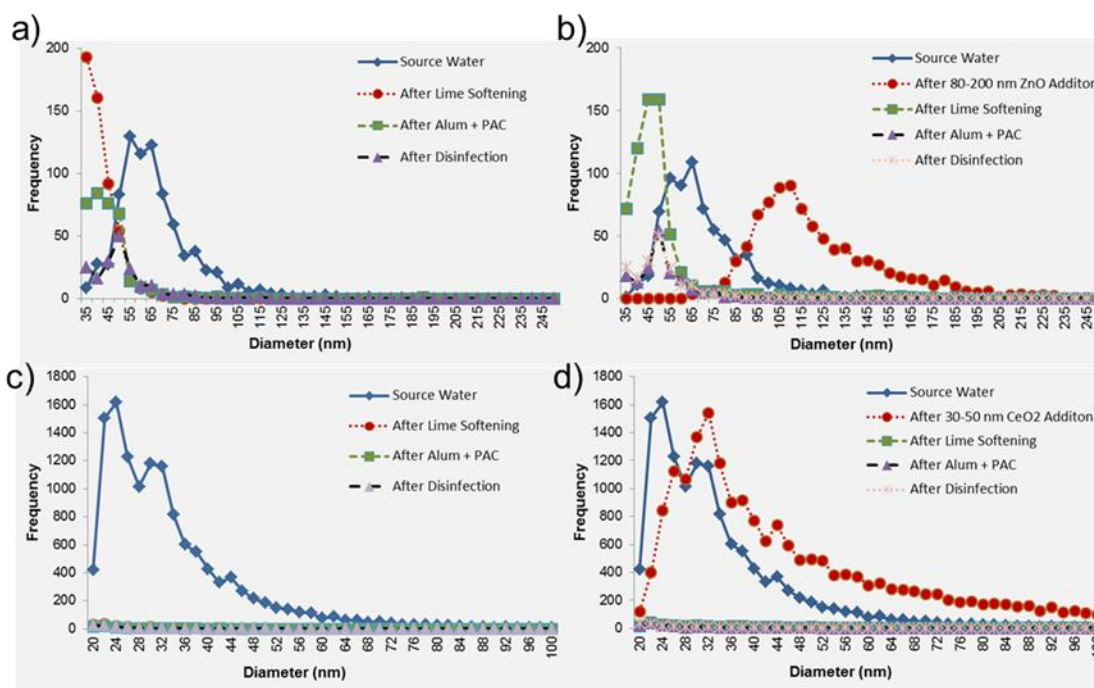


Figure 2. Change in size distribution histograms after sequential simulated drinking water treatments in Missouri River water for a) ZnO without NP addition ($n=2$), b) ZnO with 80-200 nm ZnO addition ($7 \mu\text{g/L}$ mass concentration) ($n=2$), c) CeO_2 without NP addition ($n=2$), and d) CeO_2 with 30-50 nm CeO_2 addition ($4 \mu\text{g/L}$ mass concentration) ($n=2$).

After the NPs were added, the size distribution shifted to the most frequent size of 120 nm and the dissolved Zn concentration increased from $1.11 \mu\text{g/L} \pm 0.08$ ($n=6$, RSD) to $16.45 \mu\text{g/L} \pm 0.83$ ($n=2$, relative percent difference (RPD)), indicating either the smaller (smaller than the size detection limit) ZnO NPs were detected as “dissolved” Zn, the NPs partially dissolved after addition to the water, or insoluble colloids formed from the dissolved zinc ions in solution. This result is similar to dissolved concentration when added to ultra-pure water ($16.38 \mu\text{g/L}$). The water was then treated by lime softening to pH 11, which resulted in a reduction in size distribution to around 50 nm, total particle concentration reduction by 53% and dissolved Zn to $0.36 \mu\text{g/L} \pm 0.95$ ($n=2$, RPD).

Again, the NPs may have dissolved during lime softening, but was not confirmed due to the reduction in dissolved Zn. The softened water was then treated with alum and PAC, and resulted in a further reduction in NP concentration by 79% of the original value (Figure 2b “After Alum + PAC”) and in dissolved Zn concentration of $0.46 \mu\text{g/L} \pm 6.38$ ($n=2$, RPD). No further changes were observed after disinfection. Overall, the behavior of the added engineered ZnO NPs was similar to the Zn-containing NPs in the river water.

3.3.3. Fate of Ce-Containing NP without NP Addition. Ce-containing NPs were also present in the river water collected for the removal experiments and were studied without the addition of engineered CeO₂ NPs. The actual form of the CeO₂-containing NPs could also not be determined by SP-ICP-MS. It was assumed that the NPs were present as CeO₂ NPs, and measured size was calculated as CeO₂ NPs. The water contained a size distribution histogram with a maximum at 24 nm assuming as CeO₂ with a particle size distribution arranged from DL to ~60 nm, as shown in Figure. 2c. The dissolved concentration of Ce was close or below detection limit ($0.10 \mu\text{g/L}$). The fate and removal of CeO₂ NPs during the water treatment are also important due to the toxicity of this type of NPs. For the duration of the simulation treatment experiments, the dissolved Ce levels were below the DL. After lime softening to pH 11, over 99% of the particles were removed from the water. Because the Ce-containing particle content was below the DL after lime softening, no changes were observed after alum coagulation and PAC sorption.

3.3.4. Fate of CeO₂ NP with CeO₂ NP Addition. To determine the behavior of engineered CeO₂ NPs under the same treatment conditions, 30 to 50 nm diameter CeO₂ NPs were added to the river water and subjected to the same treatments. After NP

addition, the size distribution histogram showed most frequent size at 38 nm and size distribution from detection limit to about 60 nm (Figure 2d). The dissolved Ce content was still below the DL after the NPs were added, which indicated that the NPs were not dissolving. Like the Ce-containing NPs, the CeO₂ NPs were completely (>99%) removed after lime softening. No changes were observed in the subsequent treatments. The CeO₂ results were similar to those from our previous study of TiO₂, Ag, and Au NPs removal during the simulated drinking water treatment process [27]. CeO₂, Ag, Au, and TiO₂ NPs had removal after lime softening higher than 90% without showing significant dissolution. ZnO NPs were significantly reduced after lime softening treatment (38-53%) but not completely removed. After alum coagulation and PAC sorption ZnO removal increased to 61-79% removal. Zeta potentials for similar uncoated NPs were negative in previous reports [34,35], indicating stabilization due to a negative surface charge at high pH for both NPs. Under these conditions, the cations added during lime softening may neutralize the surface charge on the NPs, causing them to settle during sedimentation. These two studies suggest that lime softening is effective in removing the selected NPs from surface water. Other studies have shown that alum coagulation can remove up to 99% of ZnO NPs [22] and up to 70% of TiO₂ and/or Ag NPs depending on treatment conditions without preceding lime softening treatment [22,23,36]. Thus, with a combination of lime softening and coagulation, it is likely that most uncoated CeO₂ NPs at low concentrations in source water of drinking water would be removed based on the results of this work.

3.4. ZnO AND CeO₂ NP OCCURRENCE IN WATER FROM THREE DRINKING WATER TREATMENT FACILITIES

Samples were taken from three large DWTFs from source water and drinking water to evaluate the occurrence of Zn- and Ce-containing NPs and their fate after full-scale drinking water treatments. DOC, pH, and turbidity measured for each water sample are presented in Table 3. The NP and dissolved ion detection results are presented in Table 4. All field blanks were below the DLs for each analyte and all dissolved element spike recoveries were between 76-123% and the reproducibility of duplicated samples was good, indicating good method performance in the collected samples. Zn-containing NPs and dissolved Zn ions were present in the source water from each facility with concentrations around 1.5×10^5 particles/mL for NPs and 5.49, 5.36, and 32.2 $\mu\text{g/L}$ Zn ions at Facilities 1, 2 and 3, respectively. Ce-containing NPs were present in source water from each facility around 5.5×10^5 particles/mL and Ce ions were present between 0.16 and 0.75 $\mu\text{g/L}$ at the three facilities. Facility 1 source water had 87 nm Zn-containing NPs (as ZnO) at $\sim 10^5$ particles/mL. After treatment, the size increased to 114 nm as ZnO, but the particle concentration decreased to $\sim 10^4$ particles/mL. It is likely that some of the particles were removed and that the remaining particles aggregated resulting in the size increase. Ce-containing NPs were in Facility 1 source water at $\sim 5 \times 10^5$ particles/mL and 30 nm as CeO₂. After treatment these particles were removed to below the DL. Facility 2 had Zn- and Ce-containing NPs in source water. Zn-containing NPs were reduced from 81 nm at $\sim 10^5$ particles/mL to 60 nm at $\sim 5 \times 10^5$ particles/mL during treatment. Ce-containing NPs were reduced from 44 nm at $\sim 5 \times 10^5$ particles/mL to 17 nm at $\sim 5 \times 10^4$ particles/mL. For this facility, it is likely that the NPs were partially dissolved during treatment. Facility 3 had Zn-containing NPs at 114 nm and $\sim 10^5$ particles/mL as ZnO and

Ce-containing NPs at 41 nm and $\sim 5 \times 10^5$ particles/mL as CeO₂. After treatment, Zn-containing NPs were reduced to 54 nm and $\sim 10^4$ particles/mL and Ce-containing NPs were reduced to below the DL. The results showed that the treatment combination in each facility was effective in removing Zn- and Ce-containing NPs from surface water using a combination of softening and ferric coagulation. While further study is needed under other conditions, these results suggest the protective nature of combined softening and ferric coagulation for general control of uncoated CeO₂ and ZnO NPs in drinking water treatment systems.

Table 3. General water quality parameters for Facilities 1-3.

Facility and Sample	DOC (mg/L)	pH	Turbidity (NTU)
Facility 1:			
Field Blank	<MDL	---	0.02
Source Water	3.93	8.57	22.90
Source Water Duplicate	4.23	8.50	22.75
Drinking Water	2.14	9.83	0.35
Drinking Water Duplicate	2.15	9.89	0.28
Facility 2:			
Field Blank	<MDL	---	0.04
Source Water	4.34	8.39	43.36
Source Water Duplicate	4.42	8.37	47.59
Drinking Water	3.17	9.20	0.02
Drinking Water Duplicate	3.28	9.32	0.02
Facility 3:			
Field Blank	<MDL	---	0.03
Source Water	4.03	8.51	43.89
Source Water Duplicate	4.56	8.43	40.53
Drinking Water	3.17	9.34	0.00
Drinking Water Duplicate	3.44	9.32	0.01

Table 4. Zn- and Ce-containing NP occurrence and dissolved Ce and Zn through drinking water treatments at three drinking water treatment facilities.

Facility and Sample	Zn			Ce		
	Most Freq. Size (nm)	Part. Conc. (pts/mL)	Diss. Conc. ($\mu\text{g/L}$)	Most Freq. Size (nm)	Part. Conc. (pts/mL)	Diss. Conc. ($\mu\text{g/L}$)
Facility 1:						
Field Blank	<MDL	<MDL	<MDL	<MDL	<MDL	<MDL
Source Water	87	1.25E+05	5.48	32	4.96E+05	0.18
Source Water Duplicate	87	1.11E+05	5.49	29	5.38E+05	0.16
Drinking Water	114	1.37E+04	<MDL	<MDL	<MDL	<MDL
Drinking Water Duplicate	114	1.76E+04	<MDL	<MDL	<MDL	<MDL
Facility 2:						
Field Blank	<MDL	<MDL	<MDL	<MDL	<MDL	<MDL
Source Water	81	1.44E+05	5.37	44	5.87E+05	0.70
Source Water Duplicate	81	1.39E+05	5.34	42	5.72E+05	0.74
Drinking Water	60	5.74E+04	1.15	17	4.95E+04	<MDL
Drinking Water Duplicate	63	8.65E+04	1.51	17	5.09E+04	<MDL
Facility 3:						
Field Blank	<MDL	<MDL	<MDL	<MDL	<MDL	<MDL
Source Water	114	1.34E+05	32.19	41	5.47E+05	0.67
Source Water Duplicate	114	1.23E+05	31.26	43	4.99E+05	0.72
Drinking Water	54	9.81E+03	0.90	<MDL	<MDL	<MDL
Drinking Water Duplicate	54	9.50E+03	0.90	<MDL	<MDL	<MDL

ACKNOWLEDGEMENTS

We acknowledge funding received from the Missouri Department of Natural Resources for this study. The NexION 300D/350D ICP-MS was provided by PerkinElmer, Inc. The authors appreciate the support from the Center for Single Nanoparticle, Single Cell, and Single Molecule Monitoring (CS³M) at Missouri

University of Science and Technology. We would also like to thank Qingbo Yang for assisting with SEM imaging.

CONFLICT OF INTEREST

The authors declare that they have no competing interests.

REFERENCES

1. Boxall A, Chaudhry Q, Sinclair C, Jones A, Aitken R, Jefferson B, et al. Current and future predicted environmental exposure to ENPs. Central Science Laboratory, Department of the Environment and Rural Affairs, London, UK 89; 2007.
2. Lin W, Xu Y, Huang CC, Ma Y, Shannon KB, Chen DR, et al. Toxicity of nano and microsized ZnO particles in human lung epithelial cells. *J Nanoparticle Res.* 2008;11(1):25–39.
3. Ma H, Williams PL, Diamond SA. Ecotoxicity of manufactured ZnO nanoparticles—a review. *Environ Pollut.* 2013;172:76–85.
4. Hussain S, AlNsour F, Rice AB, Marshburn J, Yingling B, Ji Z, et al. Cerium dioxide nanoparticles induce apoptosis and autophagy in human peripheral blood monocytes. *ACS Nano.* 2012;6(7):5820–9.
5. Gaiser BK, Fernandes TF, Jepson MA, Lead JR, Tyler CR, Baalousha M, et al. Interspecies comparisons on the uptake and toxicity of silver and cerium dioxide nanoparticles. *Environ Toxicol Chem.* 2012;31(1):144–54.
6. Lin W, Huang YW, Zhou XD, Ma Y. Toxicity of cerium oxide nanoparticles in human lung cancer cells. *Int J Toxicol.* 2006;25(6):451–7.
7. Zhang H, He X, Zhang Z, Zhang P, Li Y, Ma Y, et al. NanoCeO₂ exhibits adverse effects at environmental relevant concentrations. *Environ Sci Technol.* 2011;45(8):3725–30.

8. Xia T, Kovochich M, Long M, Mädler L, Gilbert B, Shi H, et al. Comparison of the mechanism of toxicity of zinc oxide and cerium oxide nanoparticles based on dissolution and oxidative stress properties. *ACS Nano*. 2008;2(10):2121–34.
9. Lombi E, Donner E, Tavakkoli E, Turney TW, Naidu R, Miller BW, et al. Fate of zinc oxide nanoparticles during anaerobic digestion of wastewater and posttreatment processing of sewage sludge. *Environ Sci Technol*. 2012;46(16):9089–96.
10. Ma R, Levard C, Judy JD, Unrine JM, Durenkamp M, Martin B, et al. Fate of zinc oxide and silver nanoparticles in a pilot wastewater treatment plant and in processed biosolids. *Environ Sci Technol*. 2014;48(1):104–12.
11. GomezRivera F, Field JA, Brown D, SierraAlvarez R. Fate of cerium dioxide (CeO₂) nanoparticles in municipal wastewater during activated sludge treatment. *Bioresource Technol*. 2012;108:300–4.
12. Limbach LK, Bereiter R, Müller E, Krebs R, Gälli R, Stark WJ. Removal of oxide nanoparticles in a model wastewater treatment plant— influence of agglomeration and surfactants on clearing efficiency. *Environ Sci Technol*. 2008;42(15):5828–33.
13. Brar SK, Verma M, Tyagi RD, Surampalli RY. Engineered nanoparticles in wastewater and wastewater sludge—evidence and impacts. *Waste Manag*. 2010;30(3):504–20.
14. Keller AA, Wang H, Zhou D, Lenihan HS, Cherr G, Cardinale BJ, et al. Stability and aggregation of metal oxide nanoparticles in natural aqueous matrices. *Environ Sci Technol*. 2010;44(6):1962–7.
15. Van Hoecke K, De Schamphelaere KA, Van der Meeren P, Smagghe G, Janssen CR. Aggregation and ecotoxicity of CeO nanoparticles in synthetic and natural waters with variable pH, organic matter concentration and ionic strength. *Environ Pollut*. 2011;159(4):970–6.
16. Li M, Lin D, Zhu L. Effects of water chemistry on the dissolution of ZnO nanoparticles and their toxicity to *Escherichia coli*. *Environ Pollut*. 2013;173:97–102.
17. Quik JT, Lynch I, Van Hoecke K, Miermans CJ, De Schamphelaere KA, Janssen CR, et al. Effect of natural organic matter on cerium dioxide nanoparticles settling in model fresh water. *Chemosphere*. 2010;81(6):711–5.
18. Volk C, Wood L, Johnson B, Robinson J, Zhu HW, Kaplan L. Monitoring dissolved organic carbon in surface and drinking waters. *J Environ Monit*. 2002;4(1):43–7.

19. Hassan AA, Li Z, SahleDemessie E, Sorial GA. Computational fluid dynamics simulation of transport and retention of nanoparticle in saturated sand filters. *J Hazardous Mater.* 2013;244(245):251–8.
20. Li Z, Aly Hassan A, SahleDemessie E, Sorial GA. Transport of nanoparticles with dispersant through biofilm coated drinking water sand filters. *Water Res.* 2013;47(17):6457–66.
21. Li Z, SahleDemessie E, Hassan AA, Sorial GA. Transport and deposition of CeO nanoparticles in watersaturated porous media. *Water Res.* 2011;45(15):4409–18.
22. Chalew TEA, Ajmani GS, Huang H, Schwab KJ. Evaluating nanoparticle breakthrough during drinking water treatment. *Environ Health Perspect.* 2013;121(10):1161–6.
23. Zhang Y, Chen Y, Westerhoff P, Hristovski K, Crittenden JC. Stability of commercial metal oxide nanoparticles in water. *Water Res.* 2008;42(8):2204–12.
24. Dan Y, Shi H, Stephan C, Liang X. Rapid analysis of titanium dioxide nanoparticles in sunscreens using single particle inductively coupled plasmamass spectrometry. *Microchem J.* 2015;122:119–26.
25. Dan Y, Zhang W, Xue R, Ma X, Stephan C, Shi H. Characterization of gold nanoparticles uptake by tomato plants using enzymatic extraction followed by single particle inductively coupled plasmamass spectrometry. *Environ Sci Technol.* 2015. doi: 10.1021/es506179e .
26. Mitrano DM, Ranville JF, Bednar A, Kazor K, Hering AS, Higgins CP. Tracking dissolution of silver nanoparticles at environmentally 2 relevant concentrations in laboratory, natural, and processed waters using single particle ICPMS (spICPMS). *Environ Sci Nano.* 2014;1(3):248–59.
27. Donovan AR, Adams CD, Ma Y, Stephan C, Eichholz T, Shi H. Single particle ICP-MS characterization of titanium dioxide, silver, and gold nanoparticles during drinking water treatment. *Chemosphere.* 2015;144:148–53.
28. Hadioui M, Merdzan V, Wilkinson KJ. Detection and characterization of ZnO nanoparticles in surface and waste waters using single particle ICPMS. *Environ Sci Technol.* 2015;49(10):6141–8.
29. Hadioui M, Peyrot C, Wilkinson KJ. Improvements to single particle ICPMS by the online coupling of ion exchange resins. *Anal Chem.* 2014;86(10):4668–74.

30. Montaña MD, Badiei HR, Bazargan S, Ranville JF. Improvements in the detection and characterization of engineered nanoparticles using spICPMS with microsecond dwell times. *Environ Sci Nano*. 2014;1(4):338.
31. Degueldre C, Favarger PY. Colloid analysis by single particle inductively coupled plasmamass spectroscopy: a feasibility study. *Colloid Surf A Physicochem Eng Aspect*. 2003;217(1/3):137–42.
32. Lee S, Bi X, Reed RB, Ranville JF, Herckes P, Westerhoff P. Nanoparticle size detection limits by single particle ICPMS for 40 elements. *Environ Sci Technol*. 2014;48(17):10291–300.
33. Takeno N. Atlas of EhpH diagrams. Geological survey of Japan open file report. 2005;419:102.
34. Degen A, Kosec M. Effect of pH and impurities on the surface charge of zinc oxide in aqueous solution. *J Eur Ceramic Soc*. 2000;20:667–73.
35. Berg JM, Romoser A, Banerjee N, Zebda R, Sayes CM. The relationship between pH and zeta potential of ~30 nm metal oxide nanoparticle suspensions relevant to in vitro toxicological evaluations. *Nanotoxicology*. 2009;3(4):276–83.
36. Wang H, Qi J, Keller AA, Zhu M, Li F. Effects of pH, ionic strength, and humic acid on the removal of TiO nanoparticles from aqueous phase by coagulation. *Colloid Surf A Physicochem Eng Aspect*. 2014;450:161– 5.

II. FATE OF NANOPARTICLES DURING ALUM AND FERRIC COAGULATION MONITORED USING SINGLE PARTICLE ICP-MS

Ariel R. Donovan¹, Craig D. Adams^{2,3}, Yinfu Ma^{1,2}, Chady Stephan⁴, Todd Eichholz⁵,
Honglan Shi^{1,2*}

¹Department of Chemistry and Environmental Research Center, Missouri University of Science and Technology, Rolla, Missouri, 65409, United States

²Center for Single Nanoparticle, Single Cell, and Single Molecule Monitoring (CS³M), Rolla, Missouri, 65409, United States

³Department of Civil Engineering, Saint Louis University, St. Louis, Missouri, 63103, United States

⁴PerkinElmer, Inc., 501 Rowntree Dairy Rd, Woodbridge, On, Canada, L4L 8H1

⁵Missouri Department of Natural Resources, Jefferson City, MO 65102, United States

*Corresponding Author

Address: Department of Chemistry

Missouri University of Science and Technology

400 West 11th Street

Rolla, MO 65409

Phone: 573-341-4433; Fax: 573-341-6033

E-mail: honglan@mst.edu

ABSTRACT

In this study, aluminum sulfate, ferric sulfate, ferric chloride, and poly(diallyldimethylammonium chloride) (pDADMAC) coagulation removal of citrate-stabilized silver and gold nanoparticles (NPs) and uncoated titanium dioxide, cerium dioxide, and zinc oxide NPs was investigated using a single particle (SP) ICP-MS direct monitoring technique. Zone 2 (charge neutralization) coagulation was performed in river water and more commonly used Zone 4 (sweep floc) coagulation was performed in both river and lake water with environmentally relevant concentrations of selected NPs added. SP-ICP-MS was used to detect NP and dissolved species, characterize the size distribution, and quantify particle concentration as well as dissolved species before and after treatments. Other parameters including pH, dissolved organic carbon, turbidity, and UV_{254} absorbance were monitored to characterize treatment efficiency. Charge neutralization (Zone 2) coagulation resulted in 48-85% removal of citrate-stabilized NPs and 90-99% removal of uncoated NPs from river water. Sweep floc (Zone 4) coagulation in river water resulted in 36-94% removal of citrate-stabilized NPs and 91-99% removal of uncoated NPs both with and without polymer addition. Zone 4 coagulation conditions in lake water resulted in 77-98% removal of citrate-stabilized NPs and 59-96% removal of uncoated NPs without polymer. These results indicate that NP removal depends on NP surface and stability, the nature of the source water, and the coagulant type and approach.

KEY WORDS

Water treatment by coagulation; single particle-ICP-MS; nanoparticle fate during water treatment; zinc oxide; cerium dioxide; silver nanoparticle.

1. INTRODUCTION

The manufacturing and applications of metal and metal-oxide nanoparticles (NPs) is increasing each year, resulting in higher concentrations of NPs entering the environment. Sources of NP environmental release includes leaching from outdoor facades (Kaegi et al., 2010) and wastewater discharges (Benn and Westerhoff, 2008; Brar et al., 2010; Heithmar and Pergantis, 2010; Kaegi et al., 2011; Kiser et al., 2009; Lee et al., 2008; Limbach et al., 2008; Westerhoff et al., 2011; Windler et al., 2012) among other sources (Mueller and Nowack, 2008; Sharifi et al., 2012; Yu et al., 2013) with predicted environmental concentrations on the ng/L to $\mu\text{g/L}$ level (Mueller and Nowack, 2008). While some NPs may be removed from water bodies through sedimentation, sorption, uptake, or dissolution, stabilized NPs may remain in suspension and result in potential health risks for human, animal, plant, and aquatic life (Nowack et al., 2012; Yu et al., 2013). It is imperative from a public health perspective to understand the behavior and removal of NPs during typical drinking water treatments to assess the potential for human exposure through potable water. Unfortunately, the fate of NPs through conventional drinking water treatment processes is not well understood, as limited studies have been conducted on the subject. This work has been hindered by the lack of sensitive

analytical methods to detect NPs directly in environmental matrices and has resulted in insufficient knowledge on NP occurrence in source and drinking waters.

Coagulation, flocculation and sedimentation is a predominant method used to remove colloidal material during drinking water treatment (Kim et al., 2001). Varying dosages of alum in tap water and buffered nanopure water have been shown to remove between 20-60% of TiO₂, ZnO, Fe₂O₃, NiO, and silica NPs (Zhang et al., 2008). In another study, alum coagulation resulted in Ag, TiO₂, and ZnO removal from 2-20%, 3-8%, and 48-99%, respectively, in a variety of surface, ground, and synthetic waters (Chalew et al., 2013). TiO₂ removal was evaluated by polyferric sulfate (PFS), ferric chloride (FeCl₃), polyaluminum chloride (PACl), and alum (Al₂(SO₄)₃), resulting in higher removal efficiency by ferric based coagulants (Wang et al., 2013). PFS and FeCl₃ were evaluated for TiO₂ removal under a variety of conditions, resulting in up to 90% removal under optimized conditions (Wang et al., 2014). However, each of these methods used indirect techniques for monitoring NP behavior such as digestion and inductively coupled plasma-mass spectrometry (ICP-MS) analysis, graphic furnace atomic absorption (GFAA), or turbidity measurements. These methods provide information regarding the mass content remaining after treatment, but the size, aggregation, and particle concentrations of the NPs could not be and were not determined.

Single particle (SP)-ICP-MS is an emerging and powerful technique for NP analysis due to its ability to characterize NPs directly in aqueous and environmental samples including simultaneous determination of particle size, size distribution, particle concentration, and dissolved ion concentration (Cascio et al., 2015; Dan et al., 2015; Laborda et al., 2014; Loeschner et al., 2013; Peters et al., 2015). The theory of SP-ICP-

MS has been described in detail elsewhere and, as such, will not be discussed here (Degueldre and Favarger, 2003; Degueldre and Favarger, 2004; Degueldre et al., 2004; Degueldre et al., 2006a; Degueldre et al., 2006b; Laborda et al., 2013; Montaña et al., 2014). In two recent studies, Au, Ag, TiO₂, CeO₂ and ZnO NPs were characterized during a simulated drinking water treatment and in source and drinking water from three drinking water treatment facilities using SP-ICP-MS technology (Donovan et al., 2015a; Donovan et al., 2016). Full treatment processes including lime softening (for Ca and Mg removal), alum coagulation (Zone 4) with powdered activated carbon sorption, and free chlorine disinfection were simulated. However, there is a need to evaluate the efficacy of both alum and ferric primary coagulants and polymer coagulation aids to understand how NPs behave under most coagulation conditions.

In this study, alum, ferric, and polymer-based coagulation processes were simulated in river and lake water spiked with Ag, Au, TiO₂, ZnO, and CeO₂ NPs to test the hypothesis that engineered NPs can be effectively removed by traditional treatments. By using our recently developed SP-ICP-MS methodologies, the fate and transportation of the selected NPs under both charge neutralization (Zone 2) and sweep floc (Zone 4) coagulation processes were examined in river water and lake water (Zone 4 only) using the three coagulants: alum (Al₂(SO₄)₃), ferric sulfate (Fe₂(SO₄)₃), and ferric chloride (FeCl₃). NP removal was also evaluated with and without simultaneous polymer addition under each condition using typical polymer dosages.

2. MATERIALS AND METHODS

2.1. MATERIALS

Citrate-stabilized Ag (diameters of 40, 70, and 100 nm) and Au NPs (diameters of 50, 80, and 100 nm) suspensions in 2 mM sodium citrate were obtained from nanoComposix, Inc. (San Diego, CA, USA). Uncoated TiO₂ (100 nm), CeO₂ (30-50 nm), and ZnO NPs (80-200 nm) were purchased from US Research Nanomaterials, Inc. (Houston, TX, USA). All NPs were characterized by transmission electron microscopy (TEM) and SP-ICP-MS (suspended in ultra-pure water) in our laboratory to confirm the manufacturer-reported size distribution. Dissolved Au, Ti, Ce, and Zn standards (PerkinElmer, Shelton, CT, USA) and dissolved Au standard (High-Purity Standards, Charleston, SC, USA) were used for dissolved element calibrations and NP size calibrations for Ti, Ce, and Zn NPs. Nitric acid (HNO₃, trace metal grade), aluminum sulfate (Al₂(SO₄)₃·18H₂O, alum), ferric chloride (FeCl₃·6H₂O), and ferric sulfate (Fe₂(SO₄)₃·4H₂O) were purchased from Thermo Fisher Scientific, Inc. (Pittsburgh, PA, USA). Clarifloc C-338 (poly (diallyldimethylammonium chloride) or pDADMAC) polymer was acquired from Polydyne (Riceboro, GA, USA). A Simplicity185 water purification system from Millipore (Billerica, MA, USA) was used to generate ultra-pure water (18.2 MΩ·cm).

2.2. NATURAL WATERS

Missouri River water (at Jefferson City, MO, USA) and Schuman Lake water (at Rolla, MO, USA) were collected in 20 L polypropylene bottles pre-cleaned with 3%

HNO₃ and ultra-pure water. The jugs were rinsed with river or lake water three times before sample collection. Samples were stored refrigerated and unfiltered in collection bottles until use (typically one to two days). The river water samples settled at least 24 hours prior to use.

2.3. INSTRUMENTATION

A NexION 300/350D ICP-MS and Syngistix Nano Application software were used for SP-ICP-MS analysis (PerkinElmer, Shelton, CT, USA). Dissolved organic carbon (DOC) was measured using a TOC-L analyzer with ASI-L liquid autosampler from Shimadzu Scientific Instruments (Columbia, MD, USA). A Hach 2100P portable turbidimeter (Loveland, CO, USA) was used to monitor turbidity in samples. UV₂₅₄ absorbance was analyzed by a Cary 50 Conc Scanning UV/Vis Spectrophotometer from Agilent (Santa Clara, CA, USA). A FEI (Hillsboro, OR, USA) Tecnai F20 scanning transmission electron microscope (STEM) with energy-dispersive X-ray spectroscopy (EDS) capability was used to image and confirm elemental composition of NPs. The zeta potentials of all NPs used were measured using a Zetasizer Nano --ZS90 (Malvern Instruments, Inc., Southborough, MA, USA). For zeta potential detection, NPs were suspended in 0.01 M and 0.10 M NaNO₃ and allowed to equilibrate for 24 hours before analysis. Ag and Au NPs were analyzed at 1 mg/L, TiO₂ and CeO₂ NPs were analyzed at 10 mg/L, and ZnO NPs were analyzed at 50 mg/L.

2.4. SP-ICP-MS ANALYSIS

The ICP-MS instrument and method were same as previously reported (Donovan et al., 2015b; Donovan et al., 2016). In SP-ICP-MS procedures, samples are not acidified, rather they are analyzed directly using a short dwell time (100 μ s in this study). When a single NP enters the plasma, a packet of ions is generated. The ion packet reaches the mass detector and creates a pulse signal that is correlated to the total mass per particle, and subsequently correlated to the particle size. For this study, a low abundance isotope, ^{47}Ti (7% abundance), was selected as the isotope for Ti detection to avoid interference from ^{48}Ca for ^{48}Ti (74% abundance). Au and Ag NP size calibrations were generated by analyzing three particle sizes for each element. Due to aggregation and wide size distributions in standard suspensions of TiO_2 , CeO_2 , and ZnO NPs, it was not suitable to use these NP standards directly to calibrate for size calibration of these NPs. Therefore, dissolved element calibrations were converted to particle size by the Syngistix software for TiO_2 , CeO_2 , and ZnO (Laborda et al., 2013). Dissolved calibration standards were prepared in 0.45- μ m nylon membrane filtered matrix water with background subtractions for elements present in the matrix water. Transport efficiency and sample flow rate were determined daily before each experiment. Sample flow rate was measured gravimetrically by quantifying the mass of sample uptake after three minutes (Liu et al., 2017). Transport efficiency was determined using the particle frequency method (Pace et al., 2011; Montañó et al., 2016). Dissolved ions of the metal elements were also measured simultaneously by the SP-ICP-MS methods. The calibrations were performed by adding different concentrations of the corresponding metal ion standards into matrix water. It is important to note that in SP-ICP-MS method, the particles smaller than the particle size

detection limits in water samplers was counted as dissolved elements because they do not meet the ratio cut-off to be counted as particles, thus, the signal is attributed to the dissolved fraction. Any dissolved detection using this technique will include particles that are smaller than the particle size detection limit as well as dissolved species.

2.5. JAR TEST PROCEDURE

Jar tests were conducted using six-gang stirrers with 2-L water samples in acid prewashed square beakers (Phipps and Bird, Richmond, VA, USA). 70 nm Au (5 µg/L as Au), 80 nm Ag (2 µg/L as Ag), 100 nm TiO₂ (6 µg/L as Ti), 30-50 nm CeO₂ (5 µg/L as Ce), and 80-200 nm ZnO (6 µg/L as Zn) NPs each with particle concentrations ~10⁶ particles/mL (on the upper limit of expected environmental particle concentrations (Boxall et al., 2007), possibly at the source of release) were added to designated beakers and stirred at 100 rpm for 1 minute. After mixing, samples were taken from each beaker for NP, DOC, UV₂₅₄, turbidity, and pH analysis. Pre-determined amounts of alum, ferric chloride, or ferric sulfate were added to designated beakers, stirred at 300 rpm for 30 seconds (rapid mix) followed by 58, 42, and 28 rpm for 10 minutes each (flocculation) and finally allowed to settle at 0 rpm for 3 hours (sedimentation). After settling, supernatant samples were taken for NP, DOC, UV₂₅₄, turbidity, and pH analysis. Duplicate beakers were included in all experiments to determine the reproducibility of the procedure. Jar tests have proven to be a valuable tool in determining coagulant and other chemical dosages in drinking water and are a staple in most drinking water treatment facilities that use coagulants. Standard methods, chemical dosages, stirring calculations, and detention times for each step are well-defined and were selected on the basis of

simulating typical drinking water treatment conditions (Crittenden et al., 2012). NP removal efficiency was calculated for each analysis using total particle concentration (by number) compared with those of no coagulant addition.

3. RESULTS AND DISCUSSION

3.1. SP-ICP-MS ANALYSIS

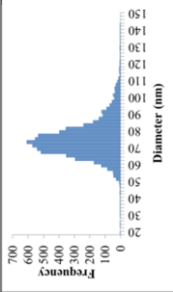
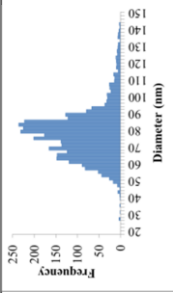
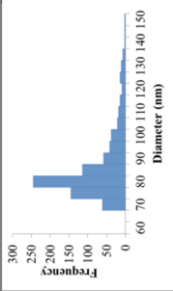
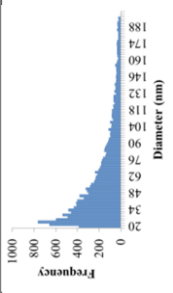
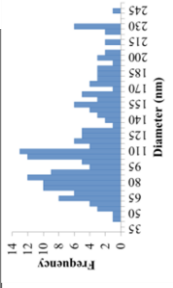
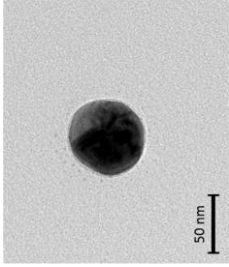
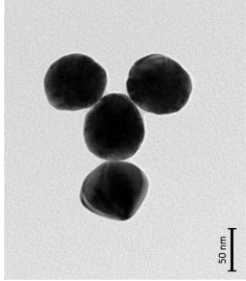
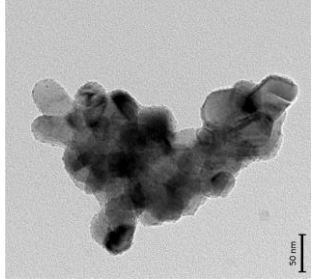
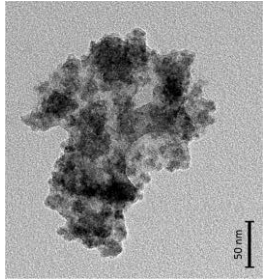
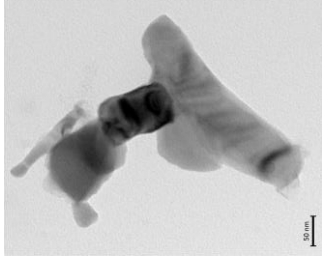
Sample flow rate and transport efficiency were determined daily and the values were approximately 0.30 mL/min and 8-10%, respectively. Methods were validated for NPs and dissolved species by calibrating and spiking in river water for Ag, Au, Ti, Ce, and Zn as NPs and dissolved elements. All spike recoveries were between 70-130% for dissolved elements and Ag and Au NP spikes. Au and Ag NPs were assumed to be 100% of the respective element. Ti-, Ce-, and Zn-containing NPs were analyzed as if their formulae were TiO_2 , CeO_2 , and ZnO , respectively, because of their numerous applications and natural occurrence (Anselmann, 2001; Klaine et al., 2008). Dissolved element detection limits (DLs) were determined by analyzing progressively lower concentrations of spikes with the lowest spike that maintained regression linearity ($R^2 > 0.99$) as the DL. NP size DLs were determined to be 5 times the standard deviation (5σ) of a sample of ultra-pure water analyzed for each element as the same way previously used (Donovan et al, 2016a, 2016b). A more stringent criterion was selected for detection limit detection to ensure all signals in blank water samples were excluded. Dissolved element DLs were 0.10 $\mu\text{g/L}$ for Ag, Au, and Ce, 0.20 $\mu\text{g/L}$ for Zn, and 0.55 $\mu\text{g/L}$ for Ti. NP size DLs were 25 nm, 30 nm, 70 nm, 23 nm, and 44 nm for Ag, Au, TiO_2 , CeO_2 , and

ZnO, respectively. Detection limits were higher for dissolved Ti and TiO₂ compared to the other elements and NPs because of the low abundance isotope used for analysis. It is important to note that particles smaller than the particle size detection limits were counted as dissolved element because they do not meet the ratio cut-off to be counted as particles. Thus, the signal is attributed to the dissolved species fraction. Any dissolved detection using this technique includes particles that are smaller than the particle size detection limit as well as dissolved species.

3.2. NANOPARTICLE CHARACTERIZATION

All NPs used for jar test experiments were analyzed by the SP-ICP-MS methods and TEM. NPs were suspended in ultra-pure water and directly analyzed by SP-ICP-MS. NP stock solutions were diluted to 10 mg/L (20 mg/L for ZnO NPs) and sonicated for 10 minutes before plating on copper grids for TEM imaging. The zeta potentials of the selected NPs were measured over pH 3-11 to determine the zero point of charge (ZPC). SP-ICP-MS size distribution histograms, TEM images, ZPC, and statistical variation among replicate samples analyzed by SP-ICP-MS during the jar tests are shown in Table 1. Ag and Au NPs were very well defined, spherical particles that exhibited minimal aggregation in both SP-ICP-MS analysis and TEM images. The metal oxides experienced aggregation that was obvious in both SP-ICP-MS (right tailing size distribution histograms) and in the TEM images.

Table 1. SP-ICP-MS size distribution histograms, TEM images, ZPC (point of zero charge), and SP-ICP-MS statistical variation for the five selected NPs.

NP Parameter	70 nm Ag	80 nm Au	100 nm TiO ₂	30-50 nm CeO ₂	80-200 nm ZnO
SP-ICP-MS Size Distribution Histogram					
SP-ICP-MS Mean NP Size Variation (% n=3)	5.7	7.2	3.8	7.1	8.7
TEM Image (50 nm scale)					
ZPC (pH)	2.3	3.1	3.8	3.0	9.2

3.3. NANOPARTICLE FATE AND REMOVAL BY CHARGE NEUTRALIZATION (ZONE 2) COAGULATION

Zone 2 coagulation requires that a stoichiometric number of cations (typically Al^{3+} or Fe^{3+}) are added to neutralize negative surface charges on colloidal and suspended particles. Once the surface charges are neutralized, the particles will aggregate and settle out of the water. The major benefits of Zone 2 coagulation are reduced sludge residuals after treatment and lower required dosages of coagulant. For this type of process, removal is related to solubility of coagulant, charge density on original particles, and surface area of original particles (Dentel, 1988). Even though there are savings when using this technique, few drinking water treatment facilities use Zone 2 coagulation due to variation in source water quality, particularly for facilities using surface water prone to turbidity fluctuations (requiring frequent jar tests to determine proper coagulant dosing). As charge neutralization coagulation is a treatment option sometimes used, and a fundamental coagulation mechanism, it is imperative to understand how NPs behave under this type of treatment. Specifically, if NPs are imparted with a negative surface charge (i.e., citrate-stabilized) or if they naturally have a negative surface charge in water, Zone 2 coagulation may result in higher removal efficiencies than other types of coagulation.

For the Zone 2 coagulation jar tests, the correct coagulant dosage was found by adding a series of dosages of alum (0, 1, 2, 4, 6, 9, and 15 mg/L) to seven 2-L square beakers filled with Missouri River water spiked with five types of NPs. It was important to find the correct dosage in water with NPs added because their surface charges add to the stoichiometric ratio of negative charges in the water, particularly the citrate-stabilized Ag and Au NPs. The optimal Zone 2 dosage was determined by evaluating turbidity among all dosages after 3 hours of sedimentation. Initial water parameters were pH of

7.89, turbidity of 30.6 NTU, UV_{254} absorbance of 0.110, and DOC of 4.57 mg/L. Based on the initial water pH, Zone 4 coagulation (sweep floc and adsorption) was expected to occur above 8 mg/L as $Al_2(SO_4)_3 \cdot 18H_2O$. All four Zones of coagulation were observed: Zone 1 (too little coagulant added) at dosages less than 4 mg/L as $Al_2(SO_4)_3 \cdot 18H_2O$; Zone 2 (charge neutralization) at 4 mg/L as $Al_2(SO_4)_3 \cdot 18H_2O$; Zone 3 (NPs stabilized by coagulant) at 6 mg/L as $Al_2(SO_4)_3 \cdot 18H_2O$; and Zone 4 (sweep floc) above 9 mg/L as $Al_2(SO_4)_3 \cdot 18H_2O$. The Zone 2 dosage was converted from $Al_2(SO_4)_3 \cdot 18H_2O$ to $FeCl_3 \cdot 6H_2O$ and $Fe_2(SO_4)_3 \cdot 4H_2O$ based on cation stoichiometry (first converted from $Al_2(SO_4)_3 \cdot 18H_2O$ to Al^{3+} , to Fe^{3+} , then to each ferric coagulant) and eight more 2-L beakers with Missouri River water spiked with NPs were dosed with and without added polymer and a beaker was treated with polymer alone. This process was duplicated in lake water, but Zone 2 was not observed.

NP concentrations and sizes were monitored before and after each treatment. Size distribution histograms are shown in Figure 1. Ag and Au NPs were not present in the river water and their size distribution histograms were similar before treatment and after the treatment process when no coagulants were added. Ti, Ce, and Zn containing NPs (treated as TiO_2 , CeO_2 and ZnO NPs in this study) were detected in the river water, and their size distribution histograms were shifted from the standard size, similar with those in the previous study (Donovan et al, 2016a, 2016b). Size distribution histograms for NPs present in the collected river water are shown in SI 1 of the Supplementary Information. There was little change for TiO_2 , and CeO_2 NPs size distribution histograms between before and after the treatment process when no coagulants were added. Slight decrease of ZnO NPs was observed after the treatment when no coagulant was added, may be due to

the well-known solubility of ZnO in water (David et al., 2012). However, this decrease was less than 5% of the original total particle concentration, as shown in Figure 2. Two removal trends were observed: citrate-stabilized Ag and Au NP removal increased with polymer addition (Figure 2a) and TiO₂, CeO₂, and ZnO NP removal was relatively constant over the various Zone 2 coagulation treatments (Figure 2b). Each NP removal trend was compared to turbidity removal after each treatment. For citrate-stabilized Ag and Au NPs, removal was between 48-58% when using Zone 2 alum and ferric chloride.

Removal increased to 75-79% when 2 mg/L pDADMAC polymer was added simultaneously with coagulant, visible in the size distribution changes in Figure 1. However, ferric chloride was slightly less efficient than alum. Ferric sulfate resulted in higher removal for these two NPs with and without polymer added (71-76% removal without polymer and 81-84% removal with polymer). When only polymer was added (2 mg/L) 74-77% of Ag and Au NPs were removed. Turbidity removal followed Ag and Au NP removal trends. For uncoated TiO₂, CeO₂, and ZnO NPs, 89-99% removal was observed using each type of coagulant with and without polymer and by polymer alone. Removal of these NPs was typically higher than overall turbidity removal. The control sample had NPs spiked and was stirred by the same program as the rest of the samples, but did not have coagulant added. Minimal settling occurred in the control sample and pH, UV₂₅₄ absorbance, and DOC were unchanged. It is likely that significant settling did not occur as that in ultra-pure water due to the DOC present in the surface water. It has been shown that DOC can significantly stabilize oxide NPs in suspension (Keller et al., 2010; Quik et al., 2010; Van Hoecke et al., 2011).

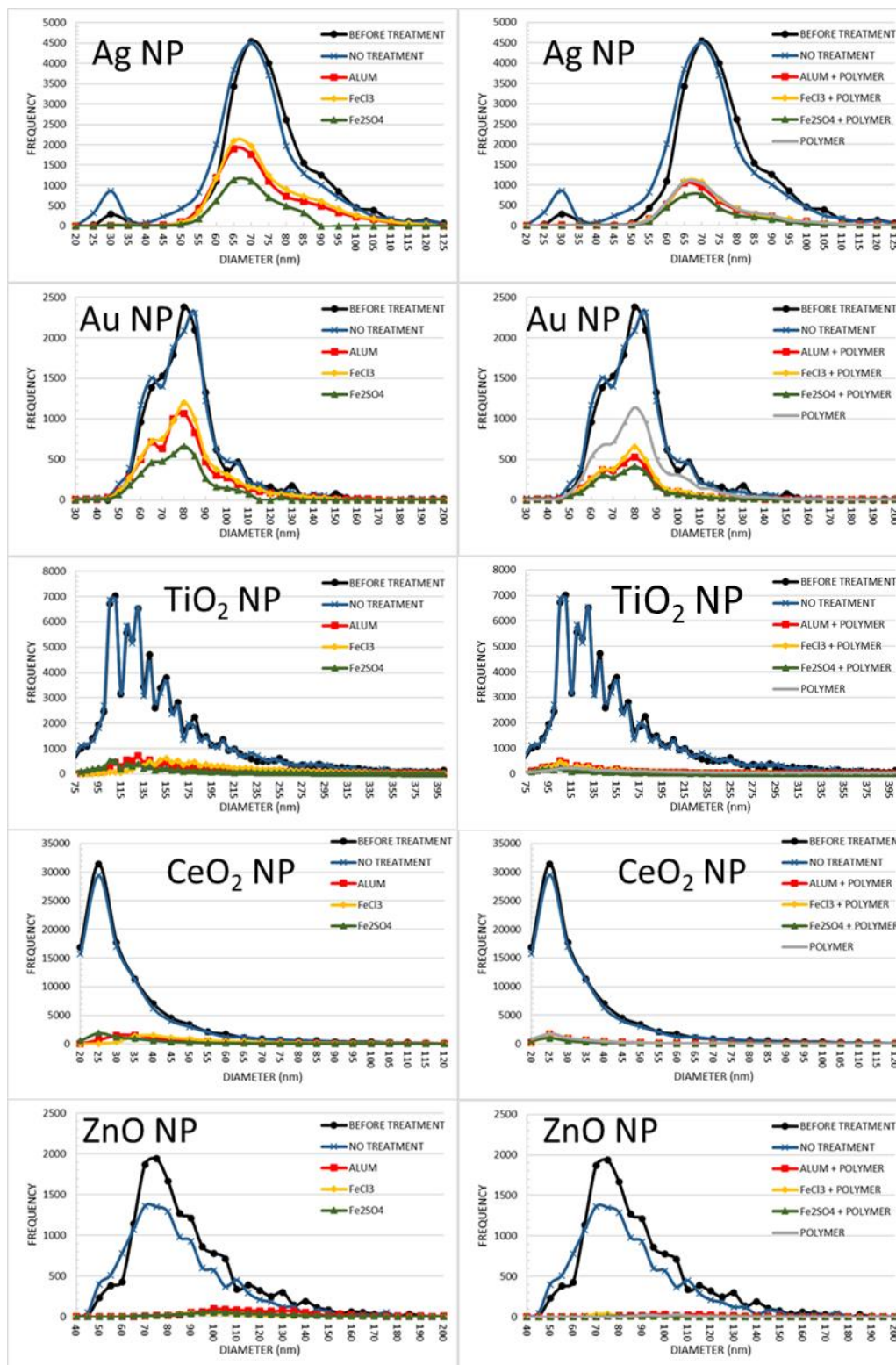


Figure 1. Size distribution histograms for all studied NPs after Zone 2 (charge neutralization) treatment in river water.

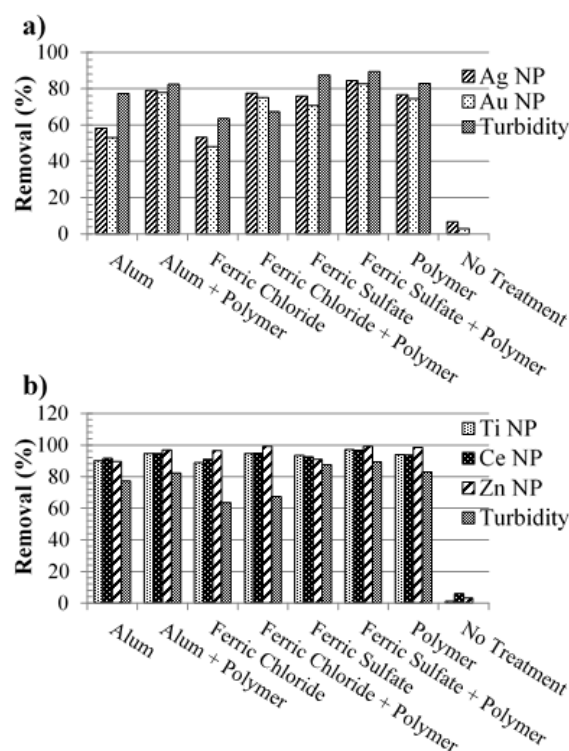


Figure 2. a) Ag NP, Au NP, and turbidity removal and b) TiO₂, CeO₂, ZnO NP and turbidity removal after various Zone 2 coagulation and polymer treatments in river water.

As previously mentioned, dissolved ion concentrations were also monitored before and after treatment by the SP-ICP-MS methods. Dissolved Ag, Au, and Ce were below the DLs before and after NP addition and after treatment. Initial dissolved Ti and Zn were present in the river water at 25.9 and 2.51 $\mu\text{g/L}$, respectively. After NP addition, the dissolved Ti concentration remained the same, but the dissolved Zn concentration increased to 10.5 $\mu\text{g/L}$ most likely due to NP dissolution and particles present in the standard that were below the NP size detection limit. Decreasing was observed in the size distribution histogram for ZnO NPs in the no treatment control sample (Figure 1). Removal of dissolved Ti and Zn after Zone 2 coagulation treatments is depicted in Figure 3. Dissolved Ti removal was between 53-92% for all of the samples. Higher removal was

observed when a coagulant was added with polymer. Dissolved Zn removal ranged from -20-40% after treatment. Addition of alum or polymer alone treatment ended with higher dissolved Zn concentrations than before treatment. This most likely meant that the particles dissolved during the treatment into Zn ions or ZnO NPs smaller than the size DL.

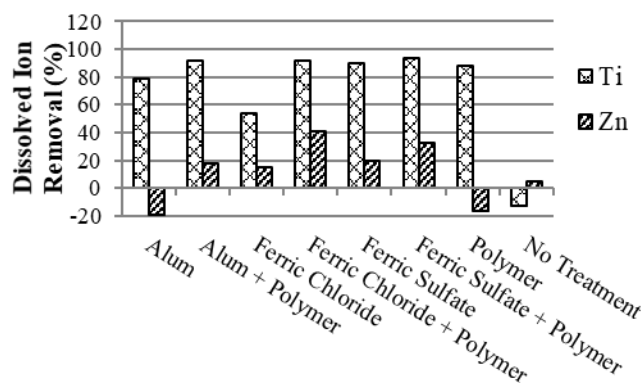


Figure 3. Dissolved Ti and Zn removal during Zone 2 coagulation experiments in river water.

Because dissolved ion concentrations were less than or approximately equal to the dissolved concentrations before treatment, it was probable that the NPs were not undergoing any physical changes during Zone 2 coagulation with and without polymer and by polymer alone. This is an important discovery because certain ions such as dissolved Ag have been shown to be more toxic than Ag NPs (Beer et al., 2012; Kittler et al., 2010; Yang et al., 2012). These results indicated that engineered NPs were removed by Zone 2 coagulation using a variety of coagulants without significant dissolution, except for ZnO NPs, and generally resulted in lower concentrations of dissolved ions and NPs. Uncoated NPs (TiO₂, CeO₂, and ZnO) were removed with higher efficiencies This may be explained due to the difference in surface charges of the NPs. Ag and Au had

many more negative surface charges due to the citrate coating while the TiO₂, CeO₂, and ZnO had no surface coating and, presumably, fewer surface charges, as reflected by ZPC measurements, making charge neutralization an easier process for the uncoated NPs.

3.4. NANOPARTICLE FATE AND REMOVAL BY SWEEP FLOC (ZONE 4) COAGULATION

Zone 4 coagulation, or sweep floc, is the process of generating insoluble precipitate by exceeding the solubility product of a coagulant (i.e., Al or Fe). The precipitate that results is a larger floc that can “sweep up” other particulate matter in the water as it settles.

Because the key water parameters that dictate coagulant solubility are pH and temperature, Zone 4 is easily implemented and robust, and thus used by many drinking water treatment facilities (Crittenden et al., 2012). Coagulant dosages for jar test experiments were determined based on typical operating ranges for alum and ferric coagulants as previously recorded (Amirtharajah and Mills, 1982). Because the river water was collected on a different date than the water used in the Zone 2 experiments, water parameters were different. For river water, initial pH was 7.30, turbidity was 113 NTU, UV₂₅₄ absorbance was 0.120, and DOC was 6.47 mg/L. For lake water, initial pH was 7.62, turbidity was 27.3 NTU, UV₂₅₄ absorbance was 0.071, and DOC was 3.53 mg/L. Size distribution histograms for Zone 4 removal of the NPs in river water are shown in Figure 4, and in lake water in Figure 5. Size distribution histograms of the natural occurrence metal containing particles in the river and lake waters without NP addition are shown in the Supplementary Information. In river water, Ag NPs were removed similarly among each treatment without polymer and the most frequent size of the particles remained the same before and after each treatment.

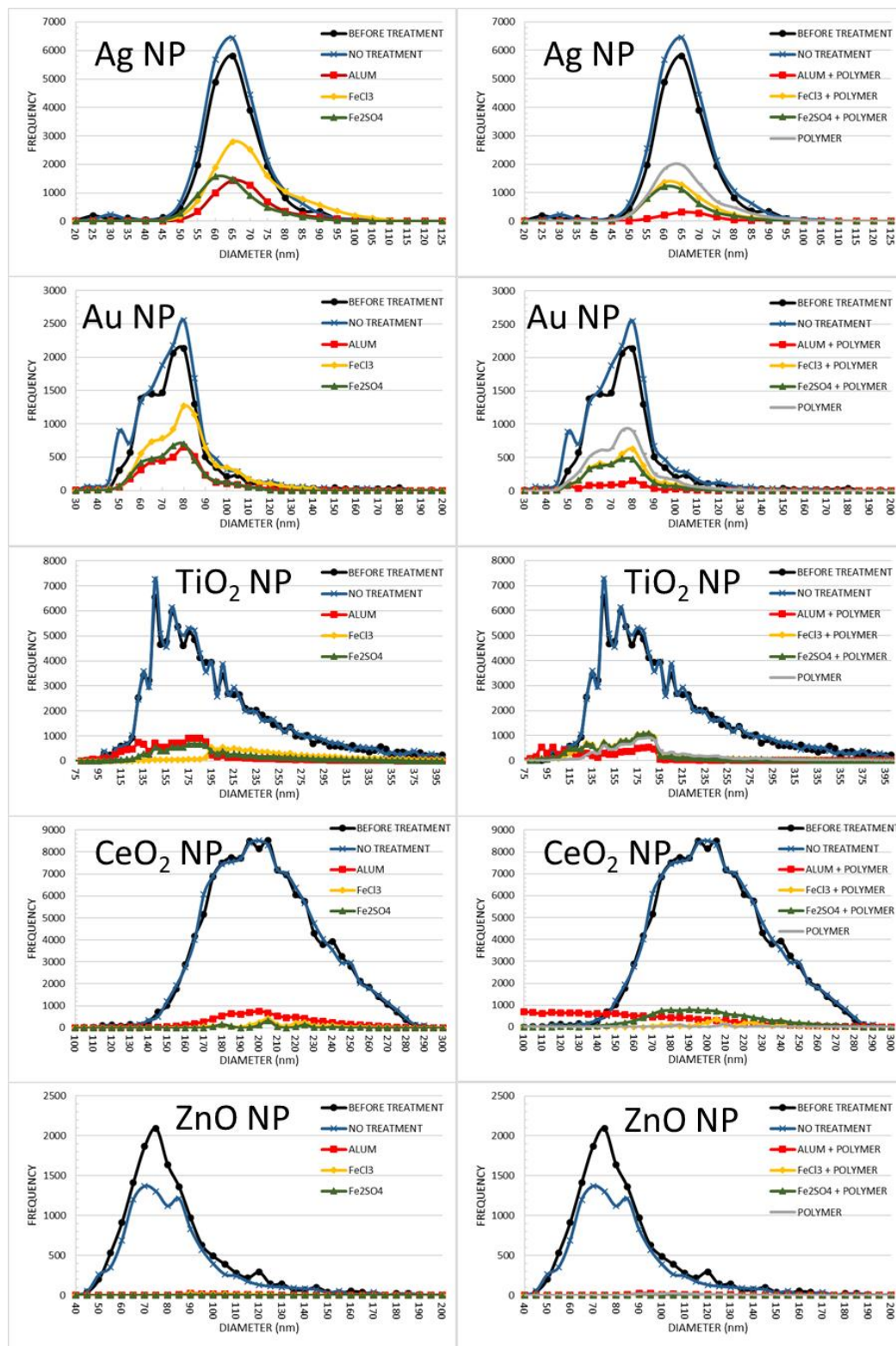


Figure 4. Size distribution histograms for all studied NPs after Zone 4 (sweep floc) treatment in river water.

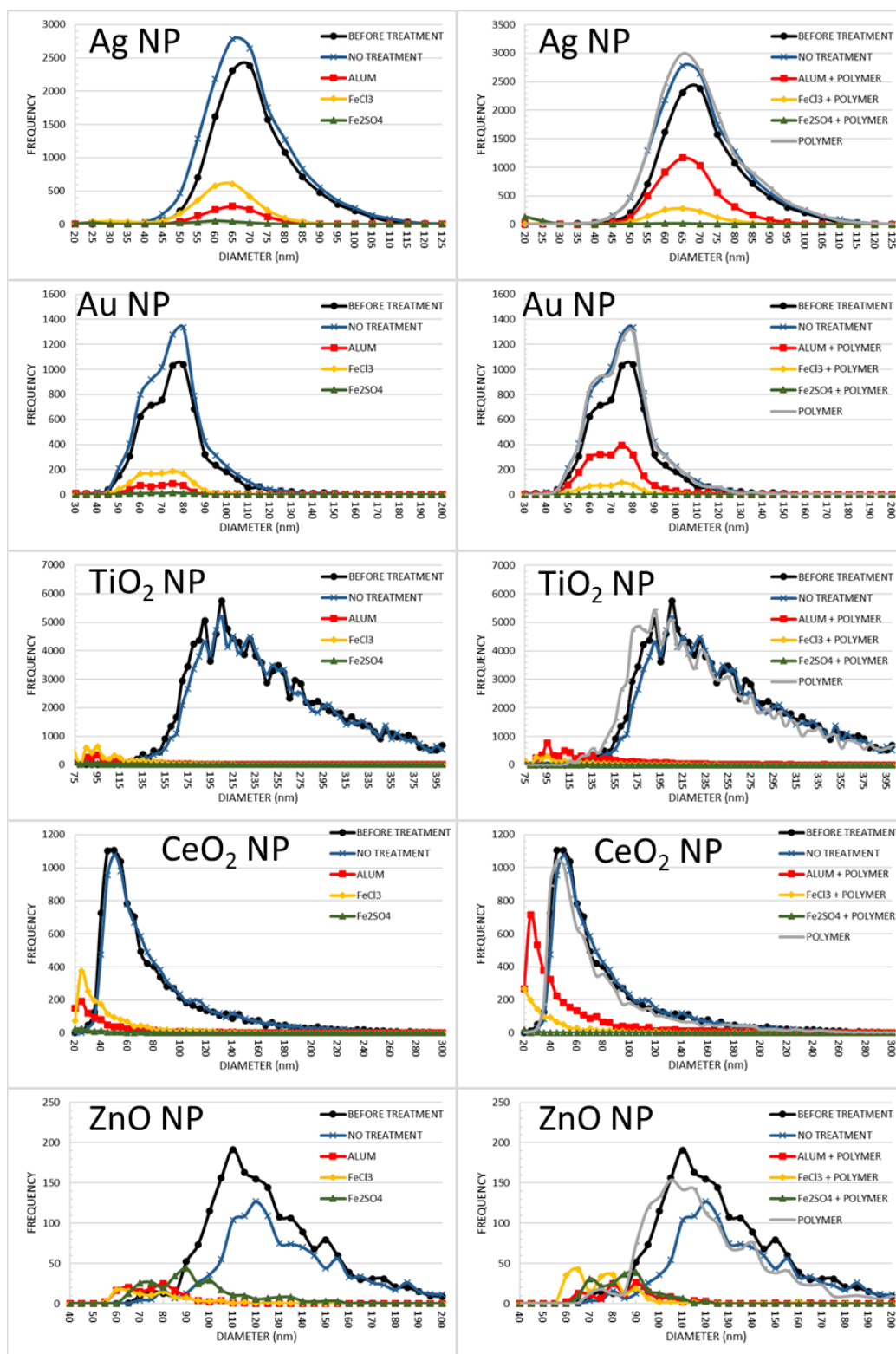


Figure 5. Size distribution histograms for all studied NPs after Zone 4 (sweep floc) treatment in lake water.

Polymer addition increased removal only when added with alum for both Ag and Au NPs. However, in lake water the polymer was not effective and when applied alone did not remove either of these particles (Figure 5). For the uncoated NPs, removal was largely the same among all treatments, resulting in similar size distributions after each in both river and lake water. CeO₂ removal in lake was an exception, with worse removal when polymer was applied with alum and ferric chloride coagulants. Dissolution was observed for ZnO NPs when no treatment was applied to both river and lake water (Figure 4 and Figure 5, respectively).

NP removal after Zone 4 coagulation using alum, ferric chloride, and ferric sulfate with and without polymer and by polymer alone are shown in Figure 6 for both river and lake water. Ag and Au NPs showed similar overall removal most likely because they were both citrate-stabilized (Figure 6a, 6b). Under Zone 4 conditions in river water, alum resulted in the highest removal of Ag and Au NP among coagulation treatments without polymer addition (Figure 6a). Ferric chloride resulted in similar removal when polymer was added simultaneously. The highest removal efficiency observed for Ag and Au NPs was after alum with polymer addition. Polymer addition enhanced removal when added at the same time as other coagulants in Zone 4.

Turbidity removal did not show a significant correlation to Ag and Au NP removal, but was reduced by over 70% for all treatments (Figure 6). Minimal settling occurred when no treatment was applied. Zone 4 coagulation treatments in lake water resulted in more than 75% of Ag and Au NP removal when alum, ferric chloride, and ferric sulfate were applied alone (Figure 6b). When polymer was added alone, significant NP removal was not observed for any of the monitored NPs in lake water (Figure 6b, 6d).

However, the polymer was effective in river water at the same dosage (Figure 6a, 6c) which indicated that the organic carbon concentrations in the water played a major role in the efficacy of the polymer. Similar results have been reported. (Jarvis et al., 2006; Matilainen et al., 2010; Rizzo et al., 2008) Dissolved Ag and Au were below the DLs in all samples.

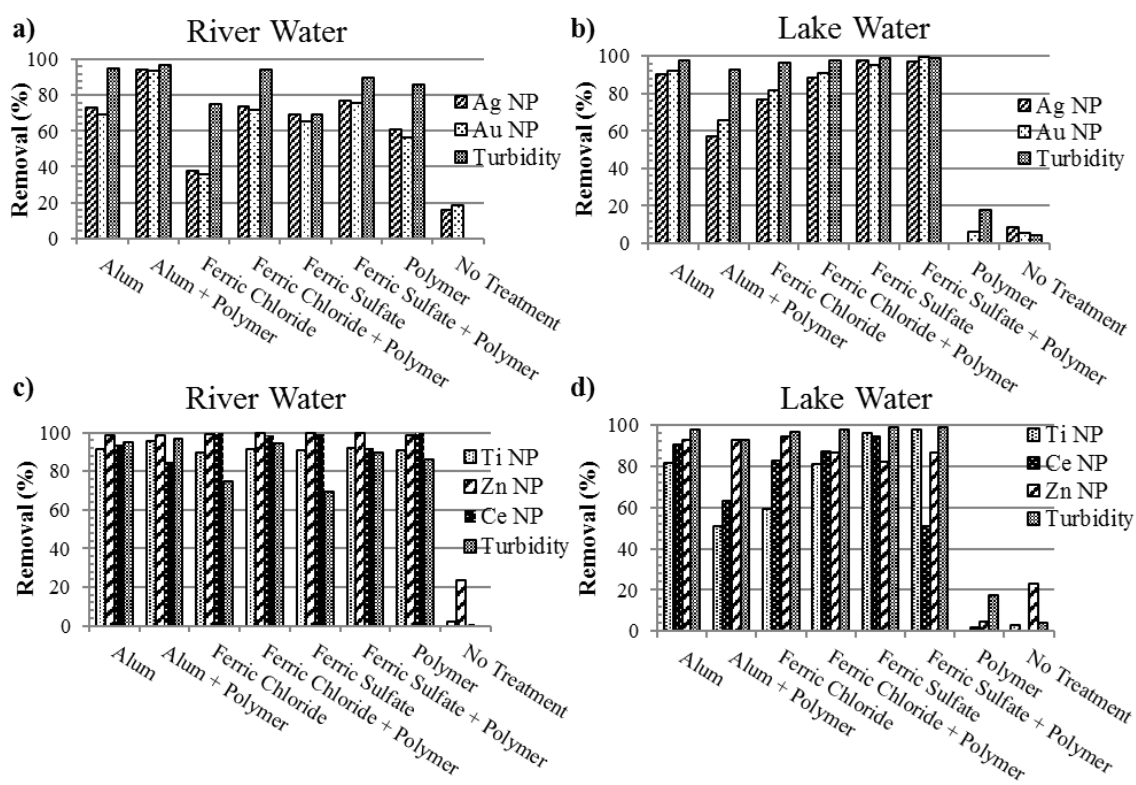


Figure 6. a) Ag NP, Au NP, and turbidity removal and c) TiO₂, CeO₂, ZnO NP and turbidity removal after various Zone 4 coagulation and polymer treatments in river water; b) Ag NP, Au NP, and turbidity removal and d) TiO₂, CeO₂, ZnO NP and turbidity removal after various Zone 4 coagulation treatments in river water.

TiO₂, CeO₂, and ZnO removal after Zone 4 treatments in river water and lake water can be seen in Figure 6c and 6d, respectively. Under each treatment condition,

removal for these NPs was between 85-99% in river water matrix, which indicated that Zone 4 coagulation effectively removed the uncoated NPs from river water even at high DOC levels (6.47 mg/L). Dissolved Ce, if present, was below the detection limit in river water samples, but dissolved Ti and Zn were present in the river water samples at 109 and 7.85 $\mu\text{g/L}$, respectively. After NP addition, dissolved Ti concentrations did not increase, but dissolved Zn increased to 23.0 $\mu\text{g/L}$. ZnO NP dissolution and those smaller than the size DL contributed to this increase in detected Zn ions. After Zone 4 coagulation treatments, dissolved Ti and Zn concentrations were reduced by 62-99% depending on treatment (Figure 7). Polymer alone resulted in the lowest dissolved ion removal. pH, UV_{254} absorbance, and DOC were also monitored before and after the various Zone 4 coagulation treatments. After Zone 4 coagulation in river water with alum, ferric chloride, and ferric sulfate, the pH decreased from 7.30 to 7.03, 7.10, and 7.10, respectively. Polymer addition had no effect on the pH. Turbidity, UV_{254} , and DOC removal by all of the coagulants, but reduced turbidity (Figure 6).

As during the Zone 2 coagulation experiments, dissolved ions did not increase after NP addition which indicated that the NPs were not undergoing any physical changes after addition to river water, except ZnO which is known to be highly soluble. Citrate-stabilized Ag and Au NPs removal was generally higher after Zone 4 coagulation compared to Zone 2, which indicated that the NPs were “swept up” into coagulant floc. Uncoated TiO_2 , CeO_2 , and ZnO NPs were removed by Zone 4 coagulation with high efficiency. Dissolved Ti and Zn removal was higher under Zone 4 conditions than Zone 2 conditions. The decrease in pH and sweep action of the Zone 4 coagulation process both contributed to this increase in removal.

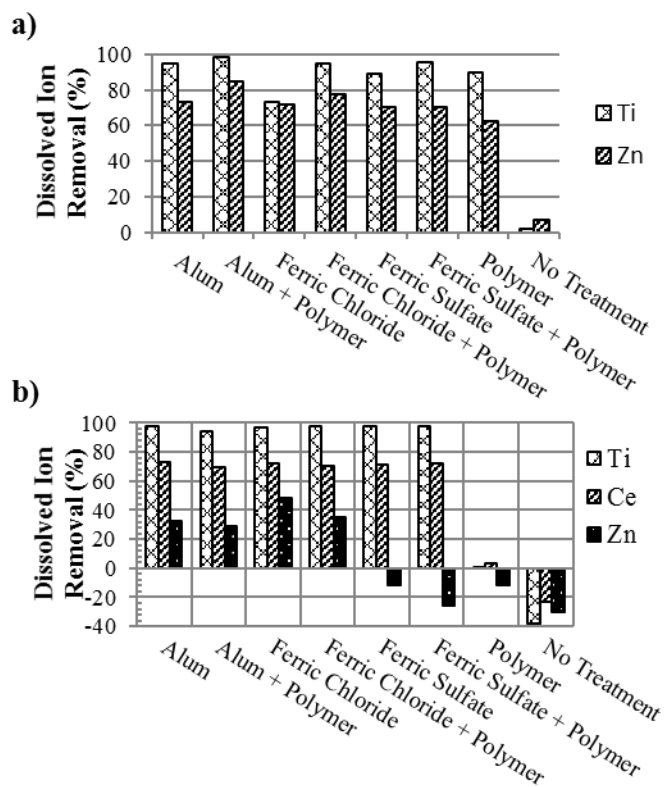


Figure 7. Dissolved Ti and Zn removal during Zone 4 coagulation experiments in a) river water and b) lake water.

4. CONCLUSIONS

As applications and production of NP increase, it is important to understand if NPs are efficiently removed during alum, ferric, and polymer coagulation processes for protection of public health as well as for future environmental and health regulations. Alum, ferric, and polymer coagulants effectively removed citrate-stabilized Ag and Au NPs and uncoated TiO₂, CeO₂, and ZnO NPs from river water under Zone 2 and Zone 4 coagulation conditions. These NPs were added at the upper limit of predicted environmental exposure ($\sim 1 \times 10^6$ particles/mL, $\mu\text{g/L}$ level mass concentrations), which

indicated that these treatments were effective under maximum predicted exposure levels. This study resulted in similar removal efficiencies with previous studies that used higher concentrations of NP, indicating that NP removal under these conditions is not concentration dependent. However, some NPs were not removed by alum, ferric, and polymer coagulation processes. If a large concentration of NPs is released into source water, it may be necessary to combine several different treatments to ensure NPs have been removed to safe limits for human consumption. As shown in previous work, lime softening effectively removed over 90% of particles from river water. By combining traditional treatment techniques, the selected NPs in this and previous studies can be removed very efficiently. More work needs to be done to evaluate the behavior of other types of NPs with various sizes and surface coatings, and SP-ICP-MS methods should be improved to reduce detection limits to improve NP characterization.

SUPPLEMENTARY INFORMATION

The supplementary information contains size distribution histograms for each metal element containing particle in the collected surface waters without added NPs.

CONFLICT OF INTEREST

None.

ACKNOWLEDGEMENTS

The authors thank the Center for Single Nanoparticle, Single Cell, and Single Molecule Monitoring (CS³M), and Environmental Research Center at Missouri University of Science and Technology for providing some facilities.

Funding: This work was supported by the Missouri Department for Natural Resources (MDNR) [award number 0045667, 2015] and PerkinElmer, Inc. by providing NexION 350D ICP-MS [number 00044422, 2013].

REFERENCES

- Amirtharajah, A., Mills, K.M., 1982. Rapid-mix design for mechanisms of alum coagulation. *Journal of the American Water Works Association*. 74, 210-216.
- Anselmann, R., 2001. Nanoparticles and nanolayers in commercial applications. *Journal of Nanoparticle Research*. 3, 329-336.
- Beer, C., Foldbjerg, R., Hayashi, Y., Sutherland, D.S., Autrup, H., 2012. Toxicity of silver nanoparticles - nanoparticle or silver ion? *Toxicology Letters*. 208, 286-292.
- Benn, T.M., Westerhoff, P., 2008. Nanoparticle Silver Released into Water from Commercially Available Sock Fabrics. *Environmental Science and Technology*. 42, 4133-4139.
- Boxall, A., Chaudhry, Q., Sinclair, C., Jones, A., Aitken, R., Jefferson, B., Watts, C., 2007. Current and Future Predicted Environmental Exposure to ENPs. Central Science Laboratory, Department of the Environment and Rural Affairs, London, UK. 1-89.
- Brar, S.K., Verma, M., Tyagi, R.D., Surampalli, R.Y., 2010. Engineered nanoparticles in wastewater and wastewater sludge--evidence and impacts. *Waste Management*. 30, 504-520.

- Cascio, C., Geiss, O., Franchini, F., Ojea-Jimenez, I., Rossi, F., Gilliland, D., Calzolari, L., 2015. Detection, quantification and derivation of number size distribution of silver nanoparticles in antimicrobial consumer products. *Journal of Analytical Atomic Spectrometry*. 30, 1255-1265.
- Chalew, T.E.A., Ajmani, G.S., Huang, H., Schwab, K.J., 2013. Evaluating Nanoparticle Breakthrough during Drinking Water Treatment. *Environmental Health Perspectives*. 121, 1161-1166.
- Crittenden, J.C., Trussell, R.R., Hand, D.W., Howe, K.J., Tchobanoglous, G., 2012. *MWH's water treatment: principles and design*. John Wiley & Sons, Hoboken, New Jersey.
- Dan, Y., Zhang, W., Xue, R., Ma, X., Stephan, C., Shi, H., 2015. Characterization of gold nanoparticles uptake by tomato plants using enzymatic extraction followed by single particle inductively coupled plasma-mass spectrometry. *Environmental Science and Technology*. 49, 3007-3014.
- Degueldre, C., Favarger, P.Y., 2003. Colloid analysis by single particle inductively coupled plasma-mass spectroscopy: a feasibility study. *Colloids and Surfaces A: Physicochemical and Engineering Aspects*. 217, 137-142.
- Degueldre, C., Favarger, P.Y., 2004. Thorium colloid analysis by single particle inductively coupled plasma-mass spectrometry. *Talanta*. 62, 1051-1054.
- Degueldre, C., Favarger, P.Y., Bitea, C., 2004. Zirconia colloid analysis by single particle inductively coupled plasma-mass spectrometry. *Analytica Chimica Acta*. 518, 137-142.
- Degueldre, C., Favarger, P.Y., Rosse, R., Wold, S., 2006a. Uranium colloid analysis by single particle inductively coupled plasma-mass spectrometry. *Talanta*. 68, 623-628.
- Degueldre, C., Favarger, P.Y., Wold, S., 2006b. Gold colloid analysis by inductively coupled plasma-mass spectrometry in a single particle mode. *Analytica Chimica Acta*. 555, 263-268.
- Dentel, S.K., 1988. Application of the Precipitation-Charge Neutralization Model of Coagulation. *Environmental Science and Technology*. 22, 825-832.
- Donovan, A.R., Adams, C.D., Ma, Y., Stephan, C., Eichholz, T., Shi, H., 2016a. Single particle ICP-MS characterization of titanium dioxide, silver, and gold nanoparticles during drinking water treatment. *Chemosphere*. 144, 148-153.

- Donovan, A.R., Adams, C.D., Ma, Y., Stephan, C., Eichholz, T., Shi, H., 2016b. Detection of Zinc Oxide and Cerium Dioxide Nanoparticles during Drinking Water Treatment by Rapid Single Particle ICP-MS Methods. *Analytical and Bioanalytical Chemistry*. 408, 5137-5145.
- Heithmar, E.M., Pergantis, S.A., 2010. Characterizing Concentrations and Size Distribution of Metal-Containing Nanoparticles in Waste Water. US Environmental Protection Agency, Office of Research and Development, National Exposure Research Laboratory.
- Jarvis, P., Jefferson, B., Parsons, S.A., 2006. Floc structural characteristics using conventional coagulation for a high doc, low alkalinity surface water source. *Water Res.* 40, 2727-2737.
- Kaegi, R., Sinnet, B., Zuleeg, S., Hagendorfer, H., Mueller, E., Vonbank, R., Boller, M., Burkhardt, M., 2010. Release of silver nanoparticles from outdoor facades. *Environ Pollut.* 158, 2900-2905.
- Kaegi, R., Voegelin, A., Sinnet, B., Zuleeg, S., Hagendorfer, H., Burkhardt, M., Siegrist, H., 2011. Behavior of metallic silver nanoparticles in a pilot wastewater treatment plant. *Environ Sci Technol.* 45, 3902-3908.
- Keller, A.A., Wang, H., Zhou, D., Lenihan, H.S., Cherr, G., Cardinale, B.J., Miller, R., Ji, Z., 2010. Stability and Aggregation of Metal Oxide Nanoparticles in Natural Aqueous Matrices. *Environmental Science and Technology*. 44, 1962-1967.
- Kim, S.-H., Moon, B.-H., Lee, H.-I., 2001. Effects of pH and dosage on pollutant removal and floc structure during coagulation. *Microchemical Journal*. 68, 197-203.
- Kiser, M.A., Westerhoff, P., Benn, T., Wang, Y., Perez-Rivera, J., Hristovski, K., 2009. Titanium Nanomaterial Removal and Release from Waste Water Treatment Plants. *Environmental Science and Technology*. 43, 6757-6763.
- Kittler, S., Greulich, C., Diendorf, J., Köller, M., Epple, M., 2010. Toxicity of Silver Nanoparticles Increases during Storage Because of Slow Dissolution under Release of Silver Ions. *Chemistry of Materials*. 22, 4548-4554.
- Klaine, S.J., Alvarez, P.J.J., Batley, G.E., Fernandes, T.F., Handy, R.D., Lyon, D.Y., Mahendra, S., McLaughlin, M.J., Lead, J.R., 2008. Nanomaterials in the environment: Behavior, fate, bioavailability, and effects. *Environmental Toxicology and Chemistry*. 27, 1825-1851.

- Laborda, F., Bolea, E., Jimenez-Lamana, J., 2014. Single particle inductively coupled plasma mass spectrometry: a powerful tool for nanoanalysis. *Anal Chem.* 86, 2270-2278.
- Laborda, F., Jiménez-Lamana, J., Bolea, E., Castillo, J.R., 2013. Critical considerations for the determination of nanoparticle number concentrations, size and number size distributions by single particle ICP-MS. *Journal of Analytical Atomic Spectrometry.* 28, 1220-1232.
- Lee, B.C., Kim, S., Shon, H.K., Vigneswaran, S., Kim, S.D., Cho, J., Kim, I.S., Choi, K.H., Kim, J.B., Park, H.J., Kim, J.H., 2008. Aquatic toxicity evaluation of TiO₂ nanoparticle produced from sludge of TiCl₄ flocculation of wastewater and seawater. *Journal of Nanoparticle Research.* 11, 2087-2096.
- Limbach, L.K., Bereither, R., Muller, E., Krebs, R., Galli, R., Stark, W.J., 2008. Removal of Oxide Nanoparticles in a Model Wastewater Treatment Plant: Influence of Agglomeration and Surfactants on Clearing Efficiency. *Environmental Science and Technology.* 42, 5828-5833.
- Liu, J., Murphy, K., Winchester, M., Hackley, V., 2017. Overcoming challenges in single particle inductively coupled plasma mass spectrometry measurement of silver nanoparticles. *Analytical and Bioanalytical Chemistry.* 409, 6027-6039.
- Loeschner, K., Navratilova, J., Kobler, C., Molhave, K., Wagner, S., von der Kammer, F., Larsen, E.H., 2013. Detection and characterization of silver nanoparticles in chicken meat by asymmetric flow field flow fractionation with detection by conventional or single particle ICP-MS. *Anal Bioanal Chem.* 405, 8185-8195.
- Matilainen, A., Vepsäläinen, M., Sillanpää, M., 2010. Natural organic matter removal by coagulation during drinking water treatment: a review. *Adv Colloid Interface Sci.* 159, 189-197.
- Montaño, M., Olesik, J., Barber, A., Challis, K., Ranville, J., 2016. Single Particle ICP-MS: Advances toward routine analysis of nanomaterials. *Analytical and Bioanalytical Chemistry.* 408, 5053-5074.
- Montaño, M.D., Badieli, H.R., Bazargan, S., Ranville, J.F., 2014. Improvements in the detection and characterization of engineered nanoparticles using spICP-MS with microsecond dwell times. *Environmental Science: Nano.* 1, 338.
- Mueller, N.C., Nowack, B., 2008. Exposure Modeling of Engineered Nanoparticles in the Environment. *Environmental Science and Technology.* 42, 4447-4453.

- Nowack, B., Ranville, J.F., Diamond, S., Gallego-Urrea, J.A., Metcalfe, C., Rose, J., Horne, N., Koelmans, A.A., Klaine, S.J., 2012. Potential scenarios for nanomaterial release and subsequent alteration in the environment. *Environ Toxicol Chem.* 31, 50-59.
- Pace, H.E., Rogers, N.J., Jarolimek, C., Coleman, V.A., Higgins, C.P., Ranville, J.F., 2011. Determining transport efficiency for the purpose of counting and sizing nanoparticles via single particle inductively coupled plasma mass spectrometry. *Anal Chem.* 83, 9361-9.
- Peters, R., Herrera-Rivera, Z., Undas, A., Lee, M.v.d., Marvin, H., Bouwmeester, H., Weigel, S., 2015. Single particle ICP-MS combined with a data evaluation tool as a routine technique for the analysis of nanoparticles in complex matrices. *Journal of Analytical Atomic Spectrometry.* 30, 1274-1258.
- Quik, J.T., Lynch, I., Van Hoecke, K., Miermans, C.J., De Schamphelaere, K.A., Janssen, C.R., Dawson, K.A., Stuart, M.A., Van De Meent, D., 2010. Effect of natural organic matter on cerium dioxide nanoparticles settling in model fresh water. *Chemosphere.* 81, 711-5.
- Rizzo, L., Di Gennaro, A., Gallo, M., Belgiorno, V., 2008. Coagulation/chlorination of surface water: A comparison between chitosan and metal salts. *Separation and Purification Technology.* 62, 79-85.
- Sharifi, S., Behzadi, S., Laurent, S., Forrest, M.L., Stroeve, P., Mahmoudi, M., 2012. Toxicity of nanomaterials. *Chem Soc Rev.* 41, 2323-2343.
- Van Hoecke, K., De Schamphelaere, K.A., Van der Meeren, P., Smagghe, G., Janssen, C.R., 2011. Aggregation and ecotoxicity of CeO₂ nanoparticles in synthetic and natural waters with variable pH, organic matter concentration and ionic strength. *Environmental Pollution.* 159, 970-6.
- Wang, H., Qi, J., Keller, A.A., Zhu, M., Li, F., 2014. Effects of pH, ionic strength and humic acid on the removal of TiO₂ nanoparticles from aqueous phase by coagulation. *Colloids and Surfaces A: Physicochemical and Engineering Aspects.* 450, 161-165.
- Wang, H.T., Ye, Y.Y., Qi, J., Li, F.T., Tang, Y.L., 2013. Removal of titanium dioxide nanoparticles by coagulation: effects of coagulants, typical ions, alkalinity and natural organic matters. *Water Sci Technol.* 68, 1137-1143.
- Westerhoff, P., Song, G., Hristovski, K., Kiser, M.A., 2011. Occurrence and removal of titanium at full scale wastewater treatment plants: implications for TiO₂ nanomaterials. *Journal of Environmental Monitoring.* 43, 6757-6763.

- Windler, L., Lorenz, C., von Goetz, N., Hungerbuhler, K., Amberg, M., Heuberger, M., Nowack, B., 2012. Release of titanium dioxide from textiles during washing. *Environ Sci Technol.* 46, 8181-8188.
- Yang, X., Gondikas, A.P., Marinakos, S.M., Auffan, M., Liu, J., Hsu-Kim, H., Meyer, J.N., 2012. Mechanism of silver nanoparticle toxicity is dependent on dissolved silver and surface coating in *Caenorhabditis elegans*. *Environ Sci Technol.* 46, 1119-27.
- Yu, S.-j., Yin, Y.-g., Liu, J.-f., 2013. Silver nanoparticles in the environment. *Environmental Science: Processes & Impacts.* 15, 78-92.
- Zhang, Y., Chen, Y., Westerhoff, P., Hristovski, K., Crittenden, J.C., 2008. Stability of commercial metal oxide nanoparticles in water. *Water Research.* 42, 2204-2212.

III. CYANOTOXIN OCCURRENCE, RELATION WITH SALINITY, AND POTENTIAL RECREATIONAL HEALTH RISKS IN U.S. ESTUARIES IN THE 2015 EPA NATIONAL COASTAL ASSESSMENT

Ariel R. Donovan^{1,2}, Zachary R. Laughrey¹, Hugh Sullivan², Sarah Lehmann², Robin A. Femmer¹, Sarena L. Senegal¹, Keith A. Loftin^{1*}

1. U.S. Geological Survey, Kansas Water Science Center, Organic Geochemistry Research Laboratory, Lawrence, KS 66049, USA
2. Department of Chemistry and Environmental Research Center, Missouri University of Science and Technology, Rolla, MO, 65409, USA
3. U.S. Environmental Protection Agency, Washington, D.C. USA

*corresponding author

Keith A. Loftin

1217 Biltmore Drive, Lawrence, KS 66049, USA

kloftin@usgs.gov

(785) 832-3543

ABSTRACT

Cyanotoxins are an emerging contaminant in estuary environments due to recent implication in marine animal illness and fatal effects. In the first nationwide study of cyanotoxins in estuarine environments, algal toxins, cyanotoxins, chlorophyll, and salinity were measured in samples collected during the EPA National Coastal Condition Assessment 2015. As no recreational guidelines exist for cyanotoxins in marine waters,

recreational exposure thresholds from the World Health Organization and EPA were applied to the data to evaluate potential recreational exposure to microcystins and cylindrospermopsin. Anatoxin-a, cylindrospermopsin, domoic acid, and microcystins (sum of ten congeners) were detected by LC/MS/MS in 0.7, 1.0, 7.9, and 2.2% of samples with mean concentrations of 0.13, 0.13, 0.55, and 0.49 $\mu\text{g/L}$, respectively. A portion of the sites were sampled twice, and domoic acid was detected in 12.1% of those samples with a mean concentration of 0.44 $\mu\text{g/L}$. Microcystins by ELISA was also evaluated, and 6.7% of samples had measurable microcystins with a mean of 0.60 $\mu\text{g/L}$. Anatoxin-a and cylindrospermopsin were detected south of 40° latitude, microcystins by ELISA nationwide (only on the east coast by LC/MS/MS), and domoic acid occurred nationwide. Microcystins and cylindrospermopsin were below WHO and EPA recreational health thresholds and agreed with the WHO chlorophyll recreational health threshold metric in 63% of samples. Anatoxin-a, cylindrospermopsin, domoic acid, and microcystins by ELISA were detected in samples with a wide range of salinities, while microcystins by LC/MS/MS only occurred in samples with salinity <5 part per thousand (PPT), however whether the cyanotoxins were produced in the estuary or were transported downstream are unclear.

KEY WORDS

Cyanotoxins, microcystins, domoic acid, estuaries, salinity, cyanotoxin recreational exposure risk

1. INTRODUCTION

Cyanobacteria, also known as blue-green algae, are photosynthetic bacteria that can cause severe water quality problems including anoxia, taste and odor problems, poor aesthetics, and in some cases production of cyanotoxins (Chorus and Bartram, 1999; Paerl et al., 2001). Cyanotoxins have been reported to cause illness and death in animals, and there are cases of human illness globally with deaths reported in one instance for dialysis patients exposed to cyanotoxin-contaminated water during treatment (Pouria et al., 1998). Recently, the impacts of cyanobacteria and cyanotoxins on coastal and estuary water systems has been of interest as reported incidents of cyanobacteria blooms occurring in eateries increase and there are observable impacts on the estuary systems and animal life (Howard et al., 2017; Lehman et al., 2005; Miller et al., 2010; Rosen et al., 2018; Tatters et al., 2017). The transport of cyanobacteria and cyanotoxins into coastal environments depends on multiple factors, including tidal patterns and weather events (rain, drought, snow, snow melt) as well as the ability of the cyanobacteria to adapt to increasing salinity (Hagemann, 2011).

The effects of increasing salinity on freshwater cyanobacteria, whether through secondary salinization of freshwater or transport to coastal and estuarine systems, are not fully understood. Figure 1 summarizes current literature concerning the salinity tolerance range of certain potentially toxin-producing cyanobacteria at the genera level including *Anabaena* spp., *Microcystis* spp., *Nodularia* spp., *Phormidium* spp., *Synechococcus* spp., and *Synechocystis* spp. This summary includes multiple strains of these genera grown under various conditions (culture medium, temperature, light source, light cycles, pH, and

exposure time) as few studies used the same species and conditions. Furthermore, the ability of a specific strain to adapt to changing salinity through production of osmoregulatory compounds will impact survivability and the ability to actively produce toxins in those environments (Black et al., 2011; Mazur-Marzec et al., 2005; Reed et al., 1986; Reed and Stewart, 1985). This has a significant impact on the comparability of the studies and serves to highlight that more work needs to be done to understand the ability of these genera to adapt to increasing salinity.

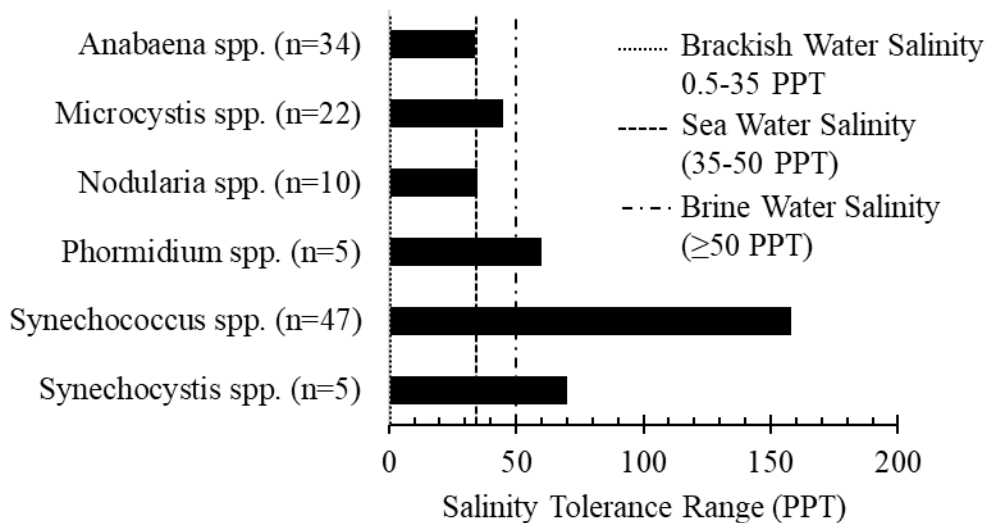


Figure 1. Salinity tolerance range of several potential toxin producing cyanobacteria genera where n is the number of instances reported salinity tolerance data. Salinity concentrations for brackish water, sea water, and briny water are noted by dashed lines. Multiple references.

Salinity tolerance ranges for the included cyanobacteria genera varied widely. Of the potential toxin-producing cyanobacteria included in Figure 1, *Anabaena* spp. and *Nodularia* spp. did not have evidence of surviving in sea water systems (>35 PPT).

Microcystis spp., known to produce microcystins, have been shown to survive in up to 45 PPT salinity (Hagemann et al., 1989), but most reports place the highest salinity tolerance <20 PPT. *Phormidium* spp., *Synechococcus* spp., and *Synechocystis* spp. are reported to tolerate salinity from freshwater into brine water range (≥ 50 PPT), also known as hypersaline environments. *Synechococcus* spp. has the largest reported salinity tolerance range, from freshwater through 158 PPT (systems like Great Salt Lake).

While there is some literature regarding the impacts of salinity on cyanobacteria toxin production and release, it is not yet well understood. Studies related to microcystin production by *Microcystis* spp. indicate that toxin production may be reduced when cells are under salt stress (Martín-Luna et al., 2015; Orr et al., 2004). Furthermore, there is some evidence to show that when *Microcystis* sp. die or have weakened membrane integrity at elevated salinities in laboratory studies, intracellular microcystins can be released from the cells, increasing the dissolved fraction of the toxin (Chen et al., 2015; Orr et al., 2004; Rosen et al., 2018). In studies regarding *Nodularia* spp., the highest levels of toxin were produced at optimal salinity levels for the cyanobacteria (Blackburn et al., 1996; Lehtimäki et al., 1997).

The interest in cyanobacteria and cyanotoxins at the marine-freshwater continuum has increased in recent years in light of findings that document cyanobacteria and cyanotoxins in estuarine and coastal systems worldwide (Howard et al., 2017; Lehman et al., 2005; Preece et al., 2017, 2015; Tatters et al., 2019, 2017). The potential effects of freshwater cyanobacteria and cyanotoxins discharged into coastal and estuarine environments was highlighted with a report of southern sea otter mortalities caused by microcystins at the Monterey Bay National Marine Sanctuary (Miller et al., 2010). Work

has been done to assess the accumulation of cyanotoxins in clams, mussels, and oysters which may result in cyanotoxin exposure of higher trophic levels. Accumulation and depuration of cyanotoxins was found to be dependent on the type of feeder, with bivalves and snails accumulating more toxin than crabs (Magalhães et al., 2003; Miller et al., 2010; Pires et al., 2004; Wood et al., 2014). The potential occurrence of marine algal toxins (domoic acid, okadaic acid, azaspiracids, pectenotoxins, and others), anthropogenic contaminants, viruses and other natural contaminants, and cyanotoxins in coastal and estuarine environments may result in increased and unknown health effects (Gibble and Kudela, 2014; Tatters et al., 2019).

To test the hypotheses that cyanotoxins occur in U.S. coastal water and to evaluate the connection between estuary salinity and cyanotoxin occurrence, a total of 21 algal toxins and cyanotoxins were analyzed by liquid chromatography tandem mass spectrometry (LC/MS/MS) in water samples collected from U.S. coastal and estuary sites for the U.S. Environmental Protection Agency (EPA) National Coastal Condition Assessment 2015 (NCCA 2015). Samples were also screened for microcystins using a commercial enzyme-linked immunosorbent assay (ELISA). Algal toxin and cyanotoxin occurrence along U.S. coastlines between June and November 2015 was evaluated against salinity associated with the samples to further understand the impacts of salinity on toxins in the water systems. Finally, World Health Organization (WHO) and EPA recreational guidelines were used to evaluate potential health risks associated with microcystins and cylindrospermopsin in coastal and estuarine waters.

2. METHODS AND MATERIALS

2.1. STUDY DESIGN

The National Coastal Condition Assessment 2015 (NCCA) (EPA, 2019) consisted of two independent designs including re-sample sites from the NCCA 2010 and the other selected new sites. A Generalized Random Tessellation Stratified (GRTS) survey design was used for both sample designs. A total of 732 unique estuary sites were sampled in June through November 2015 and analyzed for algal toxins and cyanotoxins by liquid chromatography tandem mass spectrometry (LC/MS/MS), microcystins by enzyme-linked immunosorbent assay (ELISA), and chlorophyll. A subset of 66 sites were resampled during a second visit from July through September 2015. General patterns in air temperature and precipitation during the sample collection months were described by NOAA's National Climatic Dataset (NOAA National Centers for Environmental Information, 2016).

2.2. SAMPLE COLLECTION AND PRESERVATION AND IN-SITU SALINITY MEASUREMENT

Samples collected for toxin analysis by LC/MS/MS and ELISA were collected in 500 mL high density polyethylene (HDPE) bottles. Bottles were rinsed three times with the site water before sample collection, leaving at least one inch of head space. Samples were immediately stored in a cooler on ice at the site and frozen upon return to the base site. Samples were kept frozen through shipping and until sample processing. Chlorophyll-*a* samples were collected into 2 L amber HDPE bottles using a water sampling device or water pumping system at a depth of 0.5 m or less if the station depth was less than 1.0 m.

Sampling devices and bottles were rinsed three times before sample collection, and filled bottles were placed on ice immediately after collection. Chlorophyll-a samples were filtered on shore, stored in 50-mL tube, and stored on dry ice. Salinity was measured at each site using a salinity/conductivity meter attached to a sonde that was calibrated prior to field measurements. The sonde was lowered to sampling depth and the salinity was recorded in a field measurement form and on toxin and ELISA sample bottles (EPA, 2015).

2.3. SAMPLE PROCESSING FOR ALGAL TOXIN AND CYANOTOXIN ANALYSIS BY LC/MS/MS

Samples for toxin analysis by LC/MS/MS were frozen and shipped overnight on ice to the U.S. Geological Survey (USGS) Organic Geochemistry Research Laboratory in Lawrence, KS. All samples were processed to lyse cyanobacteria cells and release intracellular toxins by three sequential freeze/thaw cycles (Graham et al., 2010; Loftin et al., 2008). Lysed samples were filtered using a 10-mL Norm-Ject polypropylene syringe (ThermoFisher Scientific, Waltham, MA, USA) coupled to a 0.70- μ m glass fiber (GF/F) syringe filter (25 mm, Whatman, Maidstone, United Kingdom). The first 2 mL of sample were discarded, and the remaining sample was filtered into a 20-mL amber vial. A miniature extraction was performed on the filter by adding 400 μ L of methanol (Optima $\text{\textcircled{R}}$ LC/MS grade, ThermoFisher Scientific, Waltham, MA, USA) with 1% formic acid (Optima $\text{\textcircled{R}}$ LC/MS grade, ThermoFisher Scientific, Waltham, MA, USA) through the filter and added to the sample. This process improved recovery for several algal toxins by reducing sorption in sample processing particularly for the lipophilic algal toxins and

cyanotoxins. The processed samples had a final methanol concentration of 4%. Samples were stored frozen until analysis.

2.4. LIQUID CHROMATOGRAPHY TANDEM MASS SPECTROMETRY (LC/MS/MS) ANALYSIS FOR ALGAL TOXINS AND CYANOTOXINS

Processed samples were analyzed by liquid chromatography tandem mass spectrometry (LC/MS/MS) for 20 algal toxins and cyanotoxins using method adapted from (Graham et al., 2010; Loftin et al., 2008). Analytes included anatoxin-a (ANAA), cylindrospermopsin (CYLS), domoic acid (DMAC), dinophysistoxin-1 (DTX-1), dinophysistoxin-2 (DTX-2), gymnodimine (GYM), 10 microcystin congeners (MCHiLR, MCHtYR, MCLA, MCLF, MCLR, MCLW, MCLY, MCRR, MCWR, and MCYR), nodularin-R (NDLR), okadaic acid (OKAC), pectenotoxin-2 (PTX-2), and 13-desmethyl spirolide c (SPX-1). Separation was performed on an Atlantis T3 analytical column (100 Å particle size, 3 µm, 4.6 mm x 150 mm) with an Atlantis T3 Sentry Guard Cartridge (Waters Corporation, Milford, MA, USA). An Agilent 1260 Bioinert LC coupled to an Agilent 6460 Triple Quadruple Mass Spectrometer with an electrospray ionization (ESI) Jet Stream Ionization Source (Agilent Technologies, Inc., Santa Clara, CA, USA). Mobile phase A consisted of water, 2 mM ammonium formate, and 0.1 % formic acid. Mobile phase B was 50/50 methanol/acetonitrile (v/v), 2 mM ammonium formate, and 0.1% tetrahydrofuran. Mobile phases were prepared using LC/MS grade solvents and reagents. Multiple reaction monitoring (MRM) was used to detect precursor and product ion fragments for quantitation, with the most abundant MRM transition designated as the quantification ion and the next most abundant MRM transition designated as the qualifier ion. Calibrations were prepared using certified reference materials from National

Research Council Canada for ANAA, CYLS, DMAC, DTX-1, DTX-2, GYM, MCLR, MCRR, NDLR, OKAC, PTX-2, and SPX-1. For compounds without certified reference materials available, standards were purchased from Enzo Life Science (MCLA, MCLF, MCLW, MCLY, MCWR, and MCYR). At the start of each run, analytes were calibrated from 0.01 – 5.00 µg/L to determine minimum reporting limits (MRLs, determined as the lowest calibration point that had at a signal to noise ratio of 5 for the quantifying MRM transition). Samples were quantitated by single-point standard addition (SA) using the stacked injection function on the Agilent 1260 LC autosampler, so that 2 µg/L of internal standard, 0.1% tetrasodium ethylenediaminetetraacetic acid (EDTA), and with 1 µg/L of all analytes when injecting a standard addition sample. Minimum reporting limits for ANAA, CYLS, DMAC, DTX-1, DTX-2, GYM, MCHiLR, MCHtYR, MCLA, MCLF, MCLR, MCLW, MCLY, MCRR, MCWR, MCRY, NDLR, OKAC, PTX-2, and SPX-1 were 0.08, 0.10, 0.20, 0.30, 0.10, 0.10, 0.10, 0.10, 0.10, 0.10, 0.10, 0.10, 0.08, 0.10, 0.10, 0.05, 0.10, 0.10, and 0.08 µg/L, respectively.

2.5. DETECTION OF MICROCYSTINS BY ENZYME-LINKED IMMUNOSORBENT ASSAY (ELISA)

EPA laboratories processed samples collected for microcystins analysis by enzyme-linked immunosorbent assay (ELISA) by three sequential freeze/thaw cycles to lyse cyanobacteria cells, then filtered by 0.45-µm glass fiber filters using Norm-ject syringes. Seawater samples were treated according to the manufacturer's directions. Briefly, a resin was prepared in a column and samples were passed through the column followed by distilled water before analysis (PN 529912, Abraxis, LLC, Warminster, PA, USA).

Samples were then analyzed using Microcystin-ADDA Test Kits (PN 520011, Abraxis, LLC, Warminster, PA, USA). The adjusted reporting range was 0.263 to 8.75 $\mu\text{g/L}$.

2.6. DETERMINATION OF CHLOROPHYLL

EPA methods 445.0 and 446.0 were recommended for chlorophyll-a analysis which entailed extracting filters with 90% acetone and analyzing the extracts by fluorometry or visible spectrophotometry (Arar and Collins, 1997a, 1997b). While these methods can be specific for chlorophyll-*a* there are known interferences from other chlorophyll analogues whose presence depend on the composition of the phytoplankton communities resulting in chlorophyll-a results being referred to as chlorophyll for this study (Arar and Collins, 1997a; Loftin et al., 2016).

2.7. DATA ANALYSIS

Statistical summaries (mean, median) were generated using Microsoft Excel (Northampton, MA, USA). All maps were generated using ArcMap version 10.6.1 (Environmental Systems Research Institute ESRI, Redlands, CA, USA). When comparing multiple parameters, analysis was performed only on samples that had data reported for all parameters. Detection frequency at or above the minimum reporting limit was determined using all available data. Concentration summary statistics were calculated using only detection data.

3. RESULTS

3.1. CLIMATE AND SALINITY

NOAA National Centers for Environmental Information release a National Climate Report annually that summarizes annual temperature and precipitation and compares it against the period of record, which included 121 years of data through 2015 (NOAA National Centers for Environmental Information, 2016). Contiguous U.S. average temperature was 12.4°C, which was above the 20th century average, making it the second warmest year in the period of record. Average precipitation was 34.47 inches, 4.53 inches above the 20th century average, making it the third wettest year in the period of record. Strong El Niño conditions were present in mid-to-late 2015. California had significant droughts with low winter precipitation that impacted reservoirs and agriculture as well as contributing to wildfires. Oregon and Washing had the warmest year in the period of record, which contributed to wildfires. Florida also had its warmest year in the period of record.

Of the 732 sites sampled for toxin analysis, 664 had salinity measurements recorded. Mean, median, and maximum salinity concentrations were 23, 27, and 55 PPT. Of these sites, 3.0% were freshwater (<0.5 PPT), 85% were brackish water (0.5 to 35 PPT), 12% were salt water (35 to 50 PPT), and 0.3% were brine water (>50 PPT). Of the 66 sites that were sampled twice for toxin analysis, 64 had salinity measurements recorded. Mean, median and maximum salinity concentrations were 25, 29, and 43 PPT. A total of 94% of these sites were considered brackish on the second visit (0.5 to 35 PPT).

3.2. OCCURRENCE OF ALGAL TOXINS AND CYANOTOXINS IN U.S. ESTUARIES AND COASTAL WATERS BY LIQUID CHROMATOGRAPHY TANDEM MASS SPECTROMETRY (LC/MS/MS)

ANAA was detected in 5 samples (0.7%) and co-occurred with DMAC in one sample. Mean, median, and maximum concentrations were 0.13, 0.14, and 0.16 $\mu\text{g/L}$, respectively. ANAA occurred on the Pacific, Gulf, and Atlantic coasts south of 40° latitude (Figure 2). CYLS was detected in 7 samples (1.0%) and did not co-occur with other toxins. Mean, median, and maximum concentrations were 0.13, 0.11, and 0.21 $\mu\text{g/L}$, respectively. CYLS occurred on the Pacific, Gulf, and Atlantic coasts south of 40° latitude (Figure 3). Mean, median, and maximum concentrations were 0.13, 0.11, and 0.21 $\mu\text{g/L}$, respectively.

Microcystin congeners by LC/MS/MS were detected in a total of 16 samples (2.2%). Two or more microcystin congeners were detected in 8 samples. MCWR was the most frequently detected (12 samples), followed by MCRR (7 samples), MCLR (6 samples), and MCYR (1 sample). MCWR also had the highest mean concentration of 0.49 $\mu\text{g/L}$. Mean, median, and maximum concentrations for total microcystins by LC/MS/MS were 0.49, 0.31, and 2.29 $\mu\text{g/L}$, respectively. Microcystins co-occurred with DMAC in 2 samples, in one of these samples two microcystin congeners were detected and in the other three congeners were detected. Microcystins were only detected by LC/MS/MS on the Atlantic coast, east of 80° longitude (Figure 4) and occurred in lower salinity water compared to the other toxins analyzed by LC/MS/MS. Estuarine and coastal samples were screened for microcystins using ELISA. Using this method, microcystins were detected in 6.7% of samples. Mean, median, and maximum concentrations were 0.60, 0.30, and 3.68 $\mu\text{g/L}$, respectively. Detections are mapped in Figure 5. Of the sites that

were sampled twice, only 1 tested positive for microcystins with a concentration of 0.20 $\mu\text{g/L}$.

DMAC was the most frequently detected toxin, with a 7.9% detection frequency with mean, median, and maximum concentrations of 0.55, 0.32, and 6.22 $\mu\text{g/L}$, respectively. The subset of sites that were sampled twice ($n=66$) tested positive for DMAC in 12.1% of samples with mean, median, and maximum concentrations of 0.44, 0.28, and 1.06 $\mu\text{g/L}$, respectively. Other toxins were not detected by LC/MS/MS in the second round of sampling for these locations. Of the locations sampled twice, only 1 location had DMAC detected on both visits. DMAC was detected on the Pacific, Gulf, and Atlantic coasts (Figure 6).

DTX-1, DTX-2, GYM, MCHiLR, MCHtYR, MCLA, MCLF, MCLW, MCLY, NDLR, OKAC, PTX-2, and SPX-1 were not detected in any sample analyzed by LC/MS/MS.

3.3. CHLOROPHYLL IN U.S. ESTUARIES AND COASTAL WATERS

All estuarine and coastal samples had measurable chlorophyll, with concentrations ranging from 0.15 to 175 $\mu\text{g/L}$ (Figure 7). A total of 64% of samples had <10 $\mu\text{g/L}$ chlorophyll present and 2% had >50 $\mu\text{g/L}$ chlorophyll. Mean and median chlorophyll concentrations were 11 and 6.5 $\mu\text{g/L}$, respectively. The highest chlorophyll concentrations occurred in the Gulf of Mexico and on the Atlantic coast east of 100° latitude.

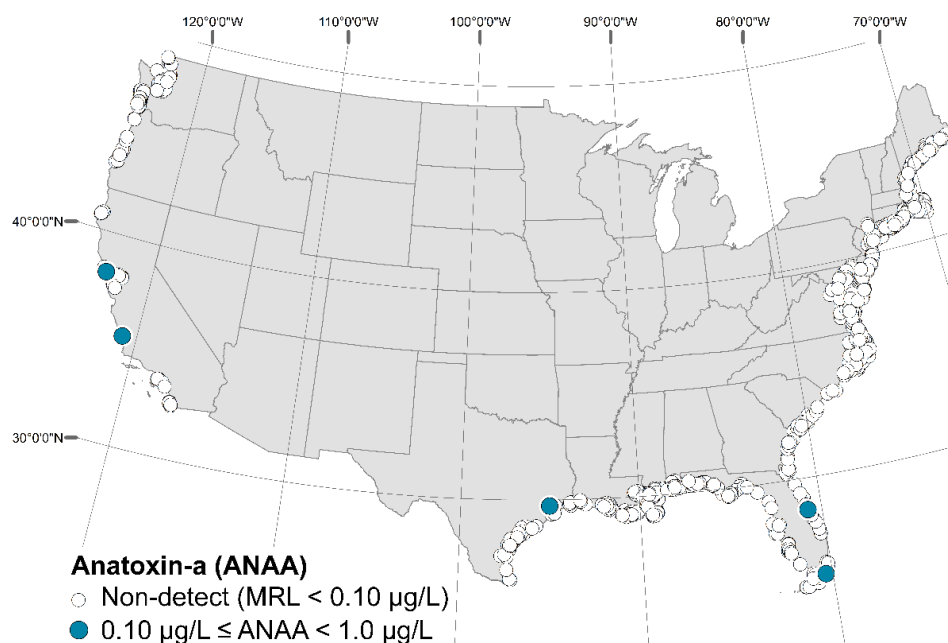


Figure 2. Anatoxin-a occurrence in U.S. estuarine and coastal samples by LC/MS/MS.

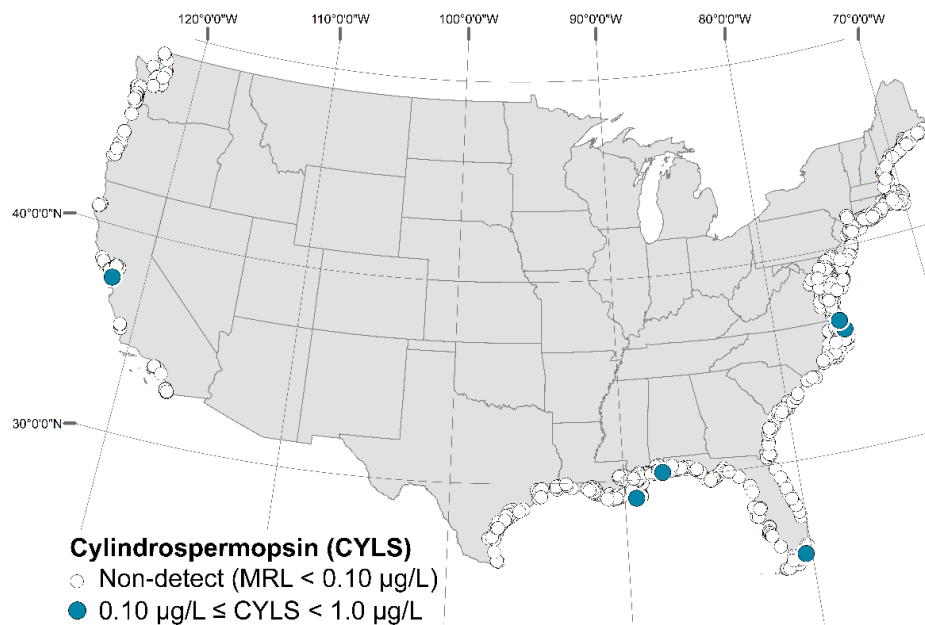


Figure 3. Cylindrospermopsin occurrence in U.S. estuarine and coastal samples by LC/MS/MS.

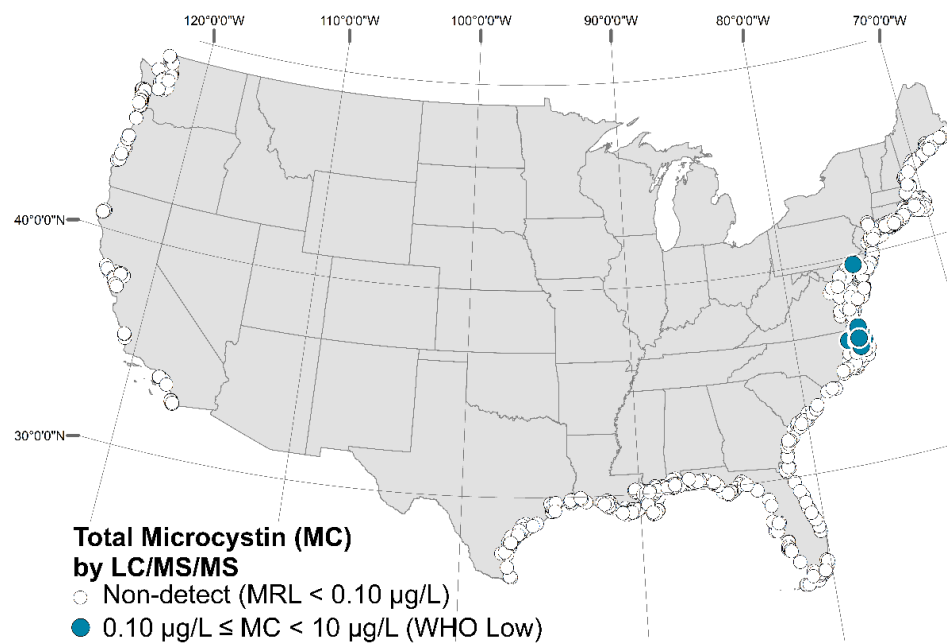


Figure 4. Total microcystin occurrence in U.S. estuarine and coastal samples by LC/MS/MS.

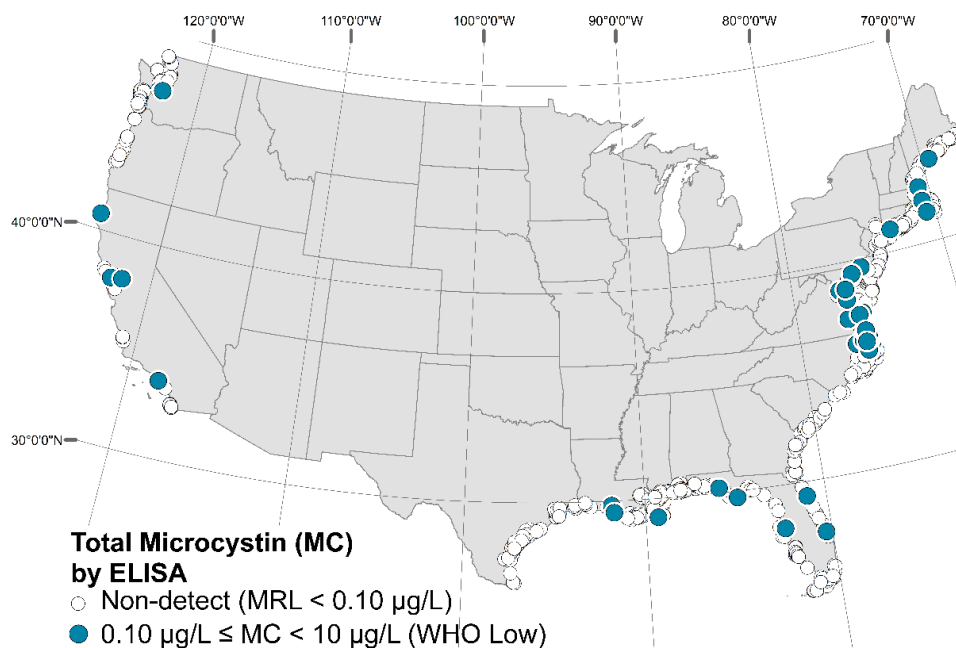


Figure 5. Microcystins occurrence in U.S. estuarine and coastal samples by ELISA.

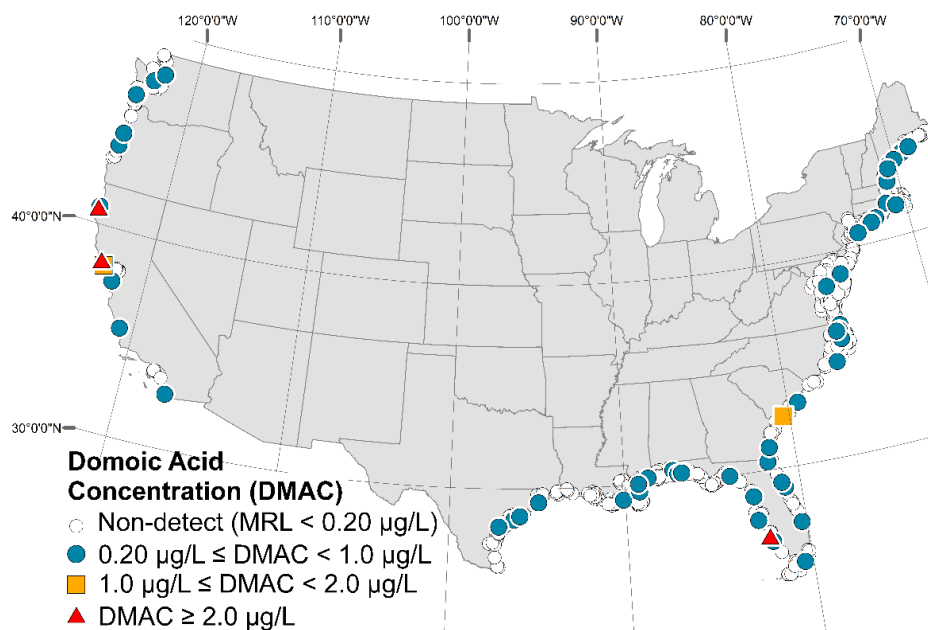


Figure 6. Domoic acid occurrence in U.S. estuarine and coastal samples by LC/MS/MS.

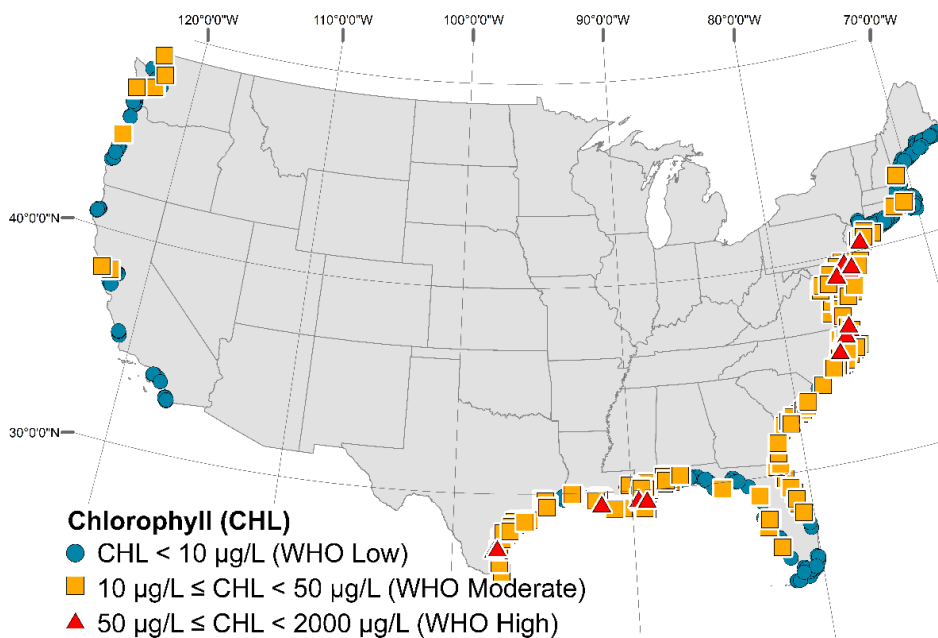


Figure 7. Chlorophyll occurrence in U.S. estuarine and coastal samples.

3.4. ALGAL TOXINS AND CYANOTOXINS OCCURRENCE IN THE CONTEXT OF MEASURED SALINITY

Algal toxin and cyanotoxin detections and chlorophyll were compared to salinity (Figure 8). ANAA and CYLS occurred over a wide range of salinity, without significant concentrations changes with increasing salinity (Figure 8a). DMAC occurred in samples with salinity ranging from 0.79 to 46 PPT (Figure 8b). The highest DMAC concentrations occurred in samples with salinity around 35 PPT. DMAC occurred in brackish (0.5-35 PPT, 90% of samples) and salt waters (35-50 PPT, 10% of samples). Microcystins by LC/MS/MS occurred in samples with salinity ranging from 0.05 to 4.5 PPT, with a mean salinity of 1.9 PPT (Figure 8c). Microcystins detected by ELISA occurred in samples with salinity ranging from 0.05 to 37 PPT, with a mean salinity of 11 PPT (Figure 8c). Twelve percent of samples with microcystins detected by ELISA occurred in freshwater, 78% in brackish water, and 10% in salt water. Chlorophyll occurred in freshwater, brackish, salt, and brine water (Figure 8d).

3.5. RECREATIONAL RISK ASSESSMENT FOR MICROCYSTIN EPOSURE IN U.S. ESTUARIES AND COASTAL WATERS BASED ON WORLD HEALTH ORGANIZATION AND U.S. ENVIRONMENTAL PROTECTION AGENCY FRESHWATER GUIDELINES

Based on recreational health thresholds established by WHO for potential microcystins exposure in freshwater, all samples analyzed for microcystins by ELISA and LC/MS/MS (total microcystins calculated as the sum of all 10 congeners analyzed) fell within the low risk level category (Table 1). On the basis of chlorophyll, 63% fell within the low threshold, 35% fell within the moderate threshold, and 1.9% fell within the high threshold.

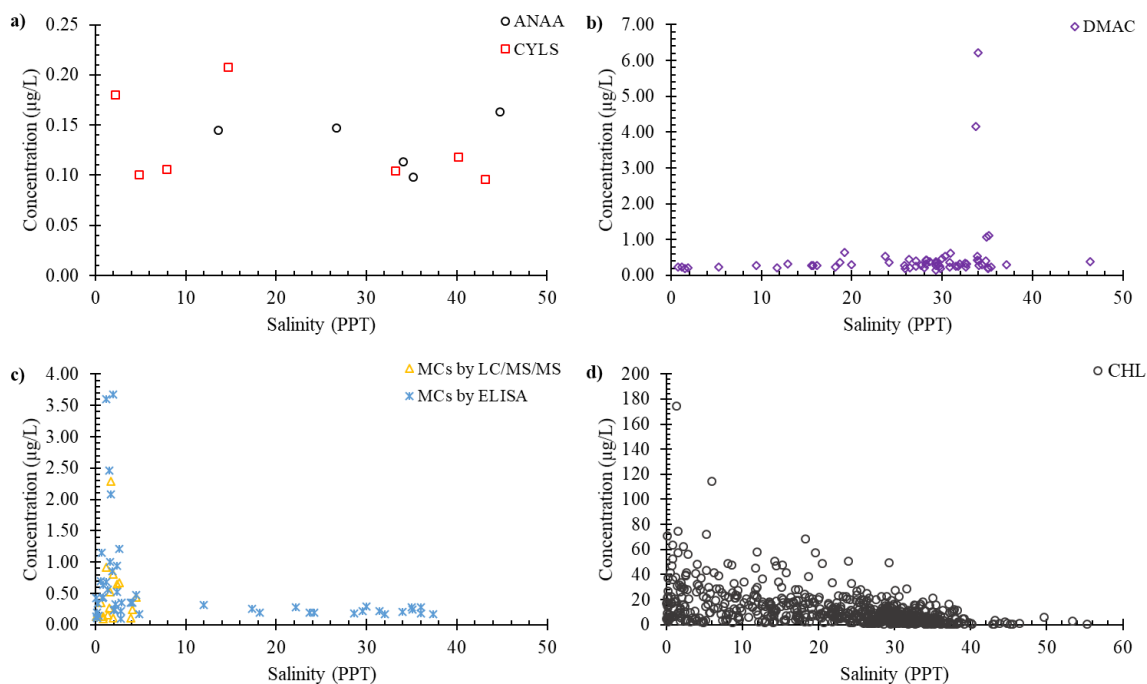


Figure 8. Comparison of a) anatoxin-a (ANAA) and cylindrospermopsin (CYLS), b) domoic acid (DMAC), c) microcystins by LC/MS/MS and ELISA, and d) chlorophyll to measured salinity.

WHO also recommends using cyanobacteria abundance to determine potential risk thresholds, but cyanobacteria were not analyzed in the coastal and estuarine samples. As mentioned in previous work, risk levels increased with less specific measurements (Loftin et al., 2016). Chlorophyll is less specific, and had samples categorized within higher risk levels compared to microcystins by ELISA and LC/MS/MS (Figures 9 and 10). Of the 50 samples that had microcystins detected by ELISA, risk levels based on microcystin and chlorophyll agreed in 17 samples (34%, Figure 9). Of the 16 samples that had microcystins detected by LC/MS/MS, risk levels based on microcystin and chlorophyll agreed in only one sample (Figure 10).

Table 1. Percentage of samples by ELISA, LC/MS/MS, and chlorophyll that fall into WHO recreational health threshold categories for potential microcystin exposure.

WHO relative health threshold	Percentage of samples (%) by category		
	Microcystin ELISA	Total Microcystins by LC/MS/MS	Chlorophyll
Low	100	100	63
Moderate	0.0	0.0	35
High	0.0	0.0	1.9
Very High	0.0	0.0	0.0

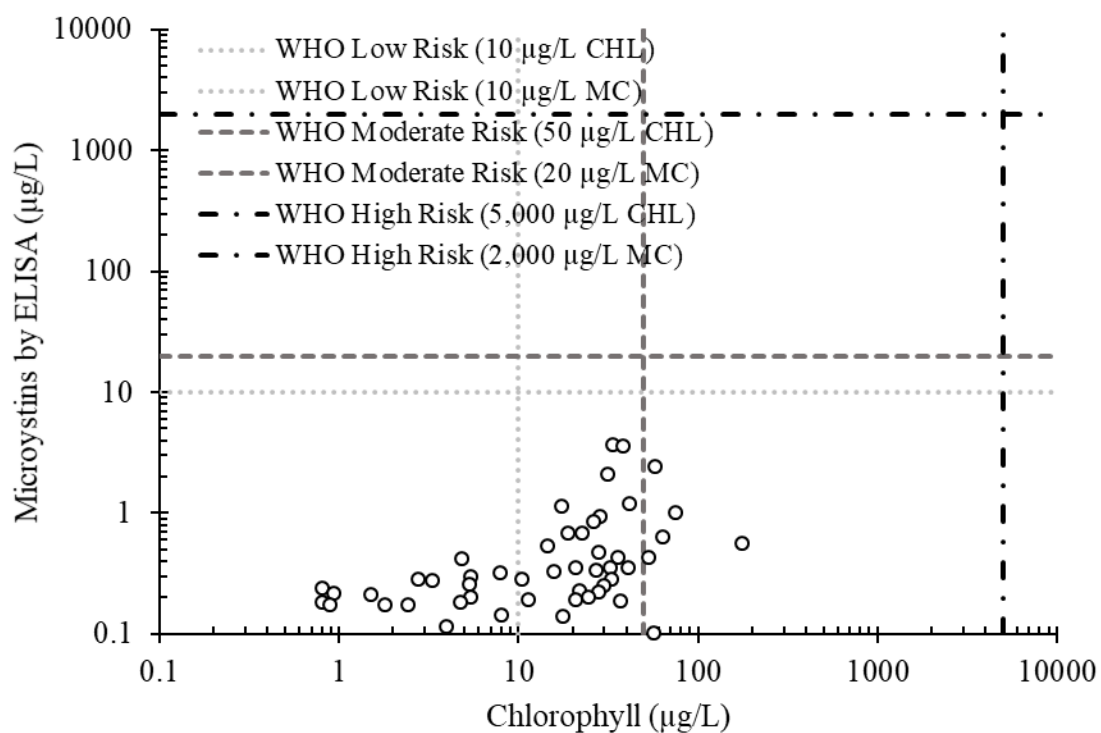


Figure 9. Comparison of microcystins measured by ELISA and chlorophyll with WHO relative health risk thresholds noted. Only samples with detections by ELISA are plotted against chlorophyll.

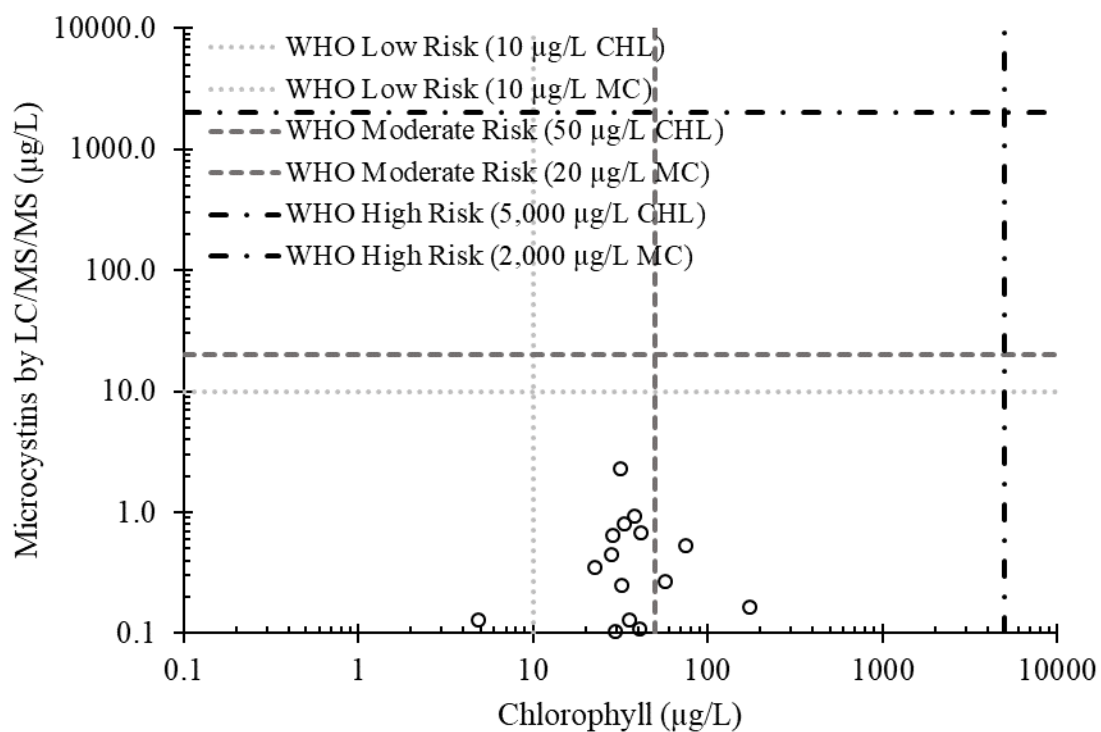


Figure 10. Comparison of microcystins measured by LC/MS/MS and chlorophyll with WHO relative health risk thresholds noted. Only samples with detections by LC/MS/MS are plotted against chlorophyll.

The U.S. EPA released recreational exposure guidelines for microcystins and cylindrospermopsin with limits of 8 µg/L and 15 µg/L, respectively (USEPA, 2019). Total microcystins by LC/MS/MS and microcystins screened by ELISA all fell under the recommended 8 µg/L concentration. Cylindrospermopsin was below the EPA recommended 15 µg/L concentration in all samples.

4. DISCUSSION

Transport of cyanobacteria and cyanotoxins from freshwater environments to coastal and estuarine systems may have consequences for human and environmental health. The major findings of this study (including samples analyzed for algal toxins, cyanotoxins, and chlorophyll from coastal and estuarine systems during the 2015 NCCA) indicate that domoic acid was the most commonly detected algal toxin in U.S. estuaries, microcystins were the most commonly detected cyanotoxin in these systems, the relationship between salinity and the presence of cyanotoxins in coastal and estuarine systems needs more study, and WHO guidelines applied to coastal and estuarine systems resulted in differing risk assessments based on the parameter used.

4.1. DOMOIC ACID WAS DETECTED IN MANY COASTAL CONTIGUOUS U.S. ESTUARY SYSTEMS TESTED

Domoic acid was detected in 76% of contiguous U.S. coastal states (Pacific, Gulf, and Atlantic) during the 2015 NCCA. States that did not have domoic acid detections included Alabama, Connecticut, New Hampshire, New Jersey, and Virginia. The most significant impacts of domoic acid in the U.S. have been documented along the west coast, but have been detected along the U.S. east coast, Gulf of Mexico, and coastlines worldwide (Pan et al., 2001; Tango and Butler, 2008; Thessen and Stoecker, 2008; Trainer et al., 2012). Cases of amnesic shellfish poisoning (ASP, domoic acid as causative agent) in humans have been minimized by the implementation of strict shellfish monitoring guidelines; however, the effects of chronic, sub-lethal doses of domoic acid on humans and animals via shellfish consumption are still unclear (Lefebvre and

Robertson, 2010). Chronic exposure to concentrations below regulatory limits in food has recently been linked to impaired cognitive function in mice (Lefebvre et al., 2017) and to structural and chemical changes in non-human primate brains (Petroff et al., 2019).

4.2. MULTIPLE CLASSES OF CYANOTOXINS OCCURRED IN U.S. ESTUARIES AND COASTAL SYSTEMS

Anatoxin-a, cylindrospermopsin, and microcystins were detected in estuary water 14, 24, and 14% of coastal states, respectively, by LC/MS/MS. Microcystins by ELISA were detected in estuaries of 52% of coastal states. Anatoxin-a has been reported in brackish water (Mazur and Pliński, 2003), and both toxins have been reported in coastal California creeks and lagoons (Tatters et al., 2019, 2017). While concentrations were low when detected, 0.10 to 0.16 $\mu\text{g/L}$ for anatoxin-a and 0.10 to 0.21 $\mu\text{g/L}$ for cylindrospermopsin, and were detected infrequently, they occurred along the Pacific, Gulf of Mexico, and Atlantic coastlines. Studies of microcystins in coastal and estuarine waters have received more attention than other cyanotoxin classes and have been measured in coastal waters worldwide (Preece et al., 2017). Microcystin producing cyanobacteria have reportedly increased in freshwater discharged in to the Atlantic Ocean on the U.S. east coast, Gulf of Mexico, and Pacific Ocean on the U.S. west coast (Howard et al., 2017; Preece et al., 2017; Tatters et al., 2019, 2017). In this study, microcystins by LC/MS/MS were detected on the east coast of the U.S. including Albemarle and Pamlico Sounds and the Delaware Bay. Microcystins were detected by ELISA on the Pacific and Atlantic coasts, as well as the Gulf of Mexico coastline. Increased detections by ELISA are likely due to the specificity of the ELISA itself, which

is designed to react with the ADDA group, common to all microcystin congeners, while only 10 congeners were monitored by LC/MS/MS.

4.3. SALINITY AND TOXINS

The relationship between salinity and algal toxins and cyanotoxins was examined. Domoic acid is primarily produced by *Pseudo-nitzschia*, a genus of marine planktonic diatoms. Laboratory and ecological studies have indicated that domoic acid production is highest when salinity is 30 PPT or greater, and that in low salinity water (<10 PPT) domoic acid production ceases (Doucette et al., 2008; Macintyre et al., 2011). In this study, the highest concentrations of domoic acid occurred when salinity was around 35 PPT (average salinity of sea water) but occurred over a wide range of salinity concentrations from 0 to 46 PPT. Concentrations of anatoxin-a and cylindrospermopsin were not impacted by salinity when they occurred, which may indicate that they are produced in situ in low amounts. Microcystins by LC/MS/MS and ELISA occurred in water with salinity up to 37 PPT, with the highest concentrations detected in water with less than 5 PPT salinity. This may indicate that the occurrence of microcystins is more strongly linked to freshening of estuaries than anatoxin-a or cylindrospermopsin.

4.4. UNKNOWN IMPACTS OF MULTIPLE TOXIN CLASSES PRESENT IN ESTUARIES AND COASTAL WATER SYSTEMS

Risk assessment for cyanotoxins in coastal and estuarine environments is challenging due to the complex nature of estuary systems. Seasonal variations in climate, precipitation events, the flux of freshwater entering coastal systems, and mixing in estuary systems impact the distribution of cyanobacteria and cyanotoxins entering the

systems as well as the fate of toxin-producing marine species. In this study, multiple classes of algal toxins and cyanotoxins occurred in U.S. coastal and estuary systems. The effects of multiple classes of toxins in estuary systems is still unknown, as synergistic effects between cyanotoxins and other toxins are still unknown. Implementation of remote monitoring for cyanobacteria in coastal freshwater bodies might be considered when performing future coastal studies for cyanotoxins to supplement the results and support findings. Because there is evidence of cyanobacteria proliferating in U.S. coastal water, evaluating whether the toxins were produced in the system or upstream is critical to human, animal, and environmental risk assessment.

SUPPORTING INFORMATION

All LC/MS/MS cyanotoxin data can be obtained via weblink (not yet public). All other National Coastal Condition Assessment 2015 data can be obtained via weblink (not yet public).

ACKNOWLEDGEMENTS

This work was supported by EPA grant # DW-14-95799601 and the USGS Toxic Substances Hydrology Program. Any use of trade, product, or firm names is for descriptive purposes only and does not imply endorsement by the U.S. Government.

REFERENCES

- Arar, E.J., Collins, G.B., 1997a. Method 445.0: In Vitro Determination of Chlorophyll a and Pheophytin a in Marine and Freshwater Algae by Fluorescence, U.S. Environmental Protection Agency. Washington, DC.
- Arar, E.J., Collins, G.B., 1997b. Method 446.0: In Vitro Determination of Chlorophylls a, b, c1 + c2 and Pheopigments in Marine And Freshwater Algae by Visible Spectrophotometry, U.S. Environmental Protection Agency.
- Albay, M., Matthiensen, A., Codd, G.A., 2005. Occurrence of toxic blue-green algae in the Kucukcekmece Lagoon (Istanbul, Turkey). *Environ. Toxicol.* 20, 277–284. <https://doi.org/10.1002/tox.20118>
- Apte, S.K., Reddy, B.R., Thomas, J., 1987. Relationship between Sodium Influx and Salt Tolerance of Nitrogen- Fixing Cyanobacteria. *Appl. Environ. Microbiol.* 53, 1934–1939.
- Arar, E.J., Collins, G.B., 1997a. Method 445.0: In Vitro Determination of Chlorophyll a and Pheophytin a in Marine and Freshwater Algae by Fluorescence, U.S. Environmental Protection Agency. Washington, DC.
- Arar, E.J., Collins, G.B., 1997b. Method 446.0: In Vitro Determination of Chlorophylls a, b, c1 + c2 and Pheopigments in Marine And Freshwater Algae by Visible Spectrophotometry, U.S. Environmental Protection Agency.
- Atkins, R., Rose, T., Brown, R.S., Robb, M., 2001. The *Microcystis* cyanobacteria bloom in the Swan River - February 2000. *Water Sci. Technol.* 43, 107–114.
- Bartolomé, M.C., D’Ors, A., Sánchez-Fortún, S., 2009. Toxic effects induced by salt stress on selected freshwater prokaryotic and eukaryotic microalgal species. *Ecotoxicology* 18, 174–179. <https://doi.org/10.1007/s10646-008-0269-y>
- Batterton, J.C., Van Baalen, C., 1971. Growth Responses of Blue-green Algae to Sodium Chloride Concentration. *Arch. Mikrobiol.* 76, 151–165.
- Batterton, J.C., Van Baalen, C., Baalen, C., 1971. Growth responses of blue-green algae to sodium chloride concentration. *Arch. Mikrobiol.* 76, 151–165. <https://doi.org/10.1007/BF00411789>
- Black, K., Yilmaz, M., Philips, E.J., 2011. Growth and Toxin Production by *Microcystis Aeruginosa* PCC 7806 (Kutzing) Lemmerman at Elevated Salt Concentrations. *J. Environ. Prot. (Irvine., Calif.)* 02, 669–674. <https://doi.org/10.4236/jep.2011.26077>

- Blackburn, S.I., McCausland, M.A., Bolch, C.J.S., Newman, S.J., Jones, G.J., 1996. Effect of salinity on growth and toxin production in cultures of the bloom-forming cyanobacterium *Nodularia spumigena* from Australian waters. *Phycologia* 35, 511–522.
- Blumwald, E., Mehlhorn, R.J., Packer, L., 1983. Studies of osmoregulation in salt adaptation of cyanobacteria with ESR spin-probe techniques. *Proc. Natl. Acad. Sci. U. S. A.* 80, 2599–602. <https://doi.org/10.1073/pnas.80.9.2599>
- Blumwald, E., Tel-or, E., 1984. Salt Adaptation of the Cyanobacterium *Synechococcus* 6311 Growing in a Continuous Culture (Turbidostat). *Plant Physiol.* 74, 183–185.
- Blumwald, E., Tel-or, E., 1982a. Structural Aspects of the Adaptation of *Nostoc muscorum* to Salt. *Arch. Microbiol.* 132, 163–167.
- Blumwald, E., Tel-or, E., 1982b. Osmoregulation and Cell Composition in Salt-Adaptation of *Nostoc muscorum*. *Arch. Microbiol.* 132, 168–172. <https://doi.org/10.3747/pdi.2011.00058>
- Bouvy, M., Molica, R., De Oliveira, S., Marinho, M., Beker, B., 1999. Dynamics of a toxic cyanobacterial bloom (*Cylindrospermopsis raciborskii*) in a shallow reservoir in the semi-arid region of northeast Brazil. *Aquat. Microb. Ecol.* 20, 285–297.
- Calandrino, E.S., Paerl, H.W., 2011. Determining the potential for the proliferation of the harmful cyanobacterium *Cylindrospermopsis raciborskii* in Currituck Sound, North Carolina. *Harmful Algae* 11, 1–9. <https://doi.org/10.1016/j.hal.2011.04.003>
- Cañedo-Argüelles, M., Kefford, B., Schäfer, R., 2019. Salt in freshwaters: Causes, effects and prospects - Introduction to the theme issue. *Philos. Trans. R. Soc. B Biol. Sci.* 374. <https://doi.org/10.1098/rstb.2018.0002>
- Chen, L., Mao, F., Kirumba, G.C., Jiang, C., Manefield, M., He, Y., 2015. Changes in metabolites, antioxidant system, and gene expression in *Microcystis aeruginosa* under sodium chloride stress. *Ecotoxicol. Environ. Saf.* 122, 126–135. <https://doi.org/10.1016/j.ecoenv.2015.07.011>
- Chorus, I., Bartram, J., 1999. *Toxic Cyanobacteria in Water: A guide to their public health consequences, monitoring and management.* Spon Press, London.
- Díez-Quijada, L., Prieto, A.I., Guzmán-Guillén, R., Jos, A., Cameán, A.M., 2019. Occurrence and toxicity of microcystin congeners other than MC-LR and MC-RR: A review. *Food Chem. Toxicol.* 125, 106–132. <https://doi.org/10.1016/j.fct.2018.12.042>

- Doucette, G.J., King, K.L., Thessen, A.E., Dortch, Q., 2008. The effect of salinity on domoic acid production by the diatom *Pseudo-nitzschia multiseries*. *Nov. Hedwigia* 133, 31–46.
- EPA, 2015. National Coastal Assessment 2015: Field Operations Manual.
- Fernandes, T.A., Iyer, V., Apte, S.K., 1993. Differential responses of nitrogen-fixing cyanobacteria to salinity and osmotic stresses. *Appl. Environ. Microbiol.* 59, 899–904.
- Gibble, C.M., Kudela, R.M., 2014. Detection of persistent microcystin toxins at the land-sea interface in Monterey Bay, California. *Harmful Algae* 39, 146–153. <https://doi.org/10.1016/j.hal.2014.07.004>
- Graham, J., Loftin, K., Kamman, N., 2009. Monitoring recreational freshwaters. *Lakeline* 29, 18–24.
- Graham, J.L., Loftin, K.A., Meyer, M.T., Ziegler, A.C., 2010. Cyanotoxin Mixtures and Taste-and-Odor Compounds in Cyanobacterial Blooms from the Midwestern United States. *Environ. Sci. Technol.* 44, 7361–7368. <https://doi.org/10.1021/es1008938>
- Hagemann, M., 2011. Molecular biology of cyanobacterial salt acclimation. *FEMS Microbiol. Rev.* 35, 87–123. <https://doi.org/10.1111/j.1574-6976.2010.00234.x>
- Hagemann, M., Erdmann, N., Schiewer, U., 1989. Salt adaptation of the cyanobacteria *Microcystis firma* and *Synechocystis aquatilis* in turbidostat cultures. I. Steady state values. *Arch. Hydrobiol. Suppl. Algal. Stud.* 57, 425–435.
- Howard, M.D.A., Nagoda, C., Kudela, R.M., Hayashi, K., Tatters, A., Caron, D.A., Busse, L., Brown, J., Sutula, M., Stein, E.D., 2017. Microcystin prevalence throughout lentic waterbodies in coastal southern California. *Toxins (Basel)*. 9, 1–21. <https://doi.org/10.3390/toxins9070231>
- Ladas, N.P., Papageorgiou, G.C., 2000. The salinity tolerance of freshwater cyanobacterium *Synechococcus* sp. PCC 7942 is determined by its ability for osmotic adjustment and presence in osmolyte sucrose. *Photosynthetica* 38, 343–348.
- Lefebvre, K.A., Kendrick, P.S., Ladiges, W., Hiolski, E.M., Ferriss, B.E., Smith, D.R., Marcinek, D.J., 2017. Chronic low-level exposure to the common seafood toxin domoic acid causes cognitive deficits in mice. *Harmful Algae* 64, 20–29. <https://doi.org/10.1016/j.hal.2017.03.003>Chronic
- Lefebvre, K.A., Robertson, A., 2010. Domoic acid and human exposure risks: A review. *Toxicon* 56, 218–230. <https://doi.org/10.1016/j.toxicon.2009.05.034>

- Lehman, P.W., Boyer, G., Hall, C., Waller, S., Gehrts, K., 2005. Distribution and toxicity of a new colonial *Microcystis aeruginosa* bloom in the San Francisco Bay Estuary, California. *Hydrobiologia* 541, 87–99. <https://doi.org/10.1007/s10750-004-4670-0>
- Lehtimäki, J., Moisander, P., Sivonen, K., Kononen, K., 1997. Growth, Nitrogen Fixation, and Nodularin Production by Two Baltic Sea Cyanobacteria. *Appl. Environ. Microbiol.* 63, 1647–1656.
- Lewitus, A.J., Brock, L.M., Burke, M.K., DeMattio, K.A., Wilde, S.B., 2008. Lagoonal stormwater detention ponds as promoters of harmful algal blooms and eutrophication along the South Carolina coast. *Harmful Algae* 8, 60–65. <https://doi.org/10.1016/j.hal.2008.08.012>
- Loftin, K.A., Graham, J.L., Hilborn, E.D., Lehmann, S.C., Meyer, M.T., Dietze, J.E., Griffith, C.B., 2016. Cyanotoxins in inland lakes of the United States: Occurrence and potential recreational health risks in the EPA National Lakes Assessment 2007. *Harmful Algae* 56, 77–90. <https://doi.org/10.1016/j.hal.2016.04.001>
- Loftin, K.A., Meyer, M.T., Rubio, F., Kamp, L., Humphries, E., Whereat, E., 2008. Comparison of two cell lysis procedures for recovery of microcystins in water samples, USGS Open-file Report 2008-1341.
- Lukatelich, R.J., McComb, A.J., 1986. Nutrient levels and the development of diatom and blue-green algal blooms in a shallow Australian estuary. *J. Phytoplankt. Res.* 8, 597–618.
- Macintyre, H.L., Stutes, A.L., Smith, W.L., Dorsey, C.P., Abraham, A., Dickey, R.W., 2011. Environmental correlates of community composition and toxicity during a bloom of *Pseudo-nitzschia* spp. in the northern Gulf of Mexico. *J. Plankton Res.* 33, 273–295. <https://doi.org/10.1093/plankt/fbq146>
- Mackay, M.A., Norton, R.S., Borowitzka, L.J., 1984. Organic Osmoregulatory Solutes in Cyanobacteria. *J. Gen. Microbiol.* 130, 2177–2191. <https://doi.org/10.1099/00221287-130-9-2177>
- Mackay, M.A., Norton, R.S., Borowitzka, L.J., 1983. Marine blue-green algae have a unique osmoregulatory system. *Mar. Biol.* 73, 301–307. <https://doi.org/10.1007/BF00392256>
- Magalhães, V.F., Marinho, M.M., Domingos, P., Oliveira, A.C., Costa, S.M., Azevedo, L.O., Azevedo, S.M.F.O., 2003. Microcystins (cyanobacteria hepatotoxins) bioaccumulation in fish and crustaceans from Sepetiba Bay (Brasil, RJ). *Toxicon* 42, 289–295. [https://doi.org/10.1016/S0041-0101\(03\)00144-2](https://doi.org/10.1016/S0041-0101(03)00144-2)

- Martín-Luna, B., Sevilla, E., Bes, M.T., Fillat, M.F., Peleato, M.L., 2015. Variation in the synthesis of microcystin in response to saline and osmotic stress in *Microcystis aeruginosa* PCC7806. *Limnetica* 34, 205–214.
- Mazur-Marzec, H., Zeglińska, L., Pliński, M., 2005. The effect of salinity on the growth, toxin production, and morphology of *Nodularia spumigena* isolated from the Gulf of Gdańsk, southern Baltic Sea. *J. Appl. Phycol.* 17, 171–179. <https://doi.org/10.1007/s10811-005-5767-1>
- Mazur, H., Pliński, M., 2003. *Nodularia spumigena* blooms and the occurrence of hepatotoxin in the Gulf of Gdańsk. *Oceanologia* 45, 305–316.
- Miller, M.A., Kudela, R.M., Mekebri, A., Crane, D., Oates, S.C., Tinker, M.T., Staedler, M., Miller, W.A., Toy-Choutka, S., Dominik, C., Hardin, D., Langlois, G., Murray, M., Ward, K., Jessup, D.A., 2010. Evidence for a Novel Marine Harmful Algal Bloom: Cyanotoxin (Microcystin) Transfer from Land to Sea Otters. *PLoS One* 5, e12576. <https://doi.org/10.1371/journal.pone.0012576>
- Moisander, P.H., McClinton, E., Paerl, H.W., 2002. Salinity effects on growth, photosynthetic parameters, and nitrogenase activity in estuarine planktonic cyanobacteria. *Microb. Ecol.* 43, 432–442. <https://doi.org/10.1007/s00248-001-1044-2>
- Moore, D.J., Reed, R.H., Stewart, W.D., 1985. Responses of Cyanobacteria to Low Level Osmotic Stress : Implications for the Use of Buffers. *J. Gen. Microbiol.* 131, 1267–1272. <https://doi.org/10.1099/00221287-131-6-1267>
- NOAA National Centers for Environmental Information, 2016. State of the Climate: National Climate Report for Annual 2015 [WWW Document]. URL <https://www.ncdc.noaa.gov/sotc/national/201513> (accessed 7.10.19).
- Oleson, D.J., Makarewicz, J.C., 1990. Effect of sodium and nitrate on growth of *Anabaena flos-aquae* (cyanophyta). *J. Phycol.* 26, 593–595.
- Orr, P.T., Jones, G.J., Douglas, G.B., 2004. Response of cultured *Microcystis aeruginosa* from the Swan River, Australia, to elevated salt concentration and consequences for bloom and toxin management in estuaries. *Mar. Freshw. Res.* 55, 277–283. <https://doi.org/10.1071/MF03164>
- Otsuka, S., Suda, S., Li, R., Watanabe, M., Oyaizu, H., Matsumoto, S., Watanabe, M.M., 1999. Characterization of morphospecies and strains of the genus *Microcystis* (Cyanobacteria) for a reconsideration of species classification. *Phycol. Res.* 47, 189–197. <https://doi.org/10.1046/j.1440-1835.1999.00162.x>

- Padisák, J., 1997. *Cylindrospermopsis raciborskii* (Woloszynska) Seenayya et Subbu Raju, an expanding, highly adaptive cyanobacterium: worldwide distribution and review of its ecology. *Arch. Für Hydrobiol. Suppl. Monogr. Beitrage* 107, 563–593.
- Paerl, H., Bland, P.T., Blackwell, J.H., Bowles, N.D., 1984. The Effects of Salinity on the Potential of a Blue-Green Algal (*Microcystis aeruginosa*) Bloom in the Neuse River Estuary, N.C.
- Paerl, H.W., Fulton, R.S., Moisander, P.H., Dyble, J., 2001. Harmful Freshwater Algal Blooms, With an Emphasis on Cyanobacteria. *Sci. World J.* 1, 76–113. <https://doi.org/10.1100/tsw.2001.16>
- Pan, Y., Parsons, M.L., Busman, M., Moeller, P.D.R., Dortch, Q., Powell, C.L., Doucette, G.J., 2001. *Pseudo-nitzschia* sp. cf. *pseudodelicatissima* - A confirmed producer of domoic acid from the northern Gulf of Mexico. *Mar. Ecol. Prog. Ser.* 220, 83–92. <https://doi.org/10.3354/meps220083>
- Pandhal, J., Ow, S.Y., Wright, P.C., Biggs, C.A., 2009. Comparative proteomics study of salt tolerance between a nonsequenced extremely halotolerant cyanobacterium and its mildly halotolerant relative using *in vivo* metabolic labeling and *in vitro* isobaric labeling. *J. Proteome Res.* 8, 818–828. <https://doi.org/10.1021/pr800283q>
- Petroff, R., Richards, T., Crouthamel, B., McKain, N., Stanley, C., Grant, K.S., Shum, S., Jing, J., Isoherranen, N., Burbacher, T.M., 2019. Chronic, low-level oral exposure to marine toxin, domoic acid, alters whole brain morphometry in nonhuman primates. *Neurotoxicology* 72, 114–124. <https://doi.org/10.1016/j.neuro.2019.02.016>
- Pires, L.M.D., Karlsson, K.M., Meriluoto, J.A.O., Kardinaal, E., Visser, P.M., Siewertsen, K., Donk, E. Van, Ibelings, B.W., 2004. Assimilation and depuration of microcystin-LR by the zebra mussel, *Dreissena polymorpha*. *Aquat. Toxicol.* 69, 385–396. <https://doi.org/10.1016/j.aquatox.2004.06.004>
- Pouria, S., De Andrade, A., Barbosa, J., Cavalcanti, R.L., Barreto, V.T.S., Ward, C.J., Preiser, W., Poon, G.K., Neild, G.H., Codd, G.A., 1998. Fatal microcystin intoxication in haemodialysis unit in Caruaru, Brazil. *Lancet* 352, 21–26. [https://doi.org/10.1016/S0140-6736\(97\)12285-1](https://doi.org/10.1016/S0140-6736(97)12285-1)
- Preece, E.P., Hardy, F.J., Moore, B.C., Bryan, M., 2017. A review of microcystin detections in Estuarine and Marine waters: Environmental implications and human health risk. *Harmful Algae* 61, 31–45. <https://doi.org/10.1016/j.hal.2016.11.006>
- Preece, E.P., Moore, B.C., Hardy, F.J., 2015. Transfer of microcystin from freshwater lakes to Puget Sound, WA and toxin accumulation in marine mussels (*Mytilus trossulus*). *Ecotoxicol. Environ. Saf.* 122, 98–105. <https://doi.org/10.1016/j.ecoenv.2015.07.013>

- Prinsloo DF, Pieterse AJH, 1994. Preliminary observations on the effect of increased concentrations of total dissolved salts on growth and photosynthetic rates in different algal species. *Water SA*.
- Rai, A.K., Abraham, G., 1993. Salinity tolerance and growth analysis of the cyanobacterium *Anabaena doliolum*. *Bull. Environ. Contam. Toxicol.* 51, 724–731. <https://doi.org/10.1007/BF00201651>
- Rai, A.K., Tiwari, S.P., 1999. NO₃- nutrition and salt tolerance in the cyanobacterium *Anabaena* sp. PCC 7120 and mutant strains. *J. Appl. Microbiol.* 86, 991–998.
- Reed, R.H., Richardson, D.L., Stewart, W.D.P., 1985. Na⁺ uptake and extrusion in the cyanobacterium *Synechocystis* PCC6714 in response to hypersaline treatment. Evidence for transient changes in plasmalemma Na⁺ permeability. *Biochim. Biophys. Acta* 814, 347–355.
- Reed, R.H., Stewart, W.D.P., 1985. Osmotic adjustment and organic solute accumulation in unicellular cyanobacteria from freshwater and marine habitats. *Mar. Biol.* 88, 1–9. <https://doi.org/10.1007/BF00393037>
- Reed, R.H., Borowitzka, L.J., Mackay, M.A., Chudek, J.A., Foster, R., Warr, S.R.C., Moore, D.J., Stewart, W.D.P., 1986. Organic solute accumulation in osmotically stressed cyanobacteria. *FEMS Microbiol. Rev.* 39, 51–56.
- Richardson, D.L., Reed, R.H., Stewart, W.D.P., 1983. *Synechocystis* PCC6803: a euryhaline cyanobacterium. *FEMS Microbiol. Lett.* 18, 99–102. <https://doi.org/10.1111/j.1574-6968.1983.tb00457.x>
- Robson, B.J., Hamilton, D.P., 2003. Summer flow event induces a cyanobacterial bloom in a seasonal Western Australian estuary. *Mar. Freshw. Res.* 54, 139–151. <https://doi.org/10.1071/MF02090>
- Rosen, B.H., Loftin, K.A., Graham, J.L., Stahlhut, K.N., Riley, J.M., Johnston, B.D., Senegal, S., 2018. Understanding the Effect of Salinity Tolerance on Cyanobacteria Associated with a Harmful Algal Bloom in Lake Okeechobee, Florida. <https://doi.org/10.3133/sir20185092>
- Sabour, B., Loudiki, M., Oudra, B., Oubraim, S., Fawzi, B., Fadlaoui, S., Chlaida, M., Vasconcelos, V., 2002. First results on *Microcystis ichthyoblabe* Kutz. toxic bloom in the hypertrophic Oued Mellah reservoir (Morocco). *Ann. Limnol. J. Limnol.* 38, 13–22. <https://doi.org/10.1051/Limn/2002001>
- Sand-Jensen, K., Jespersen, T.S., 2012. Tolerance of the widespread cyanobacterium *Nostoc commune* to extreme temperature variations (-269 to 105°C), pH and salt stress. *Oecologia* 169, 331–339. <https://doi.org/10.1007/s00442-011-2200-0>

- Sellner, K.G., Lacouture, R.V., Parrish, C.R., 1988. Effects of increasing salinity on a cyanobacteria bloom in the Potomac River estuary. *J. Plankton Res.* 10, 49–61.
- Stam, W.T., Holleman, H.C., 1979. Cultures of *Phormidium*, *Plectonema*, *Lyngbya* and *Synechococcus* (cyanophyceae) under different conditions: Their growth and morphological variability. *Acta Bot. Neerl.* 28, 45–66.
- Stam, W.T., Holleman, H.C., 1975. The influence of different salinities on growth and morphological variability of a number of *Phormidium* strains (cyanophyceae) in culture. *Acta Bot. Neerl.* 24, 379–390.
- Stulp, B.K., Stamp, W.T., 1984. Growth and morphology of *Anabaena* strains (Cyanophyceae, cyanobacteria) in cultures under different salinities. *Br. Phycol. J.* 19, 281–286. <https://doi.org/10.1080/00071618400650301>
- Tanabe, Y., Hodoki, Y., Sano, T., Tada, K., Watanabe, M.M., 2018. Adaptation of the freshwater bloom-forming cyanobacterium *Microcystis aeruginosa* to brackish water is driven by recent horizontal transfer of sucrose genes. *Front. Microbiol.* 9, 1–11. <https://doi.org/10.3389/fmicb.2018.01150>
- Tango, P.J., Butler, W., 2008. Cyanotoxins in Tidal Waters of Chesapeake Bay. *Northeast. Nat.* 15, 403–416. <https://doi.org/10.1656/1092-6194-15.3.403>
- Tatters, A.O., Howard, M.D.A., Nagoda, C., Busse, L., Gellene, A.G., Caron, D.A., 2017. Multiple Stressors at the Land-Sea Interface: Cyanotoxins at the Land-Sea Interface in the Southern California Bight. *Toxins (Basel)*. 9, 95. <https://doi.org/10.3390/toxins9030095>
- Tatters, A.O., Howard, M.D.A., Nagoda, C., Fetscher, A.E., Kudela, R.M., Caron, D.A., 2019. Heterogeneity of Toxin-Producing Cyanobacteria and Cyanotoxins in Coastal Watersheds of Southern California. *Estuaries and Coasts* 42, 958–975. <https://doi.org/10.1007/s12237-019-00546-w>
- Thessen, A.E., Stoecker, D.K., 2008. Distribution, abundance and domoic acid analysis of the toxic diatom genus *Pseudo-nitzschia* from the Chesapeake Bay. *Estuaries and Coasts* 31, 664–672. <https://doi.org/10.1007/s12237-008-9053-8>
- Tonk, L., Bosch, K., Visser, P.M., Huisman, J., 2007. Salt tolerance of the harmful cyanobacterium *Microcystis aeruginosa*. *Aquat. Microb. Ecol.* 46, 117–123. <https://doi.org/10.3354/ame046117>
- Trainer, V.L., Bates, S.S., Lundholm, N., Thessen, A.E., Cochlan, W.P., Adams, N.G., Trick, C.G., 2012. *Pseudo-nitzschia* physiological ecology, phylogeny, toxicity, monitoring and impacts on ecosystem health. *Harmful Algae* 14, 271–300. <https://doi.org/10.1016/j.hal.2011.10.025>

- USEPA, 2019. Recommended Human Health Recreational Ambient Water Quality Criteria for Swimming. <https://doi.org/10.1037//0033-2909.126.1.78>
- van Baalen, C., 1962. Studies on Marine Blue-Green Algae. *Bot. Mar.* 4, 129–139.
- Verspagen, J.M.H., Passarge, J., Jöhnk, K.D., Visser, P.M., Boers, P., Laanbroek, H.J., Huisman, J., 2006. Water Management Strategies against Toxic *Microcystis* Blooms in the Dutch Delta. *Ecol. Appl.* 16, 313–327.
- Waditee, R., Hibino, T., Nakamura, T., Incharoensakdi, A., Takabe, T., 2002. Overexpression of a Na⁺/H⁺ antiporter confers salt tolerance on a freshwater cyanobacterium, making it capable of growth in sea water. *Proc. Natl. Acad. Sci.* 99, 4109–4114. <https://doi.org/10.1073/pnas.052576899>
- Wood, J.D., Franklin, R.B., Garman, G., McIninch, S., Porter, A.J., Bukaveckas, P.A., 2014. Exposure to the Cyanotoxin Microcystin Arising from Interspecific Differences in Feeding Habits among Fish and Shellfish in the James River Estuary, Virginia. *Environ. Sci. Technol.* 48, 5194–5202. <https://doi.org/10.1021/es403491k>
- Wood, R., 2016. Acute animal and human poisonings from cyanotoxin exposure - A review of the literature. *Environ. Int.* 91, 276–282. <https://doi.org/10.1016/j.envint.2016.02.026>

SECTION

2. CONCLUSIONS

2.1. SINGLE PARTICLE ICP-MS DETECTION OF NANOPARTICLES IN SURFACE AND TREATED WATER

Single particle inductively coupled plasma mass spectrometry (SP-ICP-MS) has significant potential to be a direct monitoring technique for dissolved ions and metal oxide nanoparticles in surface and treated water. Titanium dioxide, cerium dioxide, zinc oxide, silver, and gold nanoparticles were monitored throughout various drinking water treatment processes including softening, coagulation, filtration, and disinfection. The sensitivity of this technique is applicable to anticipated environmental concentrations of these materials. However, certain assumptions must be made including particle shape, particle composition and density, and that one isotope can be monitored during a run. The next challenge for the environmental assessment of metal oxide nanoparticles is differentiating between naturally occurring nanoparticles and engineered nanoparticles and expanding instrument capability to monitor multiple isotopes in a single run. Furthermore, complementary techniques will be required to determine other salient parameters of the nanoparticles such as shape and hydrodynamic diameter.

2.2. CYANOTOXINS IN ESTUARINE ENVIRONMENTS BY LC/MS/MS

Liquid chromatography tandem mass spectrometry (LC/MS/MS) was used to detect algal toxins and cyanotoxins in estuaries of the contiguous United States. Multiple cyanotoxin classes were detected, including anatoxin-a, cylindrospermopsin, and

microcystins as well as domoic acid. Occurrence of anatoxin-a, cylindrospermopsin, and domoic acid could not be correlated to salinity, but most microcystins detections occurred in estuarine waters with <5 PPT salinity. There was a marked difference in detection frequency for microcystins by ELISA and LC/MS/MS, likely due to the principles of each technique. Using guidelines established by the WHO and US EPA, all samples fell into a low risk level category when using toxin concentration as the metric, while 37% of samples were in the moderate and high-risk categories by chlorophyll. The presence of multiple toxins co-occurring in estuary environments complicates human health risk assessment, as unknown synergistic effects may occur when multiple cyanotoxins, algal toxins, and other contaminants are present.

APPENDIX**SUPPLEMENTARY INFORMATION FOR PAPER II. FATE OF
NANOPARTICLES DURING ALUM AND FERRIC COAGULATION
MONITORED USING SINGLE PARTICLE ICP-MS**

Ariel R. Donovan¹, Craig D. Adams^{2,3}, Yinfu Ma^{1,2}, Chady Stephan⁴, Todd Eichholz⁵,

Honglan Shi^{1,2*}

¹Department of Chemistry and Environmental Research Center, Missouri University of Science and Technology, Rolla, Missouri, 65409, United States

²Center for Single Nanoparticle, Single Cell, and Single Molecule Monitoring (CS³M), Rolla, Missouri, 65409, United States

³Department of Civil Engineering, Saint Louis University, St. Louis, Missouri, 63103, United States

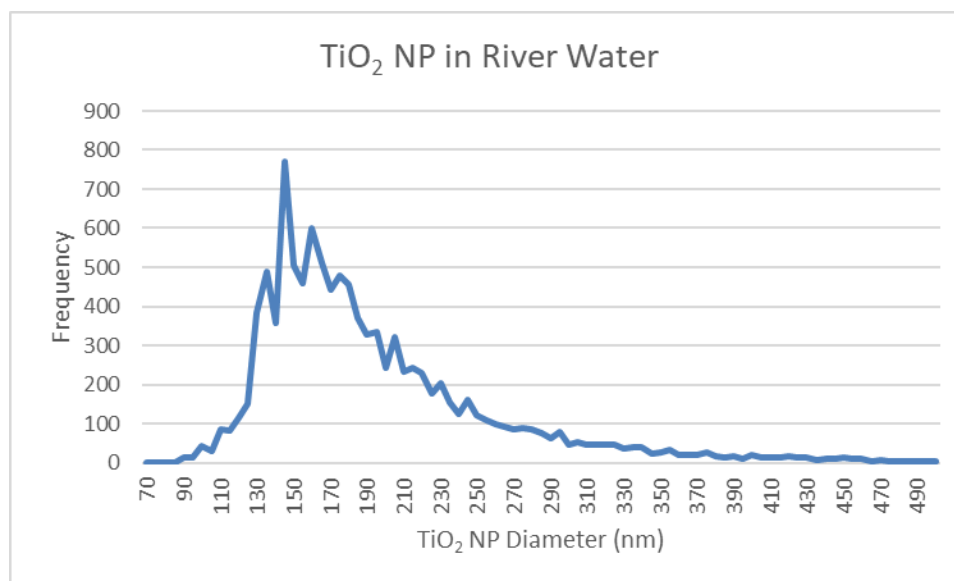
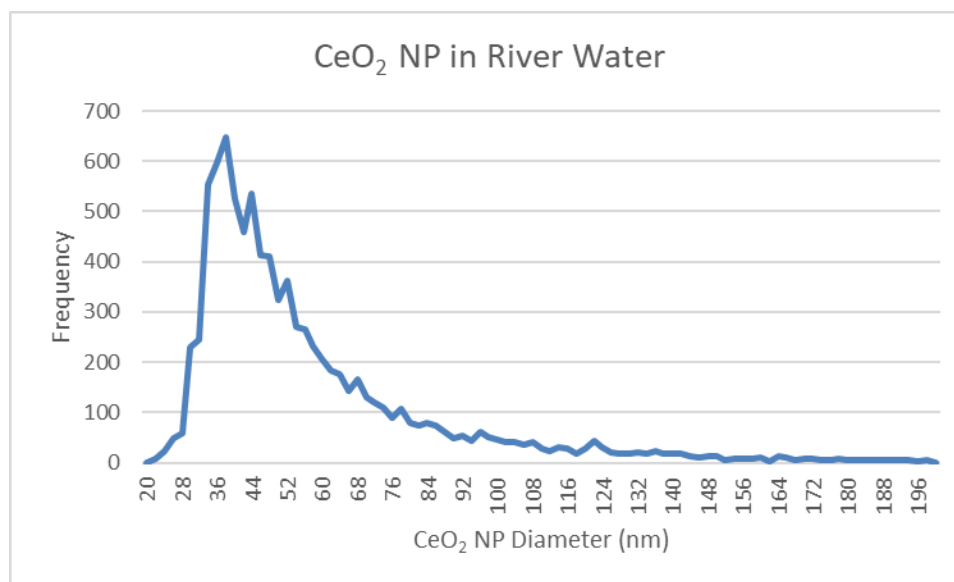
⁴PerkinElmer, Inc., 501 Rowntree Dairy Rd, Woodbridge, On, Canada, L4L 8H1

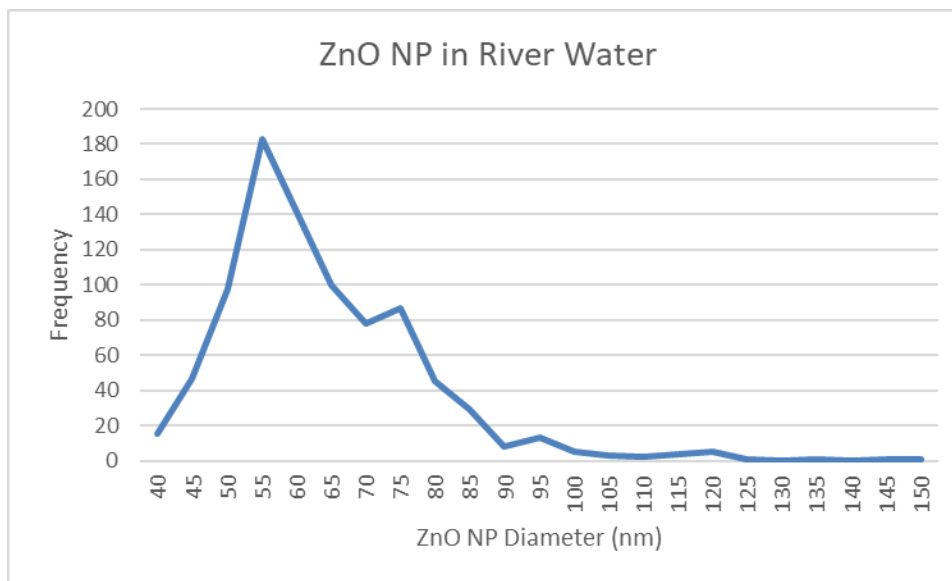
⁵Missouri Department of Natural Resources, Jefferson City, MO 65102, United States

*Corresponding Author

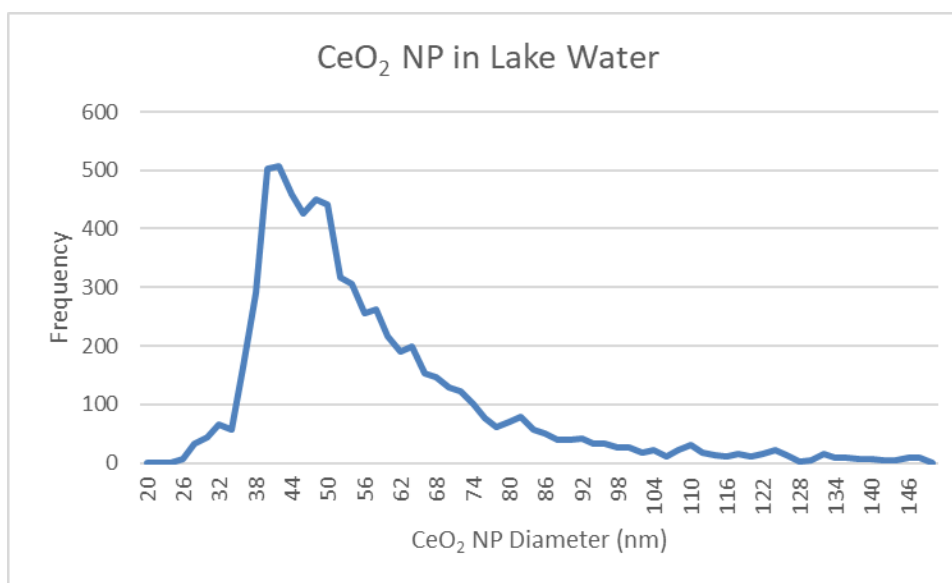
Address: Department of Chemistry
Missouri University of Science and Technology
400 West 11th Street
Rolla, MO 65409
Phone: 573-341-4433; Fax: 573-341-6033
E-mail: honglan@mst.edu

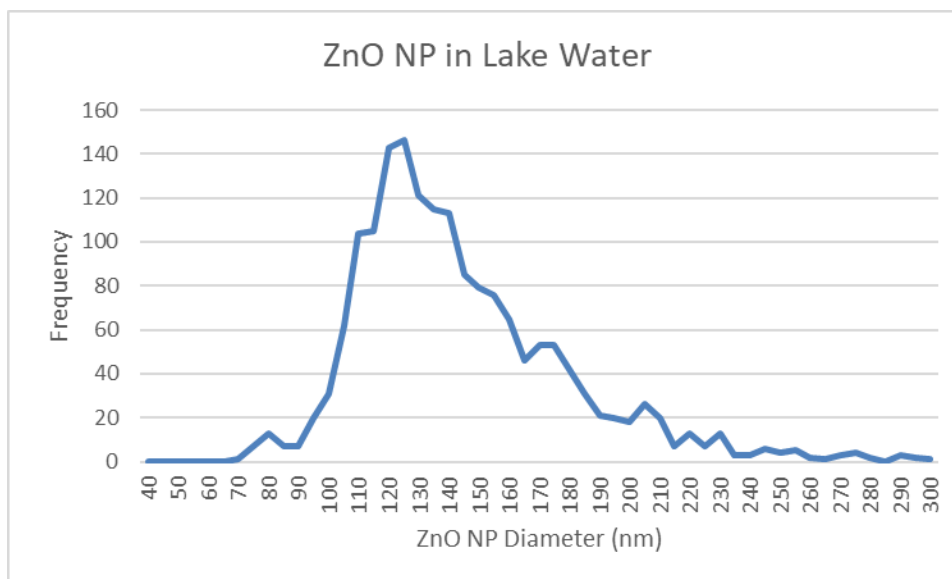
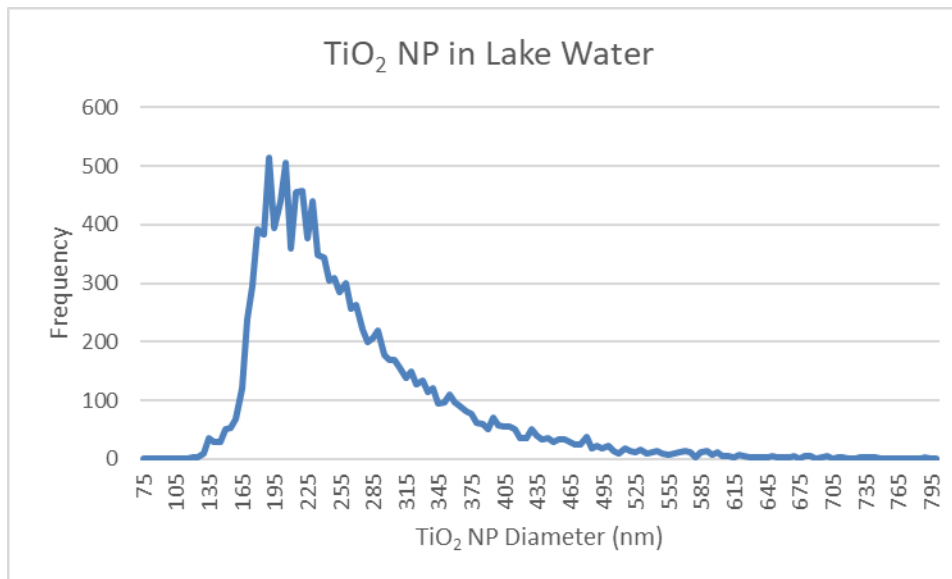
SI 1. Size distribution histograms for Ce-, Ti-, and Zn-containing NPs (treated as CeO₂, TiO₂, and ZnO respectively in this study) in river water without added NPs.





SI 2. Size distribution histograms for Ce-, Ti-, and Zn-containing NPs (treated as CeO₂, TiO₂, and ZnO respectively in this study) in lake water without added NPs.





BIBLIOGRAPHY

1. Sauvé, S. & Desrosiers, M. A review of what is an emerging contaminant. *Chem. Cent. J.* **8**, 1–7 (2014).
2. Diamond, J. M. *et al.* Prioritizing contaminants of emerging concern for ecological screening assessments. *Environ. Toxicol. Chem.* **30**, 2385–2394 (2011).
3. Crane, M., Handy, R. D., Garrod, J. & Owen, R. Ecotoxicity test methods and environmental hazard assessment for engineered nanoparticles. *Ecotoxicology* **17**, 421–437 (2008).
4. Elsaesser, A. & Howard, C. V. Toxicology of nanoparticles. *Adv. Drug Deliv. Rev.* **64**, 129–137 (2012).
5. Hassellöv, M., Readman, J. W., Ranville, J. F. & Tiede, K. Nanoparticle analysis and characterization methodologies in environmental risk assessment of engineered nanoparticles. *Ecotoxicology* **17**, 344–361 (2008).
6. Donovan, A. R. A. R. *et al.* Single particle ICP-MS characterization of titanium dioxide, silver, and gold nanoparticles during drinking water treatment. *Chemosphere* **144**, (2016).
7. Gray, E., Higgins, C. P. & Ranville, J. F. Analysis of Nanoparticles in Biological Tissues using SP-ICP-MS.
8. Schwertfeger, D. M. *et al.* Extracting Metallic Nanoparticles from Soils for Quantitative Analysis: Method Development Using Engineered Silver Nanoparticles and SP-ICP-MS. *Anal. Chem.* **89**, 2505–2513 (2017).
9. Montañó, M. D., Olesik, J. W., Barber, A. G., Challis, K. & Ranville, J. F. Single Particle ICP-MS: Advances toward routine analysis of nanomaterials. *Analytical and Bioanalytical Chemistry* (2016). doi:10.1007/s00216-016-9676-8
10. Peters, R. J. B. *et al.* Development and validation of single particle ICP-MS for sizing and quantitative determination of nano-silver in chicken meat Characterisation of Nanomaterials in Biological Samples. *Anal. Bioanal. Chem.* **406**, 3875–3885 (2014).
11. Mitrano, D. M. *et al.* Tracking dissolution of silver nanoparticles at environmentally relevant concentrations in laboratory, natural, and processed waters using single particle ICP-MS (spICP-MS). *Environ. Sci. Nano* (2014). doi:10.1039/C3EN00108C

12. Inc, P. Measurement of Titanium Dioxide Nanoparticles in Sunscreen using Single Particle ICP-MS.
13. Stewart, I., Webb, P. M., Schuler, P. J. & Shaw, G. R. Recreational and occupational field exposure to freshwater cyanobacteria - a review of anecdotal and case reports, epidemiological studies and the challenges for epidemiologic assessment. *Environ. Heal.* **5**, 1–13 (2006).
14. Wood, R. Acute animal and human poisonings from cyanotoxin exposure - A review of the literature. *Environ. Int.* **91**, 276–282 (2016).
15. *Handbook of Cyanobacterial Monitoring and Cyanotoxin Analysis*. (John Wiley & Sons, 2017).
16. Tatters, A. O. *et al.* Multiple Stressors at the Land-Sea Interface: Cyanotoxins at the Land-Sea Interface in the Southern California Bight. *Toxins (Basel)*. **9**, 95 (2017).
17. Tatters, A. O. *et al.* Heterogeneity of Toxin-Producing Cyanobacteria and Cyanotoxins in Coastal Watersheds of Southern California. *Estuaries and Coasts* **42**, 958–975 (2019).
18. Chorus, I. & Bartram, J. *Toxic Cyanobacteria in Water: A guide to their public health consequences, monitoring and management*. (Spon Press, 1999).
19. Loftin, K. A. *et al.* Cyanotoxins in inland lakes of the United States: Occurrence and potential recreational health risks in the EPA National Lakes Assessment 2007. *Harmful Algae* **56**, 77–90 (2016).
20. Nowack, B. & Bucheli, T. D. Occurrence, behavior and effects of nanoparticles in the environment. *Environ. Pollut.* **150**, 5–22 (2007).
21. *Environmental and human health impacts of nanotechnology*. (John Wiley & Sons, 2009).
22. Duncan, T. V. Applications of nanotechnology in food packaging and food safety: Barrier materials, antimicrobials and sensors. *J. Colloid Interface Sci.* **363**, 1–24 (2011).
23. West, J. L. & Halas, N. J. A gold nanoparticle bioconjugate-based colorimetric assay. 215–217 (2000).
24. Qu, X., Alvarez, P. J. J. & Li, Q. Applications of nanotechnology in water and wastewater treatment. *Water Res.* **47**, 3931–3946 (2013).

25. Smith, D. M., Simon, J. K. & Baker, J. R. Applications of nanotechnology for immunology. *Nat. Rev. Immunol.* **13**, 592–605 (2013).
26. Fabian, E. *et al.* Tissue distribution and toxicity of intravenously administered titanium dioxide nanoparticles in rats. *Arch. Toxicol.* **82**, 151–157 (2008).
27. Sharma, V., Singh, P., Pandey, A. K. & Dhawan, A. Induction of oxidative stress, DNA damage and apoptosis in mouse liver after sub-acute oral exposure to zinc oxide nanoparticles. *Mutat. Res. - Genet. Toxicol. Environ. Mutagen.* **745**, 84–91 (2012).
28. Vandebriel, R. J. & De Jong, W. H. A review of mammalian toxicity of ZnO nanoparticles. *Nanotechnol. Sci. Appl.* **5**, 61–71 (2012).
29. Akhtar, M. J. *et al.* Zinc oxide nanoparticles selectively induce apoptosis in human cancer cells through reactive oxygen species. *Int. J. Nanomedicine* **7**, 845–857 (2012).
30. Lin, W. *et al.* Toxicity of nano- and micro-sized ZnO particles in human lung epithelial cells. *J. Nanoparticle Res.* **11**, 25–39 (2009).
31. Sharma, V., Anderson, D. & Dhawan, A. Zinc oxide nanoparticles induce oxidative DNA damage and ROS-triggered mitochondria mediated apoptosis in human liver cells (HepG2). *Apoptosis* **17**, 852–870 (2012).
32. Hussain, S. *et al.* Cerium dioxide nanoparticles induce apoptosis and autophagy in human peripheral blood monocytes. *ACS Nano* **6**, 5820–5829 (2012).
33. Lin, W., Huang, Y., Zhou, X.-D. & Ma, Y. Toxicity of Cerium Oxide Nanoparticles in Human Lung Cancer Cells. *Int. J. Toxicol.* **25**, 451–457 (2006).
34. Mittal, S. & Pandey, A. K. Cerium oxide nanoparticles induced toxicity in human lung cells: Role of ROS mediated DNA damage and apoptosis. *Biomed Res. Int.* **2014**, (2014).
35. Srinivas, A., Rao, P. J., Selvam, G., Murthy, P. B. & Reddy, P. N. Acute inhalation toxicity of cerium oxide nanoparticles in rats. *Toxicol. Lett.* **205**, 105–115 (2011).
36. Hadrup, N. & Lam, H. R. Oral toxicity of silver ions, silver nanoparticles and colloidal silver - A review. *Regul. Toxicol. Pharmacol.* **68**, 1–7 (2014).
37. Sambale, F. *et al.* Investigations of the toxic effect of silver nanoparticles on mammalian cell lines. *J. Nanomater.* **16**, 1–9 (2015).

38. Alkilany, A. M. & Murphy, C. J. Toxicity and cellular uptake of gold nanoparticles: What we have learned so far? *J. Nanoparticle Res.* **12**, 2313–2333 (2010).
39. Goodman, C. M., McCusker, C. D., Yilmaz, T. & Rotello, V. M. Toxicity of gold nanoparticles functionalized with cationic and anionic side chains. *Bioconjug. Chem.* **15**, 897–900 (2004).
40. Crosera, M. *et al.* Nanoparticle dermal absorption and toxicity: A review of the literature. *Int. Arch. Occup. Environ. Health* **82**, 1043–1055 (2009).
41. Osmond, M. J. & McCall, M. J. Zinc oxide nanoparticles in modern sunscreens: an analysis of potential exposure and hazard. *Nanotoxicology* **4**, 15–41 (2010).
42. Sharma, V. *et al.* DNA damaging potential of zinc oxide nanoparticles in human epidermal cells. *Toxicol. Lett.* **185**, 211–218 (2009).
43. Freese, C., Gibson, M. I., Klok, H. A., Unger, R. E. & Kirkpatrick, C. J. Size- and coating-dependent uptake of polymer-coated gold nanoparticles in primary human dermal microvascular endothelial cells. *Biomacromolecules* **13**, 1533–1543 (2012).
44. Stefaniak, A. B. *et al.* Dermal exposure potential from textiles that contain silver nanoparticles. *Int. J. Occup. Environ. Health* **20**, 220–234 (2014).
45. Kim, J. S. *et al.* Genotoxicity, acute oral and dermal toxicity, eye and dermal irritation and corrosion and skin sensitisation evaluation of silver nanoparticles. *Nanotoxicology* **7**, 953–960 (2013).
46. Baalousha, M., Stolpe, B. & Lead, J. R. Flow field-flow fractionation for the analysis and characterization of natural colloids and manufactured nanoparticles in environmental systems: A critical review. *Journal of Chromatography A* (2011). doi:10.1016/j.chroma.2011.04.063
47. Kammer, F. von der, Legros, S., Hofmann, T., Larsen, E. H. & Loeschner, K. Separation and characterization of nanoparticles in complex food and environmental samples by field-flow fractionation. *TrAC - Trends in Analytical Chemistry* (2011). doi:10.1016/j.trac.2010.11.012
48. Degueldre, C., Favarger, P. Y. & Bitea, C. Zirconia colloid analysis by single particle inductively coupled plasma-mass spectrometry. *Anal. Chim. Acta* **518**, 137–142 (2004).
49. Degueldre, C., Favarger, P. Y. & Wold, S. Gold colloid analysis by inductively coupled plasma-mass spectrometry in a single particle mode. *Anal. Chim. Acta* (2006). doi:10.1016/j.aca.2005.09.021

50. Degueldre, C., Favarger, P. Y., Rossé, R. & Wold, S. Uranium colloid analysis by single particle inductively coupled plasma-mass spectrometry. *Talanta* (2006). doi:10.1016/j.talanta.2005.05.006
51. Stephan, C. & Neubauer, K. *Single Particle Inductively Coupled Plasma Mass Spectrometry: Understanding How and Why*. (2014).
52. Donovan, A. R. *et al.* Single particle ICP-MS characterization of titanium dioxide, silver, and gold nanoparticles during drinking water treatment. *Chemosphere* (2016). doi:10.1016/j.chemosphere.2015.07.081
53. Donovan, A. R. *et al.* Detection of zinc oxide and cerium dioxide nanoparticles during drinking water treatment by rapid single particle ICP-MS methods. *Anal. Bioanal. Chem.* **408**, 5137–5145 (2016).
54. Donovan, A. R. *et al.* Fate of nanoparticles during alum and ferric coagulation monitored using single particle ICP-MS. *Chemosphere* **195**, 531–541 (2018).
55. Peters, R. *et al.* Single particle ICP-MS combined with a data evaluation tool as a routine technique for the analysis of nanoparticles in complex matrices. *J. Anal. At. Spectrom.* **30**, 1274–1285 (2015).
56. Bitragunta, S. P., Palani, S. G., Gopala, A., Sarkar, S. K. & Kandukuri, V. R. Detection of TiO₂ Nanoparticles in Municipal Sewage Treatment Plant and Their Characterization Using Single Particle ICP-MS. *Bull. Environ. Contam. Toxicol.* **98**, 595–600 (2017).
57. Loeschner, K. *et al.* Detection and characterization of silver nanoparticles in chicken meat by asymmetric flow field flow fractionation with detection by conventional or single particle ICP-MS. *Anal. Bioanal. Chem.* (2013). doi:10.1007/s00216-013-7228-z
58. Peters, R. J. B. *et al.* Development and validation of single particle ICP-MS for sizing and quantitative determination of nano-silver in chicken meat
Characterisation of Nanomaterials in Biological Samples. *Anal. Bioanal. Chem.* (2014). doi:10.1007/s00216-013-7571-0
59. Gray, E. P. *et al.* Extraction and analysis of silver and gold nanoparticles from biological tissues using single particle inductively coupled plasma mass spectrometry. *Environ. Sci. Technol.* **47**, 14315–14323 (2013).
60. Lewicka, Z. A. *et al.* The structure, composition, and dimensions of TiO₂ and ZnO nanomaterials in commercial sunscreens. *J. Nanoparticle Res.* **13**, 3607–3617 (2011).

61. Dan, Y. *et al.* Characterization of Gold Nanoparticle Uptake by Tomato Plants Using Enzymatic Extraction Followed by Single-Particle Inductively Coupled Plasma–Mass Spectrometry Analysis. doi:10.1021/es506179e
62. Dan, Y. *et al.* Single particle ICP-MS method development for the determination of plant uptake and accumulation of CeO₂ nanoparticles. *Anal. Bioanal. Chem.* **408**, 5157–5167 (2016).
63. Zhang, Y., Chen, Y., Westerhoff, P., Hristovski, K. & Crittenden, J. C. Stability of commercial metal oxide nanoparticles in water. *Water Res.* **42**, 2204–2212 (2008).
64. Abbott Chalew, T. E., Ajmani, G. S., Huang, H. & Schwab, K. J. Evaluating nanoparticle breakthrough during drinking water treatment. *Environ. Health Perspect.* **121**, 1161–1166 (2013).
65. Wang, H. T., Ye, Y. Y., Qi, J., Li, F. T. & Tang, Y. L. Removal of titanium dioxide nanoparticles by coagulation: effects of coagulants, typical ions, alkalinity and natural organic matters. *Water Sci. Technol.* **68**, 1137–1143 (2013).
66. Wang, H., Qi, J., Keller, A. A., Zhu, M. & Li, F. Effects of pH, ionic strength and humic acid on the removal of TiO₂ nanoparticles from aqueous phase by coagulation. *Colloids Surfaces A Physicochem. Eng. Asp.* **450**, 161–165 (2014).
67. Loftin, K. A. *et al.* Cyanotoxins in inland lakes of the United States: Occurrence and potential recreational health risks in the EPA National Lakes Assessment 2007. *Harmful Algae* **56**, 77–90 (2016).
68. Graham, J., Loftin, K. & Kamman, N. Monitoring recreational freshwaters. *Lakeline* **29**, 18–24 (2009).
69. Howard, M. D. A. *et al.* Microcystin prevalence throughout lentic waterbodies in coastal southern California. *Toxins (Basel)*. **9**, 1–21 (2017).
70. Lehman, P. W. *et al.* Characterization of the Microcystis Bloom and Its Nitrogen Supply in San Francisco Estuary Using Stable Isotopes. *Estuaries and Coasts* **38**, 165–178 (2014).
71. Mountfort, D. O., Holland, P. & Sprosen, J. Method for detecting classes of microcystins by combination of protein phosphatase inhibition assay and ELISA: Comparison with LC-MS. *Toxicon* **45**, 199–206 (2005).
72. Vasas, G. *et al.* Capillary electrophoretic assay and purification of cylindrospermopsin, a cyanobacterial toxin from *Aphanizomenon ovalisporum*, by plant test (Blue-Green Sinapis Test). *Anal. Biochem.* **302**, 95–103 (2002).

73. Vasas, G. *et al.* Analysis of cyanobacterial toxins (anatoxin-a, cylindrospermopsin, microcystin-LR) by capillary electrophoresis. *Electrophoresis* **25**, 108–115 (2004).
74. Birungi, G. & Li, S. F. Y. Determination of cyanobacterial cyclic peptide hepatotoxins in drinking water using CE. *Electrophoresis* **30**, 2737–2742 (2009).
75. Mathew, J. *et al.* Dioctyl sulfosuccinate analysis in near-shore Gulf of Mexico water by direct-injection liquid chromatography-tandem mass spectrometry. *J. Chromatogr. A* **1231**, 46–51 (2012).
76. Fischer, W. J. *et al.* Congener-independent immunoassay for microcystins and nodularins. *Environ. Sci. Technol.* **35**, 4849–4856 (2001).
77. Proença, L., Tamanaha, M. S. & Fonseca, R. S. SCREENING THE TOXICITY AND TOXIN CONTENT OF BLOOMS OF THE CYANOBACTERIUM *Trichodesmium erythraeum* (EHRENBERG) IN NORTHEAST BRAZIL. *J. Venom. Anim. Toxins Incl. Trop. Dis.* **15**, 204–215 (2008).
78. Díez-Quijada, L., Prieto, A. I., Guzmán-Guillén, R., Jos, A. & Cameán, A. M. Occurrence and toxicity of microcystin congeners other than MC-LR and MC-RR: A review. *Food Chem. Toxicol.* **125**, 106–132 (2019).
79. de Figueiredo, D. R., Azeiteiro, U. M., Esteves, S. M., Gonzalves, F. J. M. & Pereira, M. J. Microcystin-producing blooms—a serious global public health issue. *Ecotoxicol. Environ. Saf.* **59**, 151–163 (2004).
80. USEPA. *Recommended Human Health Recreational Ambient Water Quality Criteria or Swimming*. (2019). doi:1037//0033-2909.I26.1.78
81. Miller, M. A. *et al.* Evidence for a Novel Marine Harmful Algal Bloom: Cyanotoxin (Microcystin) Transfer from Land to Sea Otters. *PLoS One* **5**, e12576 (2010).
82. Preece, E. P., Moore, B. C. & Hardy, F. J. Transfer of microcystin from freshwater lakes to Puget Sound, WA and toxin accumulation in marine mussels (*Mytilus trossulus*). *Ecotoxicol. Environ. Saf.* **122**, 98–105 (2015).
83. Wood, J. D. *et al.* Exposure to the cyanotoxin microcystin arising from interspecific differences in feeding habits among fish and shellfish in the James river estuary, Virginia. *Environ. Sci. Technol.* **48**, 5194–5202 (2014).
84. Gible, C. M., Peacock, M. B. & Kudela, R. M. Evidence of freshwater algal toxins in marine shellfish: Implications for human and aquatic health. *Harmful Algae* **59**, 59–66 (2016).

85. Ibelings, B. W. & Chorus, I. Accumulation of cyanobacterial toxins in freshwater “seafood” and its consequences for public health: A review. *Environ. Pollut.* **150**, 177–192 (2007).
86. Namikoshi, M. *et al.* New Nodularins: A General Method for Structure Assignment. *J. Org. Chem.* **59**, 2349–2357 (1994).
87. Chen, Y., Shen, D. & Fang, D. Nodularins in poisoning. *Clin. Chim. Acta* **425**, 18–29 (2013).
88. McGregor, G. B. & Sendall, B. C. *Iningainema pulvinus* gen nov., sp nov. (Cyanobacteria, Scytonemataceae) a new nodularin producer from Edgbaston Reserve, north-eastern Australia. *Harmful Algae* **62**, 10–19 (2017).
89. Pearson, L., Mihali, T., Moffitt, M., Kellmann, R. & Neilan, B. On the chemistry, toxicology and genetics of the cyanobacterial toxins, microcystin, nodularin, saxitoxin and cylindrospermopsin. *Marine Drugs* (2010). doi:10.3390/md8051650
90. Sellner, K. G. Physiology, ecology, and toxic properties of marine cyanobacteria blooms. *Limnol. Oceanogr.* **42**, 1089–1104 (1997).
91. Strogyloudi, E., Giannakourou, A., Legrand, C., Ruehl, A. & Granéli, E. Estimating the accumulation and transfer of *Nodularia spumigena* toxins by the blue mussel *Mytilus edulis*: An appraisal from culture and mesocosm experiments. *Toxicon* **48**, 359–372 (2006).
92. Kelly, L., Wood, S., McAllister, T. & Ryan, K. Development and Application of a Quantitative PCR Assay to Assess Genotype Dynamics and Anatoxin Content in *Microcoleus autumnalis*-Dominated Mats. *Toxins (Basel)*. **10**, 431 (2018).
93. Shams, S. *et al.* Anatoxin-a producing *Tychonema* (cyanobacteria) in European waterbodies. *Water Res.* **69**, 68–79 (2015).
94. Wonnacott, S. & Gallagher, T. The chemistry and pharmacology of anatoxin-a and related homotropanes with respect to nicotinic acetylcholine receptors. *Mar. Drugs* **4**, 228–254 (2006).
95. Rubio, F. *et al.* Colorimetric microtiter plate receptor-binding assay for the detection of freshwater and marine neurotoxins targeting the nicotinic acetylcholine receptors. *Toxicon* **91**, 45–56 (2014).
96. Mazur, H. & Pliński, M. *Nodularia spumigena* blooms and the occurrence of hepatotoxin in the Gulf of Gdańsk. *Oceanologia* **45**, 305–316 (2003).

97. Bourke, A. T. C., Hawes, R. B., Neilson, A. & Stallman, N. D. An outbreak of hepato-enteritis (the Palm Island mystery disease) possibly caused by algal intoxication. *Toxicon* **21**, 45–48 (1983).
98. de la Cruz, A. A. *et al.* A review on cylindrospermopsin: the global occurrence, detection, toxicity and degradation of a potent cyanotoxin. *Environ. Sci. Process. Impacts* **15**, 1979 (2013).
99. Rzymiski, P. & Poniedziałek, B. In search of environmental role of cylindrospermopsin: A review on global distribution and ecology of its producers. *Water Res.* **66**, 320–337 (2014).
100. Saker, M. L., Metcalf, J. S., Codd, G. A. & Vasconcelos, V. M. Accumulation and depuration of the cyanobacterial toxin cylindrospermopsin in the freshwater mussel *Anodonta cygnea*. *Toxicon* **43**, 185–194 (2004).
101. Van Dolah, F. M. Marine Algal Toxins: Origins, Health Effects, and Their Increased Occurrence. *Environ. Health Perspect.* **108**, 133–141 (2000).
102. USFDA & CFSAN. *Fish and Fishery Products Hazards and Controls Guidance. Fish and Fishery Products Hazard and Control Guidance Fourth Edition* (2011). doi:10.1039/9781847558398-00136
103. O’Dea, S. Occurrence, Toxicity, and Diversity of Pseudo-nitzschia in Florida Coastal Waters. (2012).
104. Pulido, O. M. Domoic acid toxicologic pathology: A review. *Mar. Drugs* **6**, 180–219 (2008).
105. Trainer, V. L. *et al.* Pseudo-nitzschia physiological ecology, phylogeny, toxicity, monitoring and impacts on ecosystem health. *Harmful Algae* **14**, 271–300 (2012).
106. Bates, S. S. *et al.* Pennate Diatom Nitzschia pungens as the Primary Source of Domoic Acid, a Toxin in Shellfish from Eastern Prince Edward Island, Canada. *Can. J. Fish. Aquat. Sci.* **46**, 1203–1215 (1989).
107. Perl, T. M. *et al.* An Outbreak of Toxic Encephalopathy Caused by Eating Mussels Contaminated with Domoic Acid. *N. Engl. J. Med.* **322**, 1775–1780 (1990).
108. Lefebvre, K. A. *et al.* Chronic low-level exposure to the common seafood toxin domoic acid causes cognitive deficits in mice. *Harmful Algae* **64**, 20–29 (2017).
109. Petroff, R. *et al.* Chronic, low-level oral exposure to marine toxin, domoic acid, alters whole brain morphometry in nonhuman primates. *Neurotoxicology* **72**, 114–124 (2019).

110. Goldstein, T. *et al.* Novel symptomatology and changing epidemiology of domoic acid toxicosis in California sea lions (*Zalophus californianus*): An increasing risk to marine mammal health. *Proc. R. Soc. B Biol. Sci.* **275**, 267–276 (2008).
111. Yasumoto, T., Oshima, Y. & Yamaguchi, M. Occurrence of a new type of shellfish poisoning in the Tohoku district. *Bulletin of the Japanese Society of Scientific Fisheries* **44**, (1978).
112. Fabro, E. *et al.* Distribution of Dinophysis species and their association with lipophilic phycotoxins in plankton from the Argentine Sea. *Harmful Algae* **59**, 31–41 (2016).
113. Draisci, R., Lucentini, L., Giannetti, L., Boria, P. & Poletti, R. First report of pectenotoxin-2 (PTX-2) in algae (*dinophysis fortii*) related to seafood poisoning in Europe. *Toxicon* **34**, 923–935 (1996).
114. Deeds, J. R., Wiles, K., Heideman, G. B., White, K. D. & Abraham, A. First U.S. report of shellfish harvesting closures due to confirmed okadaic acid in Texas Gulf coast oysters. *Toxicon* **55**, 1138–1146 (2010).
115. Fire, S. E. *et al.* Co-occurrence of multiple classes of harmful algal toxins in bottlenose dolphins (*Tursiops truncatus*) stranding during an unusual mortality event in Texas, USA. *Harmful Algae* **10**, 330–336 (2011).
116. An, T., Winshell, J., Scorzetti, G., Fell, J. W. & Rein, K. S. Identification of okadaic acid production in the marine dinoflagellate *Prorocentrum rhathymum* from Florida Bay. *Toxicon* **55**, 653–657 (2010).
117. Trainer, V. L. *et al.* Diarrhetic shellfish toxins and other lipophilic toxins of human health concern in Washington State. *Mar. Drugs* **11**, 1815–1835 (2013).
118. Visciano, P. *et al.* Marine Biotoxins: Occurrence, Toxicity, Regulatory Limits and Reference Methods. *Front. Microbiol.* **7**, 1–10 (2016).
119. Yasumoto, T., Murata, M., Oshima, Y. & Sano, M. Diarrhetic shellfish toxins. *Tetrahedron* **41**, 1019–1025 (1985).
120. Couesnon, A. *et al.* The dinoflagellate toxin 20-methyl spirolide-G potently blocks skeletal muscle and neuronal nicotinic acetylcholine receptors. *Toxins (Basel)*. **8**, (2016).
121. Martens, H. *et al.* Toxin Variability Estimations of 68 *Alexandrium ostenfeldii* (Dinophyceae) Strains from The Netherlands Reveal a Novel Abundant Gymnodimine. *Microorganisms* **5**, 29 (2017).

122. Pulido, O., Frémy, J.-M., Munday, R. & Quilliam, M. A. Cyclic imines (gymnodimine, spirolides, pinnatoxins, pteriatoxins, prorocontrolide and spiro-prorocentrimine). in *Assessment and management of biotoxin risks in bivalve molluscs* (eds. Lawrence, J. et al.) 99–110 (Food and Agriculture Organization of the United Nations, 2011).
123. Munday, R. *et al.* Acute toxicity of gymnodimine to mice. *Toxicon* **44**, 173–178 (2004).
124. Stirling, D. J. Survey of historical New Zealand shellfish samples for accumulation of gymnodimine. *New Zeal. J. Mar. Freshw. Res.* **35**, 851–857 (2001).
125. Takahashi, E. *et al.* Occurrence and seasonal variations of algal toxins in water, phytoplankton and shellfish from North Stradbroke Island, Queensland, Australia. *Mar. Environ. Res.* **64**, 429–442 (2007).
126. Jester, R., Rhodes, L. & Beuzenberg, V. Uptake of paralytic shellfish poisoning and spirolide toxins by paddle crabs (*Ovalipes catharus*) via a bivalve vector. *Harmful Algae* **8**, 369–376 (2009).
127. González, A. V., Rodríguez-Velasco, M. L., Ben-Gigirey, B. & Botana, L. M. First evidence of spirolides in Spanish shellfish. *Toxicon* **48**, 1068–1074 (2006).
128. Pigozzi, S., Bianchi, L., Boschetti, L., Cangini, M., Ceredi, A., Magnani, F., Milandri, A., Montanari, S., Pompei, M., Riccardi, E., Rubini, S. First evidence of spirolide accumulation in Northwestern Adriatic shellfish. *Proc. 12th Int. Conf. Harmful Algae* 319–322 (2008).

VITA

Ariel Renee Donovan completed an Associate Degree in Liberal Arts at Johnson County Community College in Overland Park, Kansas in 2011. Upon completion, she began at Missouri University of Science and Technology working toward a Bachelor of Science in Chemistry, performing undergraduate student research in Dr. Honglan Shi's research group through the completion of her BS degree in May 2014. She continued at Missouri University of Science and Technology and worked in Dr. Shi's research group into her graduate studies. She completed her Master of Science in Chemistry in 2016, before continuing onto doctoral study. In 2016, Ariel began working at the United States Geological Survey, Kansas Water Science Center with Dr. Keith Loftin. Dr. Loftin and Dr. Shi co-advised Ariel through her doctorate. Her research has focused on mass spectrometry methods for the analysis of inorganic and organic water contaminants to support environmental science research of nanoparticles and cyanotoxins in natural water systems. In December 2019 she received her PhD degree in Chemistry from Missouri University of Science and Technology